PNNL-11312
UC-2030

Pacific Northwest
National Laboratory

Operated by Battelle for the
U.S. Department of Energy

Organic Tanks Safety Program FY96 Waste Aging Studies

D. M. Camaioni
W. D. Samuels
J. C. Linehan
S. A. Clauss
A. K. Sharma
K. L. Wahl
J. A. Campbell

October 1996

Prepared for the U.S. Department of Energy
under Contract DE-AC06-76RLO 1830

PNNL-11312

DISCLAIMER

PACIFIC NORTHWEST NATIONAL LABORATORY
operated by
BATTELLE
for the
UNITED STATES DEPARTMENT OF ENERGY
under Contract DE-AC06-76RLO 1830

Printed in the United States of America

Available to DOE and DOE contractors from the Office of Scientific and Technical Information, P.O. Box 62, Oak Ridge, TN 37831; prices available from (615) 576-8401.

Available to the public from the National Technical Information Service, U.S. Department of Commerce, 5285 Port Royal Rd., Springfield, VA 22161

PNNL-11312
UC-2030

Organic Tanks Safety Program FY96 Waste Aging Studies

D. M. Camaioni
W. D. Samuels
J. C. Linehan
S. A. Clauss
A. K. Sharma
K. L. Wahl
J. A. Campbell

October 1996

Prepared for
the U.S. Department of Energy
under Contract DE-AC06-76RLO 1830

Pacific Northwest National Laboratory
Richland, Washington 99352

Summary

The underground storage tanks at the Hanford Site contain radioactive wastes generated from many years of plutonium production and recovery processes and mixed wastes from radiological degradation processes. The aging of the organic materials used in the extraction processes has a direct bearing on several specific safety issues, including hazards associated with fuel-nitrate combustion accidents. The specific purpose of this project is to learn whether the wastes are aging to lower energy content. Furthermore, the project seeks to quantify the extent to which the energy content of the waste has changed during storage. Our approach subjects non-radioactive waste simulants to a range of temperatures and doses of γ-radiation doses and then performs chemical analyses for inorganic and organic species. Conversion of the species data to data that show carbon content and energy content will allow quantitative description of the effects of temperature, radiation dose, and radiation flux on these key indicies. This report details experimental progress towards these goals.

Section 2 of this report is a revision of the corresponding section from our FY95 report (Camaioni et al. 1995). It describes an extensive series of experiments that started in FY94 and were completed this year. The simulant contained equimolar amounts of dodecane, ethylene-diaminetetraacetate (EDTA), tributyl phosphate (TBP), dibutyl phosphate (DBP), methyl isobutyl ketone (hexone), stearate, and citrate in an inorganic matrix containing hydroxide, nitrate, nitrite, aluminium hydroxide, and a variety of alkali, alkaline earth, and transition metal cations. We found that gas production is predominantly radiolytically induced. The main gases found and their radiolytic yields (G molecules/100 eV) at 70 °C are hydrogen (0.11), nitrous oxide (0.17), and nitrogen (0.08). Ammonia was also produced, but our methodology did not allow its measurement. Concurrent with gas generation starting organic compounds disappeared, and condensed-phase products, dodecanones, heptadecane, isobutyrate, succinate, oxalate, formate, and glycolate appeared. The presence of heptadecane, which must derive from stearate (a C-18 carboxylate salt), provides clear evidence that decarboxylation of carboxylates is a pathway of aging. The TBP was totally consumed in almost every run, even in unirradiated control experiments. Its consumption is attributed to alkaline hydrolysis to DBP and butanol. Disappearances of EDTA and citrate in the condensed phase fit a first-order kinetic rate law, $A=A_oe^{-kD}$ where D is the radiolytic dose. The radiation doses necessary to reduce the concentration of EDTA in the simulant by half were 0.63 MGy at 50 °C, 0.51 MGy at 70 °C, and 0.41 MGy at 90 °C (1 MGy = 100 Mrad). Citrate was less reactive, requiring about 5 times more radiation to reduce its concentration by half. Analyses for hexone, stearate, and dodecane showed significant scatter, probably the result of sample variability caused by their low solubility in the inorganic matrix of the simulant.

Section 3 reports on a recent study of a neutralized PUREX-acid sludge-simulant designated SIM-PAS-95-1c (Carlson and Babad 1996). The simulant contains 0.069 M HEDTA, 0.014 M EDTA, 0.10 M citrate, and 0.14 M glycolate in an inorganic matrix that is representative of B-Plant flow sheets. Experiments dosed the simulant with 0.3, 0.5, 1.0 and 1.5 MGy (flux ~10^3 Gy/h) at 70°C. Nearly all of the EDTA and HEDTA was consumed by a 1.5 MGy dose. Oxidation products, oxalate, formate, and carbonate increased linearly with dose (G = 0.6, 0.6 and 1.9 respetively). Analyses are in progress for chelator fragments: ethylenediaminetriacetic acid, ethylenediaminediacetic acid, nitrilotriacetic acid, iminodiacetic acid, and glycine. The relative reactivities of the starting compounds are HETA~EDTA>glycolate>citrate. The doses required to halve the initial concentrations of HEDTA, EDTA, glycolate, and citrate are 0.38, 0.46, 2.2, and 3.3 MGy, respectively. However, glycolate may be more reactive than the data suggest because the other compounds may degrade to glycolate. The nitrate reaction energies of the speciated compounds are used to estimate the change in (theoretical) energy content of the simulant with

dose. The energy content decreased linearly from 1340 J/g (dry wt basis) to 800 J/g after 150 MGy. Allowing for thermal degradation that may occur during 15 to 30 years of storage would yield an even greater reduction in energy content; the half life of glycolate in the absence of radiation is less than 1 yr at 60 °C (Barefield et al. 1995). Both TOC and nitrate reaction energies decreased with increasing dose. Correlating the two indices yields a factor of 45 J/mg C, i.e. the change in reaction energy per change in TOC (dry mix basis). This finding supports the idea that aging reduces the energy value of TOC in the tank wastes.

Subsequent sections report on studies performed to learn the possible fates of TBP hydrolysis products, sodium dibutyl phosphate (DBP) and butanol. Aging reactions of sodium butyrate were also examined because butanol may have oxidized to butyrate during the PUREX process. The disappearance and appearance of compounds are consistent with radiolytically-induced oxidation reactions. Radiolytic doses in excess of 0.6 MGy completely consumed butanol and sodium butyrate to yield formate, oxalate, acetate, glycolate, malonate (propan-1,3-dioate), malate (2-hydroxysuccinate), and possibly fumarate. These products accounted for about 25% and 40%, respectively, of the initial carbon in butyrate and butanol simulants that had received 1 MGy. Literature data suggest that alkaline hydrolysis of DBP and MBP is probably only a minor pathway for aging of DBP in tank wastes. Radiolysis experiments showed that DBP and MBP degrade by oxidation of the butyl groups. The radiolytic yield for conversion of diorganophosphates to monorganoophosphates is ~0.8 molecules/100 eV of absorbed energy. The data show that DBP is less reactive than either butanol or butyrate but more reactive than EDTA. Thus, with respect to aging, DBP and butanol rank among the more reactive organics added to tank wastes.

Contents

Tables

Figures

Schemes

Abbreviations

DBP	dibutyl phosphate
DMF	*N*,*N*-dimethyl formamide
DMSO	dimethyl sulfoxide
EDTA	ethylenediaminetetraacetate
EDDA	ethylenediaminediacetate
ED3A	ethylenediaminetriacetate
EPR	electron paramagnetic resonance
GC	Gas Chromatography
FAI	Fauske & Associates, Inc.
FY	fiscal year
HEDTA	hydroxyethylethylenediaminetriacetate
hexone	methyl isobutyl ketone
HPLC	high performance liquid chromatography
IDA	iminodiacetate
IC	Ion Chromatography
IPC	Ion-Pair Chromatography
MS	Mass Spectrometry
NMR	nuclear magnetic resonance
NPH	normal paraffinic hydrocarbons
NTA	nitrilotriacetate
PUREX	Plutonium-Uranium Extraction
REDOX	Reduction-Oxidation
RSST	Reactive Systems Screening Tool
SST	Single-Shell Storage Tanks
TBP	tributyl phosphate
TOC	total organic carbon

1.0 Introduction

Uranium and plutonium production at the Hanford Site produced large quantities of radioactive by-products and contaminated process chemicals, which are stored in underground tanks awaiting treatment and disposal. Having been made strongly alkaline and then subjected to successive water evaporation campaigns to increase storage capacity, the wastes now exist in the physical forms of salt cakes, metal oxide sludges, and partially saturated aqueous brine solutions. The tanks that contain organic process chemicals mixed with nitrate/nitrite salt wastes may be at risk for fuel-nitrate combustion accidents.

To assess hazards and provide information needed to establish safety criteria, test programs must use simulants, at least until tank samples and hot-cell test methods become available. Historical records identify the organic compounds originally purchased and potentially present in the wastes, thus allowing experimental determination of the reactivity of these starting materials with nitrates and nitrites as a first estimate of hazard (Webb et al. 1995). Aging experiments with simulated waste enable us to identify probable degradation products and evaluate the current hazard. Knowledge gained about the rates and pathways of degradation will facilitate prediction of how the hazard may change with time or with altered storage conditions. Work with aged simulated wastes contributes to the development of analytical methods for characterizing actual wastes. Finally, the simulant data provide a baseline for comparing and interpreting tank characterization data.

1.1 Objective

The purpose of the Waste Aging Task is to elucidate how chemical and radiological processes will have aged or degraded the organic compounds stored in the tanks. Ultimately, the task seeks to develop quantitative measures of how aging changes the energetic properties of the wastes. This information will directly support efforts to evaluate the hazard as well as to develop potential control and mitigation strategies.

1.2 Approach

Hazards posed by uncontrolled exothermic oxidation of organic compounds by nitrate and nitrite relate directly to the energy content and oxidation kinetics of the various organic compounds in the waste. Until sampling and analysis of the tank wastes become routine procedures, a viable approach to assessing the current organic content of the tanks is to simulate the chemical conditions of the tanks and elucidate mechanistic pathways that will reveal whether the hazards have increased, decreased, or remained constant. Accordingly, this project is using simulants in its studies of chemical aging. To facilitate studies of radiolytic-induced chemical aging, external radiation from a γ source is used rather than radioactive chemicals. Radiation doses and temperatures are selected to produce aging reactions over a few days to several months. After irradiation, the disappearance and appearance of detectable organic products in the simulant and evolved gases are determined.

1.3 Background

Each of the 177 waste tanks on the Hanford Site has a unique and uncertain composition of organic, inorganic, and radioactive elements (Agnew 1996a,b,c). Many of the single-shell waste tanks have been sampled and total organic carbon (TOC) contents measured. However, knowledge of the TOC in a particular storage tank is insufficient to bound the safety risk if the kinds of organic compounds in the waste remain unknown. Because nitrate reaction energies of organic species vary widely, we also need some information about the identity and oxidation state of the organic carbon. Organic-containing wastes have been stored in underground storage tanks at Hanford for nearly half a century. During that time the wastes have been exposed to radiation, temperatures of 20° to 140 °C (68° to 284 °F), and a reactive environment that contains high concentrations of active chemicals, including hydroxide, nitrate, nitrite, aluminate, oxides of transition metals including noble metals, radioactive elements (e.g., uranium, plutonium, cesium, strontium), and many other substances that may react with organic compounds or may catalyze or initiate organic reactions.

The organic compounds that were added to the tanks are divided into two main classes: complexants and extractants/solvents. The major organic complexants believed to have been stored in the tanks are glycolate, citrate, hydroxyethylethylenediamine-triacetate (HEDTA), and ethylenediaminetetraacetate (EDTA). Allen (1976) estimated the following approximate quantities

- glycolic acid, 8.8×10^5 kg
- citric acid, 8.5×10^5 kg
- hydroxyethylethylenediaminetriacetic acid, 8.3×10^5 kg
- ethylenediaminetetraacetic acid, 2.2×10^5 kg

Lesser amounts of other complexants were used, but amounts that actually were discharged to the tanks are not known.

Process solvents of concern that were used in chemical processes and stored in the tanks are tributyl phosphate (TBP), normal paraffin hydrocarbons (NPHs), and methyl isobutyl ketone (hexone). Sederburg and Reddick (1994) examined material balances at the Plutonium-Uranium Extraction (PUREX) plant from 1955 to 1991[1]; their findings indicate that 7.22×10^5 and 1.31×10^6 kg of TBP and NPH, respectively, went to tank storage. Other processes also used organic solvents and organic phosphate extractants, but less is known about the quantities they added to the tanks. Di(2–ethylhexyl)phosphate diluted with hydrocarbon solvent was used in the waste fractionation and encapsulation process. The reflux solvent extraction process used TBP/carbon tetrachloride (Cleveland 1967) and dibutyl butyl phosphonate/carbon tetrachloride for extraction solvents (Kingsley 1965). Considerable quantities of hexone were used in the REDOX plant as both extractant and solvent. For example, 65000 kg (65 metric tons) of hexone were retrieved from one storage tank, treated, and sent off-site (Gerber et al. 1992).

The evidence suggests that the quantities of organic solvents added to the tanks rival the quantities of complexants. However, the fraction of organic solvents that have escaped the wastes through evaporation or, in the case of phosphate esters, been saponified in the alkaline wastes

---

[1]The amount of organic entrained in PUREX wash waste discharged to the tanks was estimated to be 2,479 m^3 (655,000 gal). Assuming the composition of this waste was similar to the PUREX solvent (nominally 30 vol% TBP and 70 vol% NPH), then approximately 7.22×10^5 and 1.31×10^6 kg of the respective solvents would have been discharged to the waste tanks.

(Burger 1955) is not known. Sederburg and Reddick (1994) pointed out that during early PUREX operations, the organic wash waste was combined with high-level wastes that generated enough thermal heat to boil the tank wastes.

At the start of this project in FY94, little work had been performed on aging of organic solvent components. Therefore, we performed a series of aging studies on a simulant that contained both organic solvent compounds and complexants. This simulant was designated SY1-SIM-94C. Samples were irradiated in the γ-irradiation facility during FY94 and FY95. Most of the analyses were completed in FY95, and the rest in FY96. Thus, we include a revised version of the this work in Section 2.

Energetics and reactivity tests performed by Fauske & Associates, Inc. (Fauske 1996, 1995, Webb et al. 1995, Fauske and Epstein 1995) have shown that complexants and organic salts pose the greatest risk of propagating reactions. Attempts to ignite sodium nitrate-organic solvent mixtures (Fauske 1995, Webb et al. 1995) in either a Reactive Systems Screening Tool (RSST) (Creed and Fauske 1990) or in a tube propagation device (Webb et al. 1996) did not lead to propagating reactions, despite the high potential energy content of test compounds, such as dodecane, mineral oil, tributyl phosphate and sodium di-2-ethylhexyl phosphate, calcium dibutyl phosphate and sodium stearate. Instead, the solvent components vaporized away from the ignition source. Although tributyl phosphate and dibutyl phosphate have low or negligible vapor pressures, they tend to decompose, liberating hydrocarbon gases, before ignition temperatures are attained. Presumably, the complexants and low molecular weight carboxylate salts (e.g., acetate, butyrate, and succinate) have sufficiently high thermal stability to keep them in contact with an ignition source until melt temperatures (~200° to 250 °C) are attained and propagating reactions ensue. Accordingly, these finding focused our concern on how aging affects the distribution of organic waste components that can sustain propagating reactions.

Subsequent sections of this report describe a series of aging studies of simulants. Section 3 describes a recent study of a neutralized PUREX Acid Sludge (PAS) simulant containing HEDTA, EDTA, glycolate and citrate. Section 4 compares TOC measurements of aged simulants with amounts expected from speciation data. Sections 5 and 6 describe studies of relatively simple simulant compositions that contained single organic compounds in alkaline solutions of nitrate and/or nitrite. These special studies were started late in FY95 to learn how reactive dibutyl phosphate, butanol and sodium butyate may be in tank wastes and what products they may produce.

2.0 Aging Studies of Organic Tank Waste Simulant SY1-SIM-94C

At the start of this task in FY94, a review of the PUREX plant operations had shown that significant quantities of NPH and TBP had been disposed to the tanks (Sederburg and Reddick 1994). Although the Flammable Gas Safety Program had made extensive use of simulants to mimic the pertinent chemistry of the flammable gas-producing wastes, their simulants did not include TBP and NPH or other organic solvents, such as hexone, that had been widely used in the processing plants. Thus, the Organic Tank Safety Aging Studies set out to examine both complexant and organic solvent aging phenomena. Scoping experiments were performed to optimize procedures and establish the range of conditions over which to collect data. Then, we began a series of long-term aging experiments that spanned FY94, FY95, and FY96. For completeness, all our findings are reported here and in the Appendices.

The simulant composition was determined by consensus of PNNL and WHC investigators involved with tank safety programs and having knowledge of the chemical process streams that were fed to the underground waste storage tanks. The simulant was formulated with nonradioactive chemicals and is designated as SY1-SIM-94C. Table 2.1 shows its composition.

Table 2.1. Composition of Simulant SY1-SIM-94C[a]

Species	mg/g	Species	mg/g	Species	mg/g
Ag^{+}	0.64 ppm	Ni^{+2}	0.043	$EDTA^{4-}$	17.5
Al^{+3}	30.7	NO_2^-	100	Stearate (-1)	16.0
Ca^{+2}	0.220	NO_3^-	114	Citrate (-3)	10.6
Cl-	0.004	OH^-	27.8	TPB	15.9
CO_3^{-2}	3.00	Pb^{+3}	1.23	DBP (-1)	12.4
Cr^{+3}	3.91	Pd^{+2}	0.006	Hexone	6.0
Cs^{+}	0.013	PO_4^{-3}	6.1	Dodecane	10.1
F^-	113 ppm	Rh^{+3}	0.006		
Fe^{+3}	0.266	Ru^{+4}	0.006		
H_2O	309	$SO4^{-2}$	3.8		
K^{+}	3.11	Sr^{+2}	0.001		
Mn^{+2}	0.327	Zn^{+2}	0.019		
Na^{+}	186	Zr^{+2}	0.434		

[a]Density = 1.52 g/mL

The inorganic composition of SY1-SIM-94C is similar to that of SY1-SIM-93A (Hohl 1993, Bryan and Pederson 1994) which is based on analyses of core samples taken from Tank 241-SY-101 (Herting et al. 1992a,b). Sodium nitrate, nitrite, and hydroxide comprise the largest share of the mass of inorganic and non-radioactive species. Significant amounts of aluminum species are present. Noble metals (palladium, rhenium, ruthenium) were added based on the Reynolds (1993)

report. Zirconium was added and halide concentrations were lowered in concordance with the chemical compositions of strontium and cesium removal waste streams (Scheele et al. 1995).

The organic components were limited to seven, each added on an equimolar basis, to facilitate analyses of reactants and products in the condensed phase. Stearate, a long chain carboxylate anion, and dibutyl phosphate were included in the simulant to reflect partial oxidation of NPH and hydrolysis of TBP under plutonium extraction (PUREX) process conditions or alkaline hydrolysis. Glycolate and HEDTA were excluded to simplify analyses and because their radiolysis had been studied by Meisel et al. (1992, 1993).

2.1 Results and Discussion

Most of the simulant irradiation experiments were run at 50°, 70°, and 90 °C with samples receiving radiation doses of 0.07 to 1.2 MGy at a flux of 2660 to 3100 Gy/h. A few experiments were run at a much lower flux. Several duplicate experiments (runs 13 through 16, 18, and 21) were run to determine reproducibility. In most experiments argon and oxygen gases were in the headspace of the reaction vessel at the start of the irradiations. However, three experiments (31, 32, and 34) were run with only argon in the headspace to learn how oxygen affects radiolytic and thermal reactions of the simulant. Finally, experiments 2, B1, B2, B3, and X1 were run without radiation to determine thermal conversion levels.

2.1.1 Gas Phase Results

All scheduled experiments have been run. The analytical data are in the Appendix (Tables A.1 and A.2). The quantities of gases found were calculated from reactor head pressures and mass spectral analyses of headspace gases drawn from the reactor (see Sections 2.2.3 and 2.2.4). This methodology was not able to measure ammonia which was also generated in the aging tests.

Figure 2.1 is a plot of the reactor headspace gas pressures as a function of radiation dose and temperature. The pressures were corrected for increase in reactor temperature from ambient to run temperatures. In control experiments B1, B2, and B3, which were run in the absence of radiation, little gas increase is apparent after correction for temperature changes. Therefore, the pressure increases are due to radiolytically-induced gas-producing reactions. Although the data show considerable scatter at 70° and 90 °C, inspection of gas pressure vs. time collected for individual runs showed that pressure increased linearly with dose.

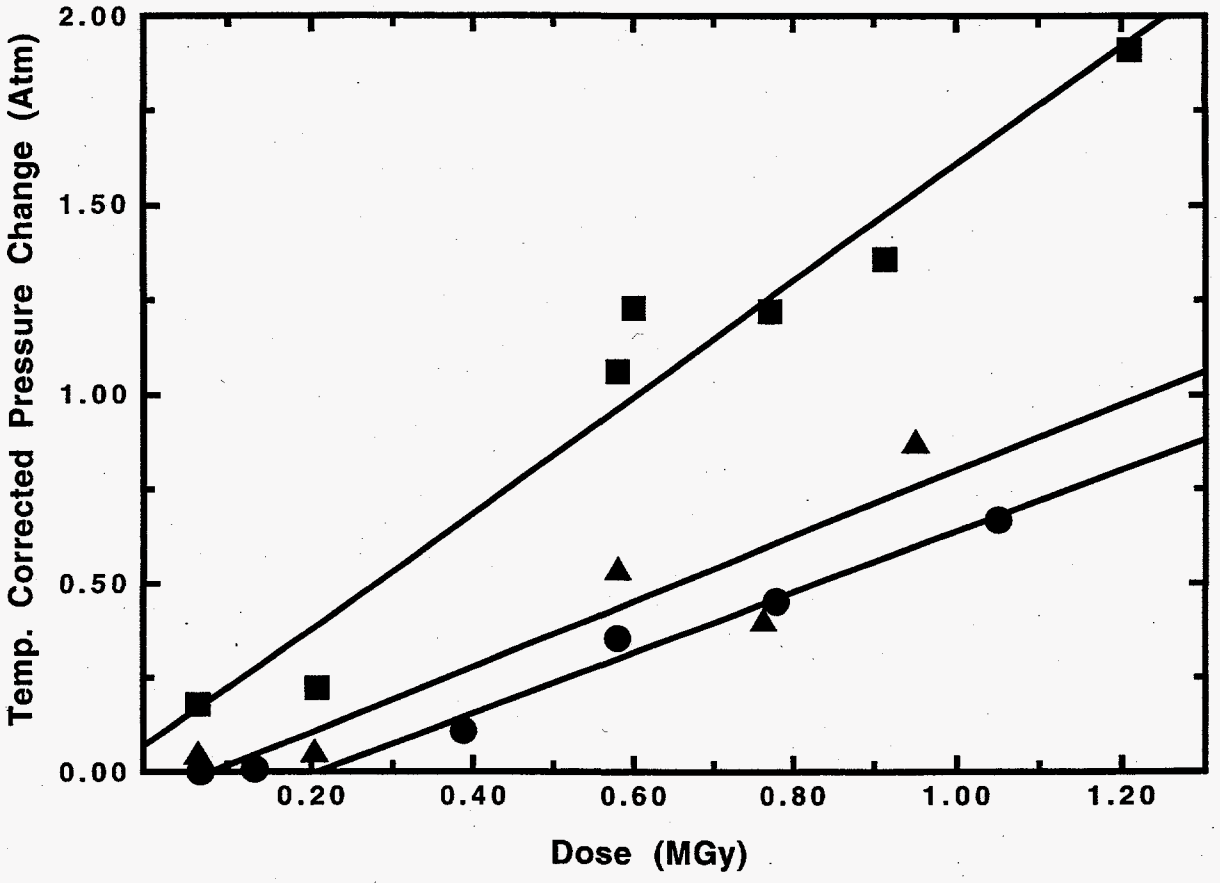

Figure 2.1. Temperature-Corrected Reactor Headspace Pressures Plotted vs. Simulant Dose at 50 °C(●), 70 °C(▲) and 90 °C (■). 1 MGy = 100 Mrad.

Induction periods for gas production were observed. For example at 50 °C, the rate of gas production increased significantly after the simulant received about 0.2 MGy. The linear increase in gas pressure with dose after the induction period indicates that gas production obeys zero-order kinetics, p=kD where d is dose. Induction periods decreased with increasing temperature.

Hydrogen, nitrogen, and nitrous oxide are the major gaseous products produced during irradiation of the simulant. The yield of individual gases was similar (except for greater scatter of the data) to that of total gas. Figures 2.2 and 2.3 are plots of the production of these gases at 50°, 70°, and 90 °C. Yields listed in Table A.2 and shown in Figures 2.2 and 2.3 are total amounts found in the reactor headspace above the simulant. For reference, the 24-mL headspace initially contained 752 µmol of argon and 192 µmol of oxygen in a volume of 24 mL. Linear fits to the yield data in Figures 2.1, 2.2, and 2.3 provide zero-order rate constants for production of H_2, N_2 and N_2O. Figure 2.4 plots these rate constants vs. inverse temperature in K. The rates of production and radiolytic yields (G) are reported in Table 2.2.

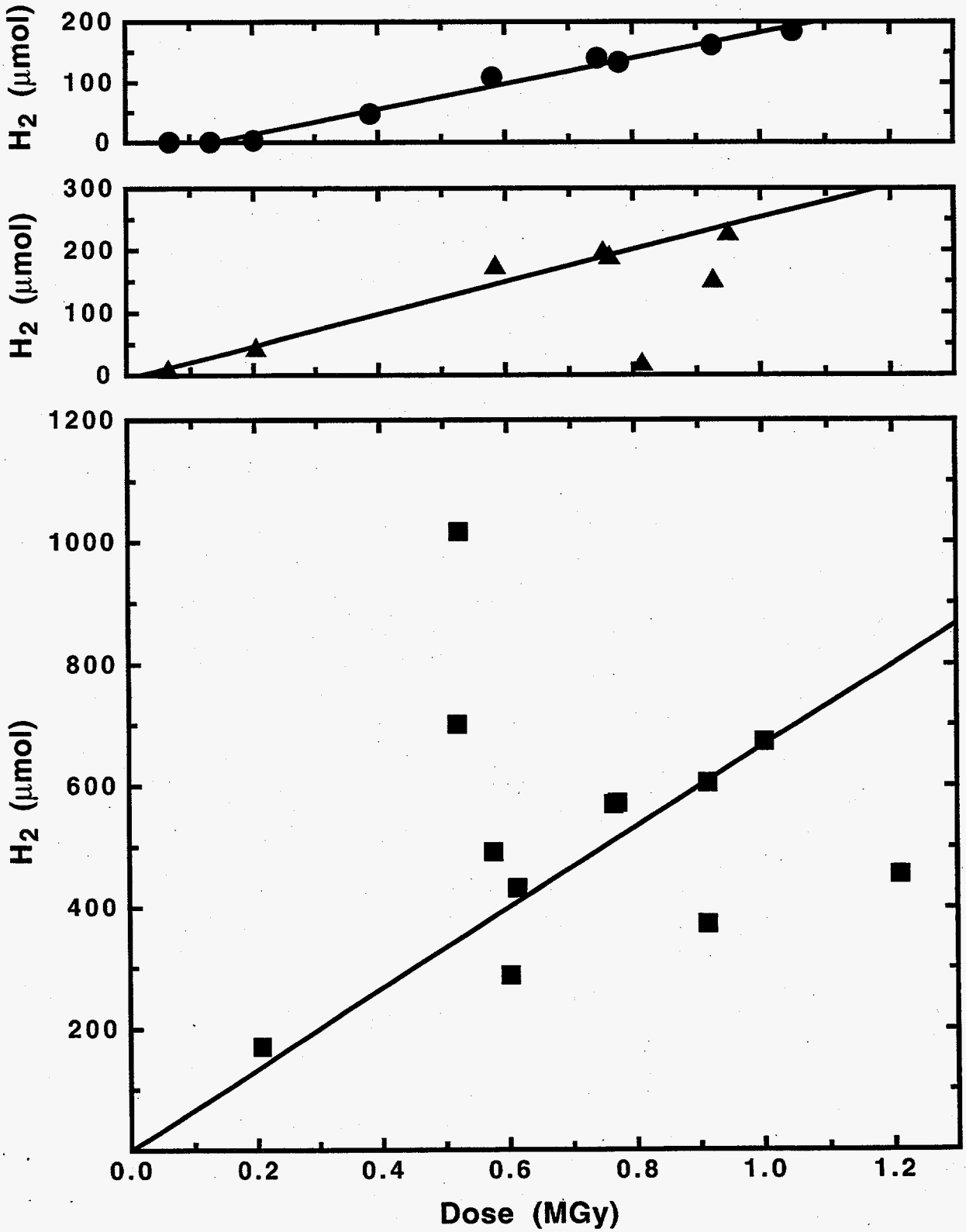

Figure 2.2. Yield of H_2 Gas from Irradiated Simulant as a Function Dose at 50 °C (●), 70 °C (▲) and 90 °C (■). 1 MGy = 100 Mrad.

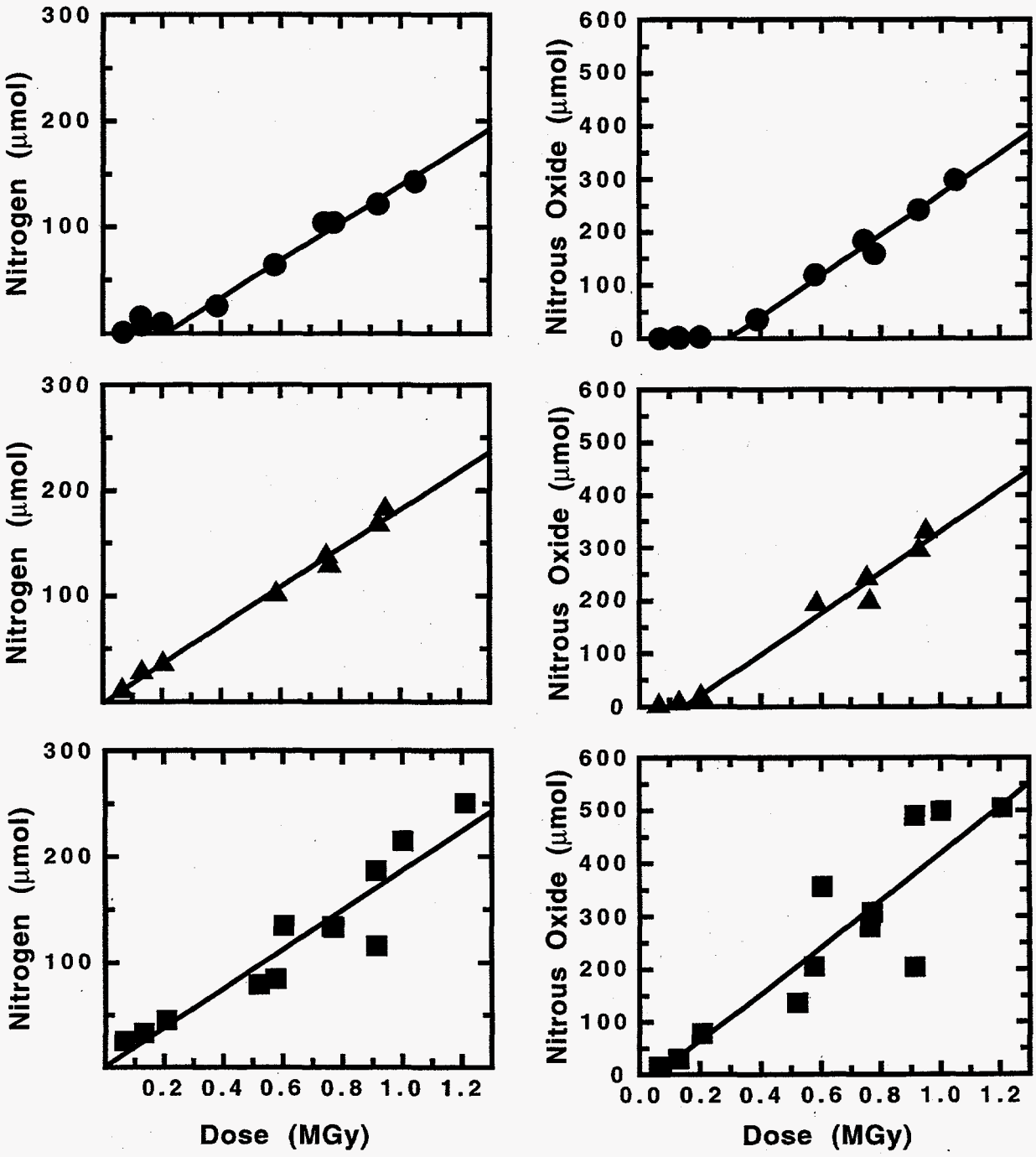

Figure 2.3. Yields of N_2 and N_2O Gases from Irradiated Simulant as a Function of Dose at 50 °C (●), 70 °C (▲) and 90 °C (■). 1 MGy = 100 Mrad.

Table 2.2. Rates of Production and Radiolytic Yields for Major Gases Produced by Radiolysis of SY-SIM-94C

	H_2			N_2			N_2O		
T (°C)	Rate[a] (M/MGy)	G[b]	% err	Rate[a] (M/MGy)	G[b]	% err	Rate[a] (M/MGy)	G[b]	% err
50	0.0141	0.09	5.3	0.0118	0.075	7.3	0.0217	0.14	7.5
70	0.0172	0.11	8	0.0122	0.077	3.5	0.0259	0.17	11
90	0.0444	0.28	15	0.0124	0.079	11.4	0.0295	0.19	16

[a]Moles of gas in headspace per liter of simulant per megagray of radiation
[b]Units of molecules/100 eV

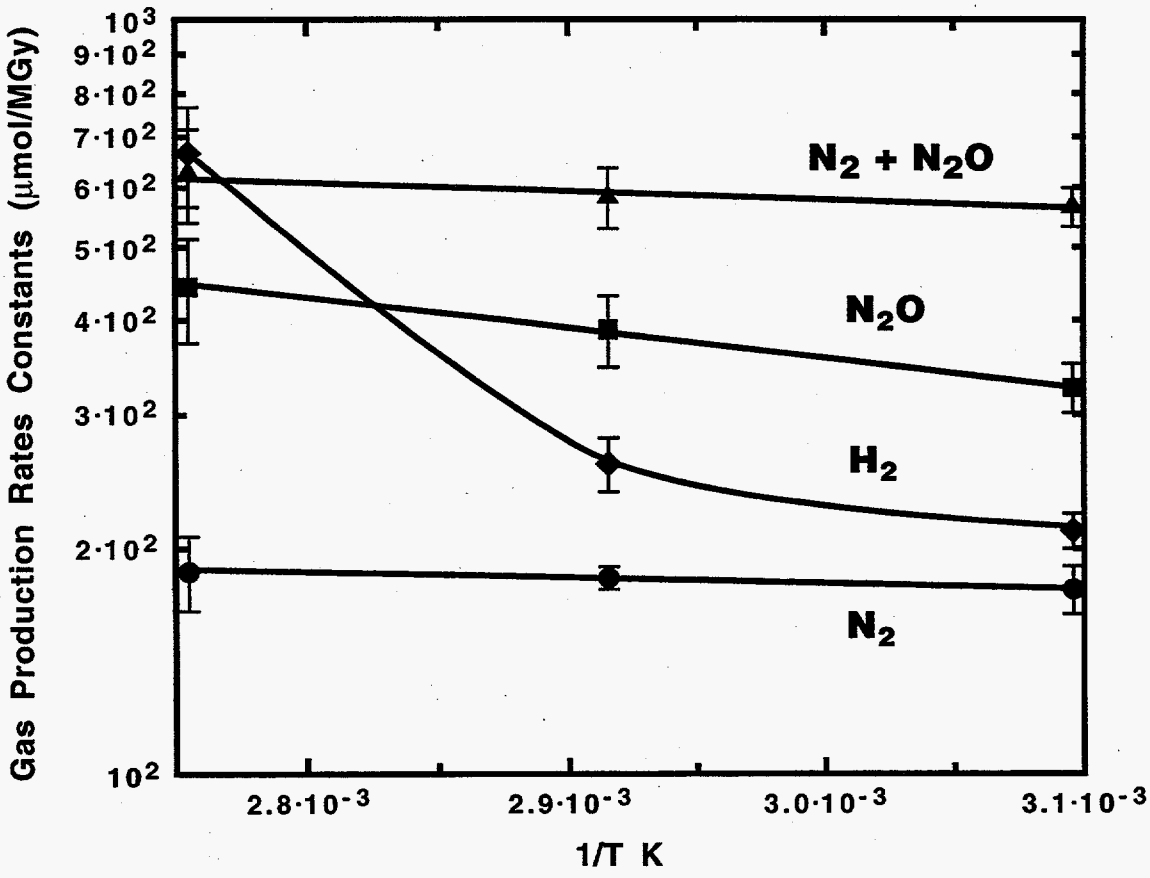

Figure 2.4. Plots of Formation Rate Constants k vs. 1/T in K for H_2, N_2, and N_2O.

As shown in Figures 2.2 and 2.4, production of H_2 increases markedly from 70 °C to 90 °C. Scatter in the data is also much greater at 90 °C. This behavior is attributed to the initiation of thermal pathways for generating hydrogen from organic degradation products. Meisel et al. (1991b, 1992, 1993) found that irradiation of simulated wastes containing glycolate, EDTA, HEDTA, and citrate showed enhanced subsequent production of H_2 during thermal treatment.

they suggested that radiolytic degradation of chelators produced formaldehyde and glyoxylate, which decompose thermally H_2.

Figure 2.3 shows that, after an induction period, production of nitrogen-containing gases obeys a zero-order kinetic rate law, m=kD, where m is moles of a gas in the headspace and D is dose. N_2O is produced in greater amounts than N_2. Ratios of N_2 to N_2O approach ~0.5 at higher doses and decrease with increasing temperature. As a result, Arrhenius activation energy (Figure 2.4) is larger for N_2O production than for N_2 production. The activation energies are 7±3 kJ/mol for N_2O and 1±3 kJ/mol for N_2. The smallness of these barriers is in accord with the mechanism offered by Meisel et al. (1993) in which N_2 and N_2O gases derive from radiolytically-generated organic radicals and NO, (Equations 1 to 5).

$$\gamma + \text{waste} \rightarrow\rightarrow\rightarrow NO + R_2CH\bullet \quad (2.1)$$

$$R_2CH\bullet + NO \rightarrow R_2CHNO \quad (2.2)$$

$$R_2CHN{=}O \rightarrow R_2C{=}NOH \quad (2.3)$$

$$R_2C{=}NOH + H_2O \rightarrow R_2C{=}O + H_2NOH \quad (2.4)$$

$$H_2NOH + NO_2^- \rightarrow\rightarrow [HO\text{-}N{=}N\text{-}OH] \rightarrow N_2O + H_2O \quad (2.5)$$

$$\downarrow$$

$$N_2 + 2\,HO\bullet$$

According to this mechanism, the combined yields of N_2 and N_2O are dependent on the production of oximes; whereas, the relative amounts of N_2 and N_2O depend on how hyponitrous acid (HO-N=N-OH) partitions. Meisel et al. (1993)proposed that the oximes originate from combination of radiolytically-generated NO and organic radicals.

We ran control experiments were run to examine how organic compounds in the simulant might promote the generation of gases. Table 2.2 compares results of these runs and the SY1-SIM-94C runs with and without irradiation. In experiments B4 through B6 the inorganic portion of the simulant contained a small amount of citrate, which had been added as zirconium citrate. It amounted to 1/70th the molar amount of the total organic constituents in the SY1-SIM-94C simulant. Amounts of nitrogen-containing gases in runs B4 to B6 were 10% to 25% of the amounts obtained from irradiated SY1-SIM-94C runs. Hydrogen gas yields were similarly smaller. Runs B1 to B3 with SY1-SIM-94C and no radiation produced very little gas. These results clearly show synergy between radiation and organic compounds in promoting gas production.

Table 2.3. Effects of Reaction Variables on Gas Production and Oxygen Consumption

Conditions	Expt no.	T °C	Dose MGy[a]	H_2	CH_4	N_2	N_2O	O_2[b]
				μmol				
High Flux	11	50.5	0.78	133	4	105	160	72
High Flux	15	50.4	0.75	140	4	104	184	94
High Flux	12	70.0	0.75	195	6	137	242	71
High Flux	14	68.0	0.76	187	6	128	198	65
High Flux	13	90.4	0.77	572	11	133	308	78
High Flux	10	91.1	0.77	700	7	134	281	85
High Flux	6	92.4	0.58	432	11	85	206	74
Low flux	29	88.4	0.61	1017	32	216	151	25
Low flux	X2	18.9	0.61	55	1.4	61	56	124
No Irradiation	B1	49.7	0	0.08	0.7	18	0.1	155
No Irradiation	B2	70.0	0	0.08	0.7	18	0.1	155
No Irradiation	B3	90.6	0	5	0.6	16	0.3	32
low TOC[c]	B4	50.0	0.73	12	1	24	89	181
low TOC[c]	B5	70.2	0.81	16	1	39	67	129
low TOC[c]	B6	88.4	0.81	16	3	21	35	86
No O_2	31	91.0	0.52	455	7	83	163	0.2
No O_2	32	83.6	0.93	297	5	67	172	0.5
No O_2	34	89.1	0.71	447	6	80	156	0.3
No flux, no O_2	X1	50.0	0	0.3	1	37	0.1	2

[a]1 MGy = 100 Mrad

[b]192 μmol at start of run

[c]Organic carbon only present as 0.01 M citrate

Oxygen in the headspace above the simulant was consumed in both the presence and absence of radiation (compare runs 11 through 13 with B1 through B3 in Table 2.3). Figure 2.5 plots headspace oxygen levels in μmols as function of dose and temperature. Oxygen levels in the headspace decreased to a non-zero steady state during irradiation at 90 °C. Although 50 °C and 70 °C runs were not observed long enough to attain steady state, the disappearance data from these runs are well fit by assuming exponential decay to a steady-state level of O_2 . Rates of disappearance and steady-state levels increased markedly with temperature. Fitted rate constants and equilibrium O_2 levels are 1.1 MGy^{-1} and 9.8 μmol at 50 °C, 3.2 MGy^{-1} and 57.9 μmol at 70 °C, and 18.8 MGy^{-1} and 77.1 μmol at 90 °C. These equilibrium levels correspond to 5%, 30%, and 40% of the starting amount of O_2 in the reactor headspace.

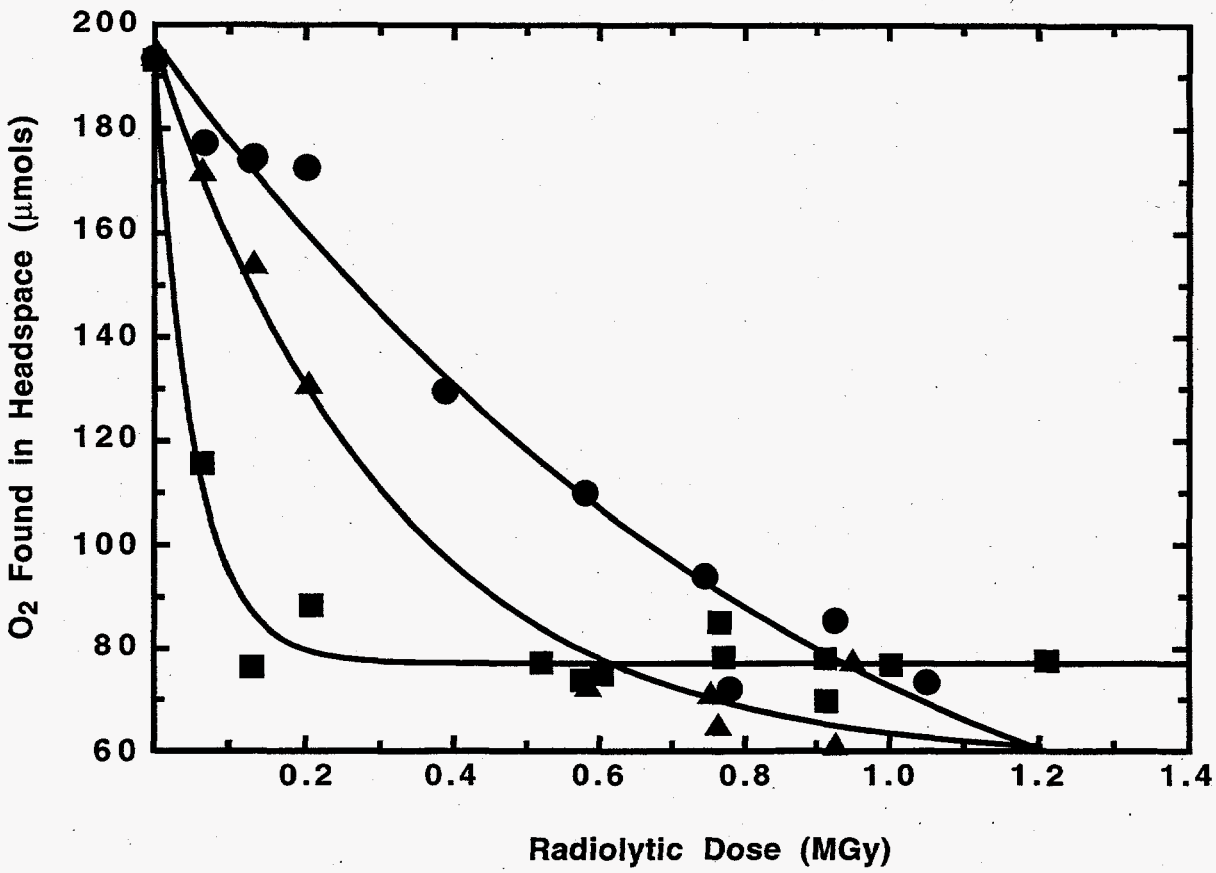

Figure 2.5. Plots of Oxygen Levels in the Reactor Headspace as a Function of Radiation Dose at 50 °C (●), 70 °C (▲) and 90 °C (■). Fitted lines correspond to the equation, $y = (y_o - y_{ss})e^{-k*dose} + y_{ss}$, where y_o and y_{ss} are initial and steady-state O_2 levels. 1 MGy = 100 Mrad.

In a simple reversible reaction (A⇆B) the steady-state level is the level at which the rates of consumption and production are equal. Runs 31, 32, and 33 (Table 2.3) tested whether steady-state O_2 levels could be reached by starting without O_2. Oxygen production in these runs was much slower than the rates of disappearance in runs starting with 21% O_2 in the headspace. Perhaps it should not be surprising that the chemical kinetics are much more complex than those of a simple reversible reaction, given the complexity of the simulant and of radiolytic processes in general.

Experiments run in the absence of radiation provide additional evidence that the oxygen steady-state levels are due to radiolysis. The concentration of oxygen decreased to well below the steady-state concentration reached during irradiation. The disappearance in a given interval of time is dependent on the temperature of the reaction, as is seen in experiments B1 to B3, in which the only variable was temperature. Approximately 84% of the initial oxygen was consumed at 90 °C in 11 days, which is the time needed for a sample to receive a dose of 0.80 MGy in the γ–facility.

Small quantities of other gases (RH in Table A.2) were detected in the mass spectrometric analyses, but the ions could not be unambiguously assigned. To learn the identities of these gases,

we analyzed headspace gases from run 4 by GC/MS according to the procedure of Stromatt (1989). Butanol was present at 0.2 mg/L and hexone at 4.4 mg/L in the vapor phase. Butene and acetone, the possible products of TBP and hexone decomposition, which have been identified in the vapor of Tank 241-C-103 (Huckaby and Story 1994), were evidently below detection limits.

2.1.4 Condensed Phase Results

Table A.3 contains condensed-phase analytical data for all irradiated samples. Only the data for EDTA and citrate lend themselves to kinetic analysis. Data for the disappearance of hexone, dodecane, and stearate are inconsistent and scattered. Control experiments indicate that current analytical methods can provide excellent recoveries of these compounds from the unirradiated simulant. These compounds are not expected to be soluble in the aqueous phase of the simulant. Therefore, sampling errors caused by inhomogeneity may account for the scatter.

Destruction of TBP was nearly complete at all irradiation times (Table A.3). Interestingly, TBP disappeared from the simulant more rapidly than expected even while stored at 4 °C (see last entries of Table A.3). The rate of hydrolysis was ~4 mg/L/h. By comparison hydrolysis of pure TBP in 1.0 M NaOH was estimated to be ~0.1 mg/L/h from rate data in Burger's (1955) report.(1) It was not clear why TBP was more reactive in this simulant.

Recovery of DBP from the unirradiated simulant was only 6% by the derivatization GC-MS method. Ion chromatography could not be used because of interference by high nitrite concentrations. Therefore, analytical data for DBP in irradiated samples are not discussed. Section 4.0 describes aging studies of DBP in a less complex simulant using ^{31}P NMR and ion chromatography.

The disappearances of EDTA and citrate from the condensed phase fit the first-order kinetic rate law, $A=A_oe^{-kD}$ (Figures 2.6 and 2.7. The radiation doses necessary to reduce the concentration of EDTA in the simulant by half were 0.63 MGy at 50 °C, 0.51 MGy at 70 °C, and 0.41 MGy at 90 °C. Citrate was much less reactive, requiring 5.9 MGy at 50 °C, 4.4 MGy at 70 °C, and 2.6 MGy at 90 °C to reduce its concentration by half. The greater reactivity of EDTA relative to citrate is consistent with the greater number of C-H bonds in EDTA. Statistically, one would expect an EDTA:citrate reactivity of 3:1. However, all of the hydrogens in EDTA are bonded to carbons adjacent to amine groups. Therefore, EDTA hydrogens may show enhanced reactivity towards electrophilic radicals relative to citrate hydrogens.

---

(1) The hydrolysis rate at 4 °C was estimated from data in Table IV of Burger's report (1955) by fitting ln (rate) vs. 1/Tto a second order polynomial. Data are provided for hydrolysis of pure TBP at 30°, 40°, 50°, 60°, 70°, and 100 °C. To estimate the hydrolysis rate at other temperatures, the data were fit to the following equation:

$$\ln(R) = 54.8 - 2.55 \times 10^4 (1/T) + 2.69 \times 10^6 (1/T)^2$$

where T is the temperature in K, R is the rate in mg/L/h. The equation is the Arrhenius equation with a quadratic term added to better fit the dependence. Curvature in the Arrhenius plot is understandable because the hydrolysis rates are not corrected for solubility, which also changes with temperature. TBP diluted in dodecane may hydrolyze more slowly. The data in Burger's report also show that hydrolysis rates for 20% TBP in kerosene are ~60% slower than pure TBP at 60 °C.

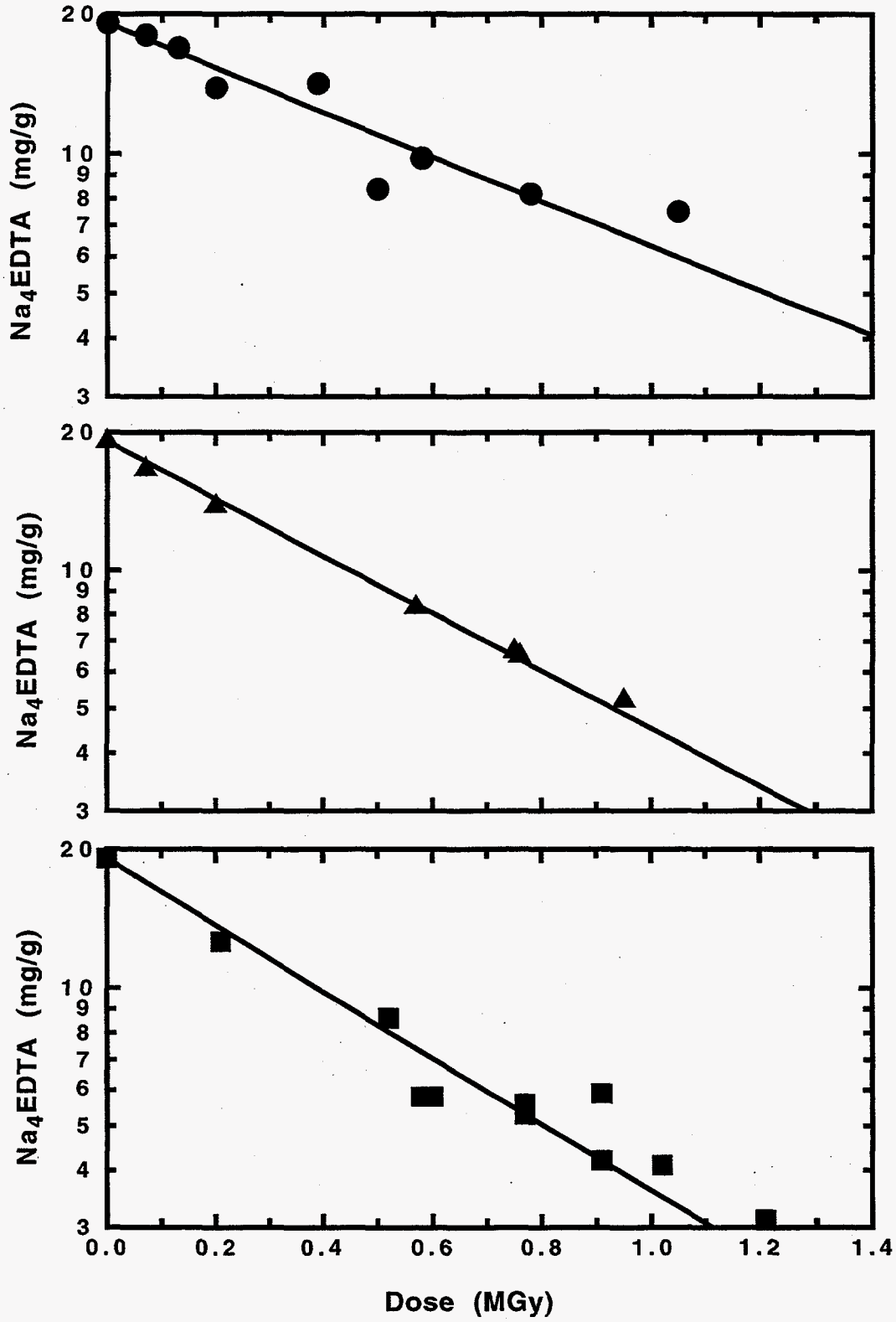

Figure 2.6. First-Order Kinetic Fits to Disappearance of EDTA in the Irradiated Simulant as Function Dose at 50 °C(●), 70 °C (▲) and 90 °C (■). 1 MGy = 100 Mrad.

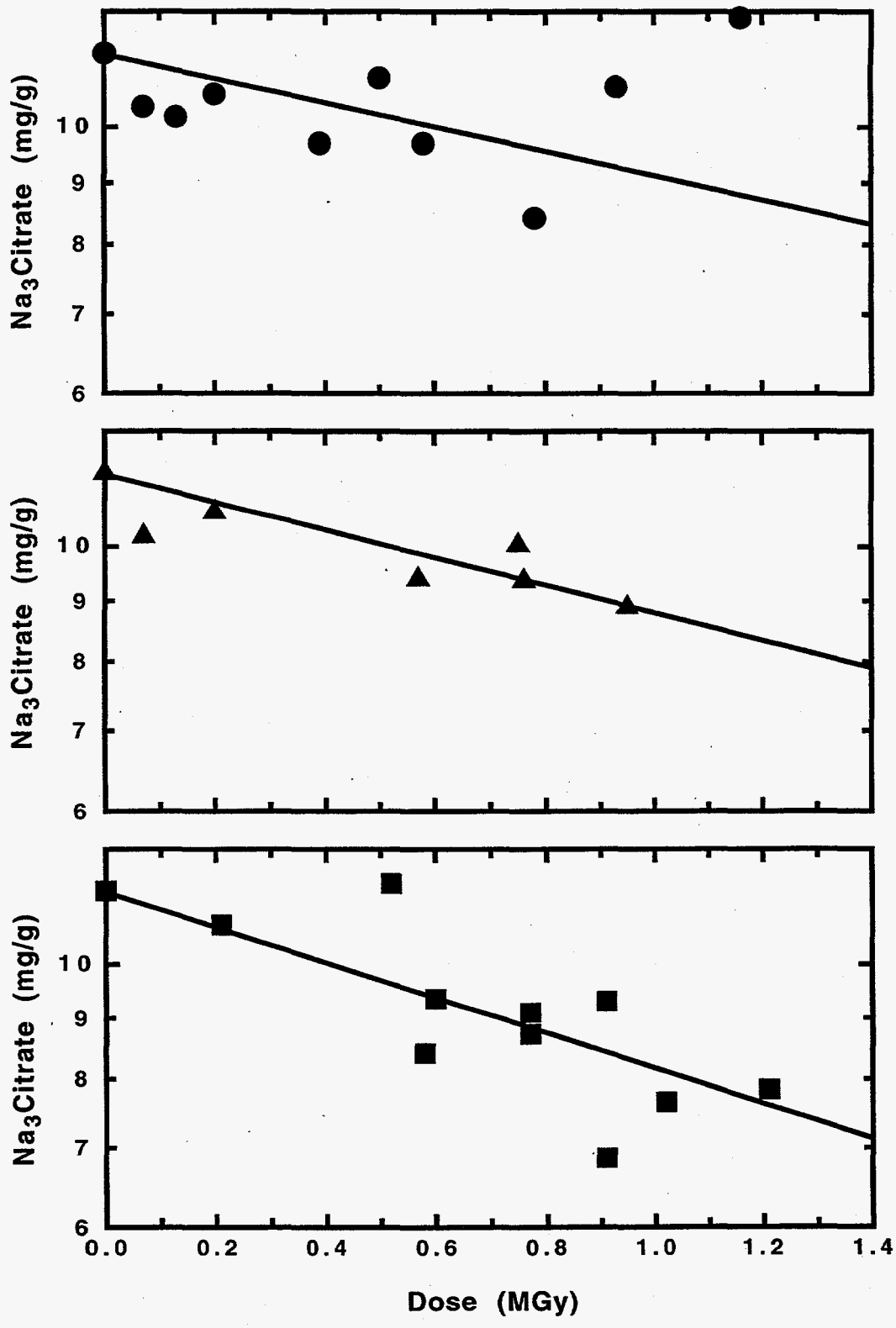

Figure 2.7. First-Order Kinetic Fits to Disappearance of Citrate in the Irradiated Simulant as Function Dose at 50 °C (●), 70 °C (▲) and 90 °C (■). 1 MGy = 100 Mrad.

Figure 2.8 plots the disappearance rate constants vs. inverse temperature (K) for EDTA and citrate. Least-squares fits of the standard error-weighted rate constants yielded activation energies of 9.7±2.5 kJ/mol for EDTA and 18.9±8.7 kJ/mol for citrate. These small activation energies are consistent with attack on these compounds by radiolytically-generated nonselective reactive intermediates, such as H•, O-•, and NO_3•.

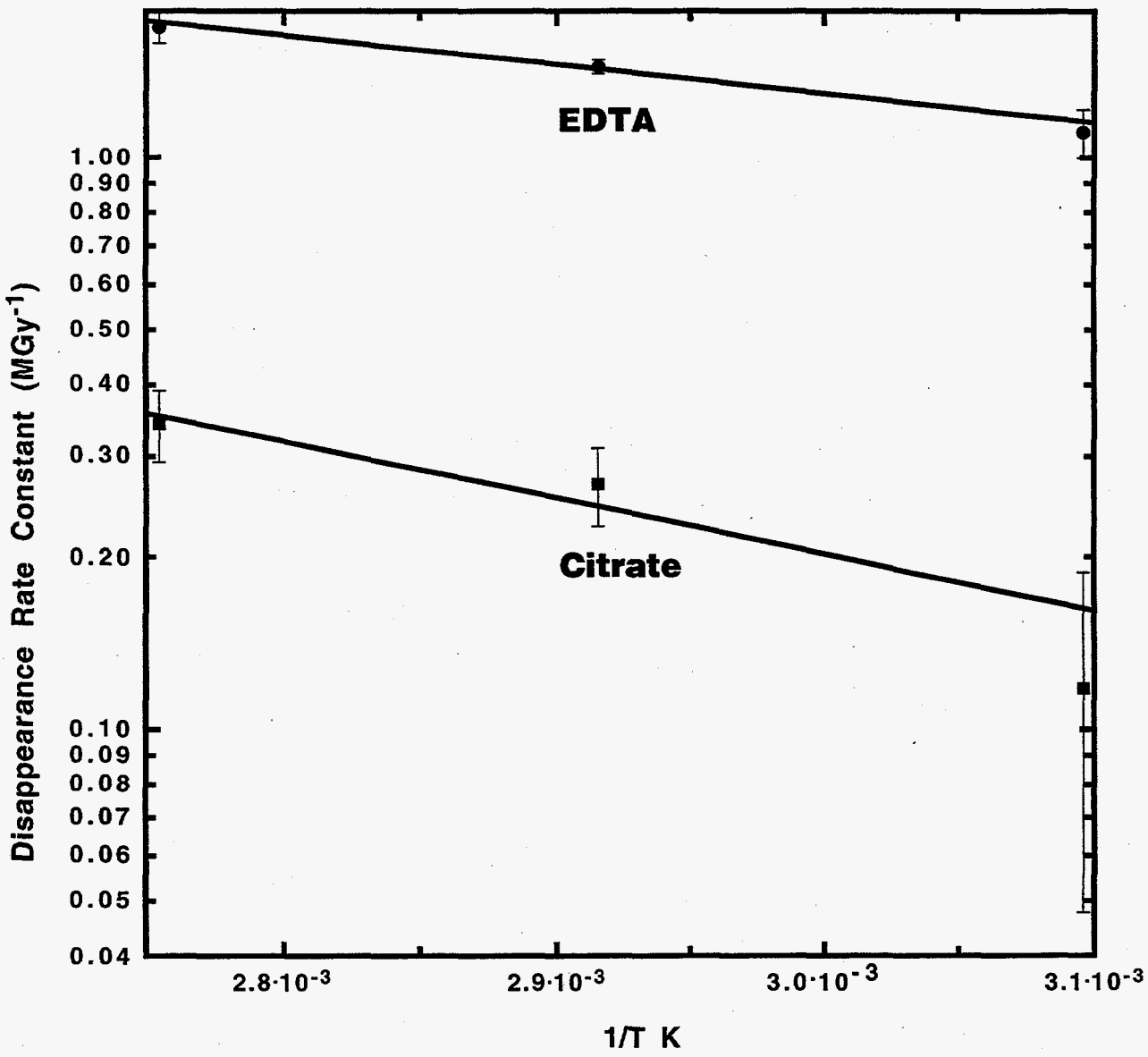

Figure 2.8. Plots of Pseudo First-Order Rate Constants (MGy^{-1}) vs. 1/T (°K) for Disappearance of EDTA and Citrate During Simulant Irradiation Experiments

Several solution-phase products have been identified, including dodecanones, heptadecane, isobutyrate, succinate, oxalate, formate, and glycolate. Table 2.4 lists amounts of glycolate, acetate, formate, succinate, and oxalate by IC analyses of the irradiated simulant. We suspect that

docecanones are from dodecane, heptadecane is from stearic acid, isobutyrate is from hexone, and oxalate, formate, and glycolate are from EDTA and citrate. Significant quantities of succinate are found in runs B1, 27, and 28, which received little or no radiation. Of the organic components in the simulant, TBP was consumed consistently and totally during these runs. Thus, TBP and its aging products are plausible sources of succinate.

Table 2.4. Low MW Carboxylates (mg/g) Found in Waste Simulant Aging Runs.

no.	T °C	MGy[a]	Acetate + Glycolate	Formate	Succinate	Oxalate
7	50	0.58	1.1	1.0	3.2	1.3
11	50	0.78	1.0	1.0	2.7	1.8
15	50	0.5	1.4	1.4	3.6	2.2
B1	50	[b]	0.3	0.3	3.1	0.5
19	90	0.52	2.1	1.8	4.6	3.0
22	50	0.39	0.4	0.7	7.1	0.9
26	50	0.13	0.5	0.5	8.0	0.8
27	50	0.07	0.5	0.4	7.5	0.6
28	70	0.07	0	0.4	7.3	0.7

[a]1 MGy = 100 Mrad. [b]Run held at 50 °C for 11 d without irradiation.

Generally, our studies used high radiation fluxes to simulate aging of waste over 1 to 14 days, times that are experimentally and programmatically practical. We ran a few experiments to assess the effect of flux. In these experiments, similar doses were delivered over 90 to 104 days. Only two experiments (29 and 6) run at 90 °C are directly comparable. The simulant received a dose of ~0.6 MGy in each experiment although the flux differed by a factor of 12. Levels of EDTA, the kinetically best behaved of the simulant organic compounds, were similar at high and low fluxes: 5.8 and 7.5 mg/g, respectively. Stearate and hexone levels were similar in both runs, but less citrate was present after the low flux run (8.4 vs. 3.4 mg/g) as would be consistent with a thermal contribution (Ashby et al. 1994) to its degradation at longer times. The gas data also correspond. The combined yield of N_2 and N_2O in the low flux run is 1.24 times that for the high flux run; and H_2 after the low flux run is 2.35 times greater than after the high flux run. Greater thermal contributions to H_2 yields are expected (Meisel et al. 1993; Ashby et al. 1994). These few results provide tentative evidence that the radiolytic degradation of organic compounds may scale with flux. Clearly, additional study is needed.

In summary, thermally- and hydrolytically-stable waste components, EDTA, citrate, hexone, and NPH undergo radiation-induced degradation. The observed gaseous and condensed-phase products and supporting published data (Bryan et al. 1996, Bryan and Pederson 1996, 1995, 1994, Meisel et al. 1991b, 1993, Camaioni et al. 1994, Ashby et al. 1994), support the concept that the organic compounds in the tank wastes are degrading by oxidative processes. Radiolytic degradation rates depend mainly on the strength (flux) of the radiation field and, to a lesser extent, on temperature.

2.2 Experimental Section

All chemicals used in this study were purchased from Aldrich Chemical Company, Eastman Kodak, or Baker Chemicals. The purity of the chemicals was reagent grade or better, and they were not further purified. A high-shear mixer (Poyltron™ PT6000, Brinkman Instruments Inc., Westbury, NY), was used to mix the simulant. The mixer speed was ~6000 rpm. Water used for preparing the simulant was deionized by a Milli-Q™ Deionization System (Millipore Corporation, San Francisco, CA).

2.2.1 Simulant Preparation

The simulant used in this portion of the study is designated SY1-SIM-94C (see Table 2.1). The simulant was prepared by first dissolving the total amount of sodium hydroxide in 700 mL of water. Sodium aluminate was added slowly, with stirring. The remainder of the inorganic constituents were weighed and added successively to the mixture with periodic mixing to homogenize the ingredients. The organic constituents were weighed into a separate container and then combined with the inorganic mixture. Finally, the remainder of the water was used to wash the organic residue into the complete simulant, which was mixed for an additional 10 minutes. The resultant light-green solution had the appearance and consistency of a milk shake. The simulant was stored in a tightly capped polyethylene jar at ~4 °C.

2.2.2 Irradiation

Sample irradiation experiments were performed in the γ–irradiation facility at Pacific Northwest National Laboratory. The facility contains 37 stainless steel irradiation tubes in a 2.13-m-diameter by 4.19-m-deep stainless steel in-ground tank. Two arrays of ^{60}Co γ-sources with a combined inventory of 1.184×10^{16} Bq are near the bottom of the tank. For radiation shielding purposes, the tank is completely filled with water, and a concrete wall, 1.1 m in height, surrounds the top of the tank. The irradiation tubes, which are sealed on the bottom, range in length from 4.9 to 5.5 m, and in diameter from 4.6 to 5.1 cm. The irradiation fluxes of the tubes range from 2 to 2×10^4 Gy/h. The uniform flux region is 15.2 cm from the tubes closest to the sources and more than 30.5 cm from the tubes farthest from the sources.

Vessels of the simulant are manually lowered into the irradiation tubes to the desired flux, where they are left for a specific length of time to attain the required exposure. Because no nuclear activation products are produced by γ–irradiation, the samples and sample vessels can be transported to other facilities for examination after being removed from the tubes.

Other ancillary equipment at the γ–irradiation facility increases the repeatiblity of thermal control and sampling procedures. The gas-manifold system connects reaction vessels to the initial headspace gas source, pressure monitoring equipment, and a port for headspace vapor removal. The data logger controls both the automated temperature and pressure measurements of the reaction vessels.

2.2.3 Reactor Vessel

The reactor vessel for this study was made from 1.59 cm inner-diameter 316 stainless steel pipe. One end was sealed by welding a plate of 316 steel to the pipe. The other end was welded to a flange, 1.59 cm inner-diameter by 3.49 cm outer-diameter. The reactor cover has two openings. One opening was fitted with a 0.16 cm Swagelok™ fitting (Swagelok Company, Solon, OH) to connect to the gas manifold via small-diameter stainless steel tubing. The other opening was fitted with a 0.32 cm Swagelok™ fitting through which a K-thermocouple was inserted 15.2 cm into the body of the reactor from the top of the flange. The volume of the vessel to the top of the flange was approximately 30 mL.

The reactor vessel was heated to operating temperature by heating tape that had been wrapped around the outside of the vessel. The internal temperature of the reaction vessel was maintained by feedback control to minimize thermal gradient problems (Bryan and Pederson 1994). Reaction vessel temperatures and pressures were monitored using a data logger.

2.2.4 Filling and Placing the Reactor

The simulant was removed from storage at ~4 °C, warmed to room temperature, and resuspended by mixing with the high-shear mixer. An aliquot of 15 mL was measured out and transferred to the reactor. The reactor was then sealed and transported to the γ-irradiation facility.

The staff at the γ-irradiation facility performed all the experiments according to a set procedure (Table 2.5). Valves and other equipment listed in Table 2.5 refer to features on the gas manifold system. The procedure involves purging the gas manifold lines, purging and venting the vessel, leak testing, heating the vessel to temperature, placing the vessel into an irradiation tube, monitoring pressure and temperature during the course of the reaction, sampling the reaction, and removing the reactor from the facility. This procedure is similar to the one developed by the Flammable Gas Safety Program (Bryan and Pederson 1994) except that the vapor was collected in our experiments before the reactor was cooled to room temperature, and we used a mixture of 79.5% argon and 20.5% oxygen as the gas phase, instead of air, to facilitate analyses of nitrogen gas.

Table 2.5. Procedure for Irradiating the Simulant and Collecting Gas Samples

1. Close vent, open purge valves, and turn on headspace gas mixture for 10 min
2. Close purge valves and turn off gas
3. Open vent
4. Hook up vessels; close vent
5. Open gas (oxygen/argon) inlet (2.7 atm)
6. Slowly open purge valves; let the vessel sit for 5 to 10 min; leak check fittings on the lid with leak detector solution
7. Take readings of temperature and pressure; close purge valves; open vent; let the vessel sit for 30 to 60 min
8. Take pressure readings to verify that the vessel does not leak
9. Slowly open each purge valve until bubbles are gone; close purge valves
10. Turn gas on and vent manifold; close vent
11. Slowly open purge valves; let the vessel sit for 5 to 10 min
12. Close purge valves; close gas inlet
13. Open vent
14. Repeat steps 6 to 10

Table 2.5. Continued.

15. Repeat 6; take readings, including pressure
16. Repeat 7 and continue at step 17
17. Open purge valves slowly and wait until the pressure reaches ~2.7 atm; let the vessel sit for 5 to 10 min
18. Take readings; close purge valves
19. Close gas supply; open vent. Shut off regulator
20. Leave vessel at pressure overnight
21. Check pressures
22. If pressures are OK, then open vent; slowly open each purge valve until bubbles are gone
23. Close purge valves
24. Connect thermocouple and heat tape to temperature controller; place vessel in the pit if irradiating
25. Bring vessel up to temperature slowly; stabilize at temperature for 1 to 2 hours
26. Take readings and start data logging
27. Record time and pressure before gas sample is collected
28. Discontinue heating of the vessel and remove it from the γ-irradiator
29. Seal reactor and disconnect it from the gas manifold
30. Remove the sample from the reactor and clean the vessel

2.2.5 Gas Collection and Analyses

The vapor phase of the reaction was removed at the end of the irradiation time at temperature. A stainless steel sample vessel evacuated to between 2×10^{-6} atm and 5×10^{-7} atm was attached to the manifold and filled by opening the gas sampling valve for 5 min, closing it, and then removing the vessel from the manifold. The vapor was later analyzed according to the procedure by Goheen (1988). Total moles of gases produced were calculated from the measured pressure and temperature, and the known total volume (24 mL) of the gas phase of the reaction vessel and gas manifold lines. Concentrations (mol%) of individual components in the gas sample were determined by mass spectrometric analyses. The quantities of specific gases generated were calculated from the total moles of gas generated and the mole fraction data.

No attempt was made to extract product gases that were either dissolved in the simulated waste mixtures or present as gas bubbles. For all product gases except ammonia, which has significant solubility in the concentrated simulant mixtures (Bryan and Pederson 1994), this approach should result in negligible errors. Solubilities of H_2, N_2, and N_2O are lower in concentrated brines than in pure water (Schumpe 1993; Bryan and Pederson 1994). Gas bubbles will contribute to the measured pressure in the test vessel, much as if the bubbles were brought to the slurry surface and eliminated, provided that simulant surface tension does not significantly compress the bubbles.

Bryan and Pederson (1994) estimated errors for measurements of H_2, N_2, and N_2O generated from simulated wastes. Among several known contributors to measurement error uncertainty of temperature can be a major contributor. Bryan and Pederson (1994) estimated that for an activation energy of 104.6 kJ/mol, approximately that reported for gas generation and related reactions (Delegard 1980, 1987, Schmidt et al. 1993, Meisel et al. 1993, Ashby et al. 1993, 1994, Person 1993), a 1 °C difference from 90°C would cause a 10% change in rate, a 2 °C difference, a 20% change in rate; and a 5 °C difference, a 60% change. For activation barriers of ~104.6 kJ/mol, this degree of precision leads to a 5% error. Other direct contributors to measurement uncertainties are

mass spectrometry analyses (approximately 2%) and pressure measurements (approximately 1%) (Bryan and Pederson 1994). Variances in volumes of the reaction vessels and the quantities of simulant introduced into the reaction vessels exceed 1%. Bryan and Pederson (1994) estimated the combined errors for 30-mL reaction vessels to be approximately 20% (assuming a 104.6 kJ/mol activation barrier for gas generation). They assumed a 1 °C to 2 °C drift in temperature. The errors for our work are likely ~15%, because the reaction vessels were independently temperature controlled throughout the tests to within ±0.50 °C. The activation barriers for gas-producing reactions of the simulant being studied here are not known at this time. Activation energies smaller than 104.6 kJ/mol would give rise to smaller errors.

2.2.6 Condensed Phase Analyses

After the gas sample was removed, the reactor was cooled to below 35 °C, removed from the manifold, sealed, and transported to another laboratory to retrieve the condensed phase. The lid was removed, and the mixture was stirred with a spatula. For runs 1 through 10, the mixture was divided into two samples of ~7.5 mL. One sample was combined with other washings from the reactor to a total volume of ~20 mL and stored at -2 °C. The other sample was analyzed for the organic constituents. For all other runs, the mixture removed from the reactor (to the extent possible) and analyzed without being divided. This change was made to reduce sampling errors.

Three different analyses were used to quantify the organic starting components and identify degradation products. A flowsheet diagram of the analytical procedures appears in Figure 2.9.

Gas chromatography/mass spectrometry (GC/MS) was used to quantify dodecane, stearic acid, hexone, and TBP. This procedure neutralized the caustic sample with phosphoric acid and extracted with dichloromethane (CH_2Cl_2). Two surrogates, dodecane-d_{26} and palmitic acid, were added before extraction to track the efficiency of the sample preparation procedure. After extraction, diazomethane was added to methylate stearic acid and thereby enhance its volatility for GC/MS analysis. Analyte recoveries for the CH_2Cl_2 extraction and sample preparation procedure were determined by spiking known amounts of the organic analytes of interest into the inorganic portion of the simulant recipe. Triplicate tests gave recoveries of 102% for dodecane, 96% for TBP, and 98% for stearic acid. Average recovery of DBP with this sample preparation method was only 6%. Therefore, this method is not viable for this analyte. Alternatives for analyzing DBP are being pursued under the Advanced Organic Analysis Task. Precision of the GC/MS analysis, as determined through replicate sample injections, had a standard deviation of less than 2% for all analytes.

Ion-pair chromatography (IPC) was the method of choice for the analysis of EDTA. An aliquot of the aqueous layer remaining after CH_2Cl_2 extraction was diluted to a concentration within the dynamic range of the IPC technique. Copper sulfate was added to enhance EDTA detection. Error estimates for sampling and analysis have been determined for EDTA in similar inorganic mixtures (Campbell et al. 1994). Replicate sample preparations and instrument injections produced standard deviations of 5%.

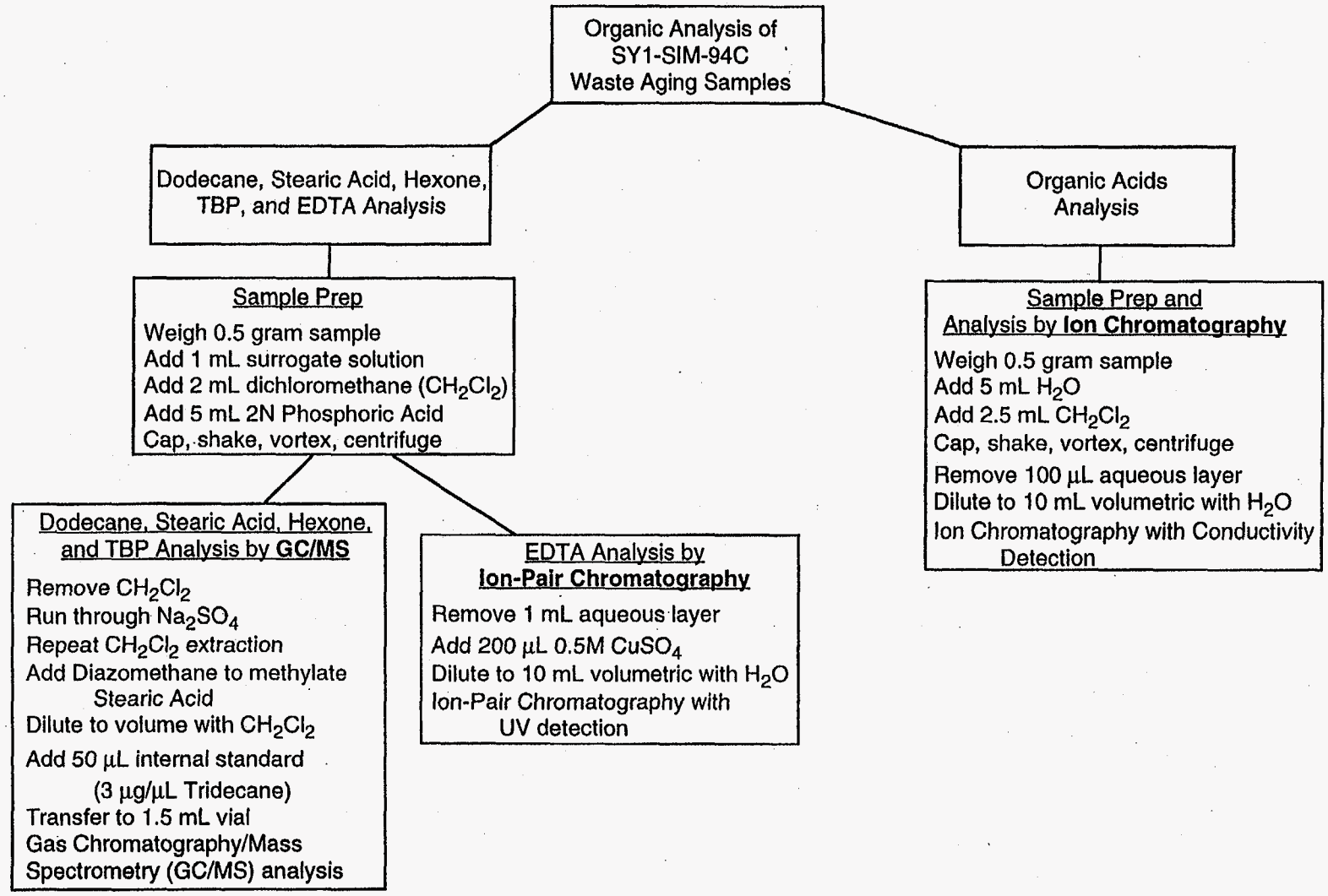

Figure 2.9. Diagram of the Sample Preparation and Analysis Scheme for Simulant Waste Samples

Ion chromatography (IC) with conductivity detection was used to analyze for citrate and products listed in Table 2.4. This technique was developed under the Flammable Gas Safety Project (Campbell et al. 1994) for detection of low molecular weight organic acids in waste tank matrices. Aliquots of the run samples were diluted with water, and dichloromethane was added to remove non-polar organics that may interfere with the IC method. Recovery studies of citric acid spiked into the simulant inorganic matrix yielded a recovery of 97%. Triplicate weighing and sample preparation yielded a sampling error (standard deviation) of 9%. Multiple injections of the same sample yielded a precision of 1%. Therefore, the total error for the IC analysis was 10%.

The sample preparation procedures, in addition to instrumental conditions currently used for GC/MS, IPC, and IC analysis, are described in the following subsections of this report.

2.2.6.1 Gas Chromatographic/Mass Spectrometric Sample Preparation/Analyses

The steps taken to prepare a sample of the simulant for GC/MS analyses are listed in Table 2.6 below.

Table 2.6. Procedure to Prepare Simulant Samples for GC/MS Analyses

1. Weigh 0.5 gram of sample into screw top test tube
2. Add 1 mL of dichloromethane (CH_2Cl_2) that contains 2.5 mg/mL of the surrogates dodecane-d_{26}, and palmitic acid; shake briefly to mix
3. Add 5 mL of 2 N phosphoric acid; a precipitate forms
4. Cap and shake, carefully release pressure on test tube; carbonate in these samples foams during neutralization
5. Centrifuge for 20 minutes at 1500 RPM
6. Remove CH_2Cl_2 layer and run through anhydrous Na_2SO_4 into a 100 mL volumetric flask
7. Repeat extraction (steps 2, 4-6)
8. Save the aqueous layer for EDTA analysis (see Ion-Pair Chromatography analyses)
9. Add diazomethane solution to the 100 mL volumetric flask containing the CH_2Cl_2 extract until the yellow color persists; this methylates the stearic and palmitic acids and DBP
10. Dilute to volume with dichloromethane
11. Transfer 1.5 mL of this solution to an autosampler vial containing 25 µL of 3 µg/µL tridecane internal standard; this sample is ready for GC/MS analysis

The prepared samples were run on a Hewlett-Packard 5970 MSD GC/MS instrument at the column and instrument settings in Table 2.7.

Table 2.7. Column and Instrument Setting for GC/MS Analyses

Analytical Column:	Rtx®-1, 30m x 0.25mm, 0.25 µm film
Head pressure:	5 psi He
Injection Temperature:	260 °C
Interface Temperature:	280 °C
Ion Source Temperature:	200 °C
Oven Temperature Program:	40 °C for 2 min ramp to 280 °C @ 15 °C/min hold for 2 min.

The *m/z* values of the ions chosen to quantify each of the analytes are as follows (compound *m/z*): hexone 58, dodecane-d_{26} (surrogate) 66, dodecane 71, tridecane (internal standard) 85, TBP 99, methyl palmitate (surrogate) 74, methyl stearate 74.

2.2.6.2 Ion-Pair Chromatography Analyses

The sample preparation was the same as that described in Table 2.6 for GC/MS analyses except that 1 mL of the aqueous layer from step 7 was placed in a 10 mL volumetric flask to which 200 µL of 0.5M $CuSO_4$ was added and diluted to volume with water. The solution was analyzed on a Waters high-performance liquid chromatography (HPLC) instrument with columns and conditions listed in Table 2.8.

Table 2.8. Columns and Conditions Used for HPLC Analyses

Guard column:	Adsorbosphere® C-8 cartridge
Analytical Column:	Adsorbosphere® C-8 (25 cm x 4.6 mm, 5-µm particle size)
Flow:	1.5 mL/min
Sample Volume:	5 µL
Detection:	UV, 280 nm, as copper complex
Mobile phase:	0.002 M dodecyltrimethylammonium bromide and 0.05 M potassium dihydrogen phosphate, pH 6.5

2.2.6.3 Ion Chromatography Preparation/Analyses

The steps taken to prepare simulant samples for ion chromatography analyses are listed in Table 2.9.

Table 2.9. Preparation of Simulant Samples for Ion Chromatography Analyses

1. Weigh 0.5 gram of sample into screw-top test tube
2. Add 5 mL of deionized water, and about 2.5 mL of CH_2Cl_2
3. Cap, shake, and vortex the sample tube
4. Centrifuge for 20 minutes at 1500 RPM
5. Remove 0.100 mL of the aqueous layer, place in a 10 mL volumetric, and dilute to volume with deionized water

Ion Chromatography analysis were performed on a Dionex Ion Chromatograph at the columns and conditions listed in Table 2.10.

Table 2.10. Columns and Instrument Settings Used for Ion Chromatography Analyses

Guard column:	Dionex® AG11
Analytical Column:	Dionex® AS11
Anion Suppressor:	SRS 2 mmol
Flow:	2.0 mL/min.
Detection:	Conductivity, @ 10 µS
Mobile phase:	15 mM NaOH

3.0 Irradiation of Simulant SIM-PAS-95-1c

Aging tests were performed using a simulant that was developed for FAI energetics and reactivity tests (Carlson and Babad 1996). The simulant, designated SYM-PAS-95-1c, is a modified version of the SIM-PAS-94 simulant, which Scheele (1995) developed from B-plant chemical inventories and process flow sheets. The results of the tests provide estimates of the distributions of organic compounds in tank wastes that have aged for 15 or more years.(1) This information may then be used to develop simulants for FAI testing that are representative of aged wastes. In addition, the data may be used to test and develop models for predicting how exposure to γ-radiation and temperature alters the organic composition and energetics of Hanford Defined Wastes (Agnew 1996a,b,c).

The simulant used in these tests (Table 3.1) is a heterogeneous mix of metal oxide/hydroxide precipitates and aqueous solutions containing Na_3HEDTA, Na_4EDTA, citrate, and glycolate. The density is 1.27 g/mL and the carbon content is 21 g/L or 4.8 wt% (dry basis).

Table 3.1. Ion Composition of Simulant SIM-PAS-95-1c

Species	mg/g	Species	mg/g	Species	mg/g
$HEDTA^{-3}$	16.9	Al^{+3}	1.493	Ca^{+2}	0.080
$EDTA^{-4}$	3.1	F^-	1.281	Mn^{+2}	0.068
$Citrate^{-3}$	17.3	Pb^{+2}	1.066	Cr^{+3}	0.044
$HOCH_2CO_2^-$	11.3	PO_4^{-3}	0.507	Cl^-	0.004
NO_3^-	109	SO_4^{-2}	0.506	Pd^{+2}	0.003
Na^+	107	Bi^{+2}	0.419	Rh^{+3}	0.003
OH^-	39.3	Ce^{+3}	0.377	Ru^{+4}	0.003
NO_2^-	37.9	Ni^{+2}	0.099	H_2O	640
Fe^{+3}	2.61				

Four aging tests were run, one each at 0.3, 0.5, 1.0 an 1.5 MGy at 70 °C. To foster reproducible results in our aging tests, the simulant was prepared before each irradiation by measuring exact quantities of 3 homogeneous stock solutions into the reactor vessel (see Section 3.3). The same vessel was used for each irradiation, and it was placed in the same location relative to the radiation source. The radiation flux was 3 kGy/h ($3x10^5$ rad/h). After irradiation, the contents of the vessel were quantitatively transferred, and analyzed for organic compounds, carbonate, nitrate, and nitrite. In addition, a control simulant was mixed and then analyzed without having been irradiated. Additional information about experimental methods is in Section 3.3.

(1)Using Sr-90 and Cs-137 single-shell storage tank (SST) inventories from the HDW Model (Agnew 1996b), doses of approximately 0.8 MGy and 1.4 MGy corresponds to 15 and 30 y storage times. The mass of the waste was estimated from the current SST waste volume (35200 kgal) assuming an average density of 1.5 g/mL.

3.1 Results

The results are divided into 2 sections. The first section presents analytical results showing how the distribution organic compounds, nitrate, nitrite, and carbonate change with radiation dose. The second section uses these data to show how organic carbon and nitrate reaction enthaplies (ΔH_{rxn}) of the simulant change with radiation dose. This latter treatment of the data is of particular interest because energy content and TOC are used to assess the likelihood of of propagating reactions in tank wastes.

3.1.1 Effect of Radiation Dose on the Distribution of Organic Compounds, Nitrate, Nitrite, and Carbonate

Table 3.2 lists results of analyses performed on the unirradiated and irradiated simulant. The analytes found in the unirradiated simulant compare well with the composition expected from mixing the stock solutions (see Section 3.3),with the exception for glycolate, which is only ~70 % of the expected amount. The reason for this discrepancy is not known. Carbonate in the unirradiated simulant is the product of CO_2 absorption during preparation of the stock solutions and transfer to the reactor vessel. Its concentration is substantially greater in the irradiated simulants. Some of this may also be attributable to absorption of CO_2 during handling, but much of it is probably a product of radiolysis. Other products derived from the organics include formate, oxalate, and chelator fragments, such as ED3A, NTA, IDA, and EDDA. These compounds have been identified by GC-MS analyses but have not yet been quantified. Acetic and succinic acids are also detected, but in insignificant amounts at all doses. For example, acetate reached a maximum concentration of 0.5 mg/mL (0.007 M) after 1.5 MGy, and the concentration of succinate was 1% of that.

Table 3.2. Concentrations[a] of Reactants and Products in SIM-PAS-95-1c as a Function of γ Dose

Dose (MGy)	CO_3^{2-}	Formic Acid	Oxalic Acid	Glycolic Acid	Citric Acid	HEDTA	EDTA	NO_2^-	NO_3^-
0	1.42			8.34±0.03	15.4±0.1	15.1±0.1	3.1±0.1	39.2	108.3
	0.030			*0.139*	*0.102*	*0.0689*	*0.0136*	*1.08*	*2.15*
0.30	4.51	0.8±0.1	1.7±0.1	7.54±0.11	14.9±0.1	8.7±0.2	2.1±0.1	42.3	102.7
	0.096	*0.022*	*0.024*	*0.126*	*0.0984*	*0.0397*	*0.0090*	*1.17*	*2.04*
0.50	6.56	1.7±0.2	2.8±0.2	6.77±0.02	13.8±0.1	5.1±0.1	1.3±0.1	44.4	98.9
	0.14	*0.048*	*0.040*	*0.113*	*0.0910*	*0.023*	*0.0055*	*1.23*	*1.96*
1.00	13.4	2.5±0.1	3.5±0.2	5.91±0.01	12.6	2.1±0.1	0.9±0.1	49.3	88.2
	0.283	*0.070*	*0.050*	*0.099*	*0.0830*	*0.0097*	*0.0038*	*1.36*	*1.75*
1.50	17.4	4.5±0.2	8.5±0.2	5.30±0.01	11.4±0.1	1.0±0.1	0.2±0.1	22.2	87.1
	0.367	*0.12*	*0.12*	*0.088*	*0.0752*	*0.0045*	*0.0010*	*0.61*	*1.73*

[a]Concentrations of organic acids and inorganic anions given in mg/g and M units (M in italics). Uncertainties are standard deviation for 2 measurements.

Figure 3.1 plots the concentrations of starting organic compounds and products as a function of radiation dose. Lines through the data points are best fits to either exponential or linear rate functions. Clearly the starting compounds, EDTA, HEDTA, and glycolate, are well fit by exponential decay functions. Citrate fits exponential and linear rate functions equally well, because little of it has reacted. The products, oxalate, formate, and carbonate all increase linearly. Although not plotted in Figure 3.1, nitrate decreases and nitrite increases linearly with dose up to at least 1 MGy. At the highest dose (1.5 MGy) the nitrite concentration was lower than at 1.0 MGy and the nitrate was approximately the same.

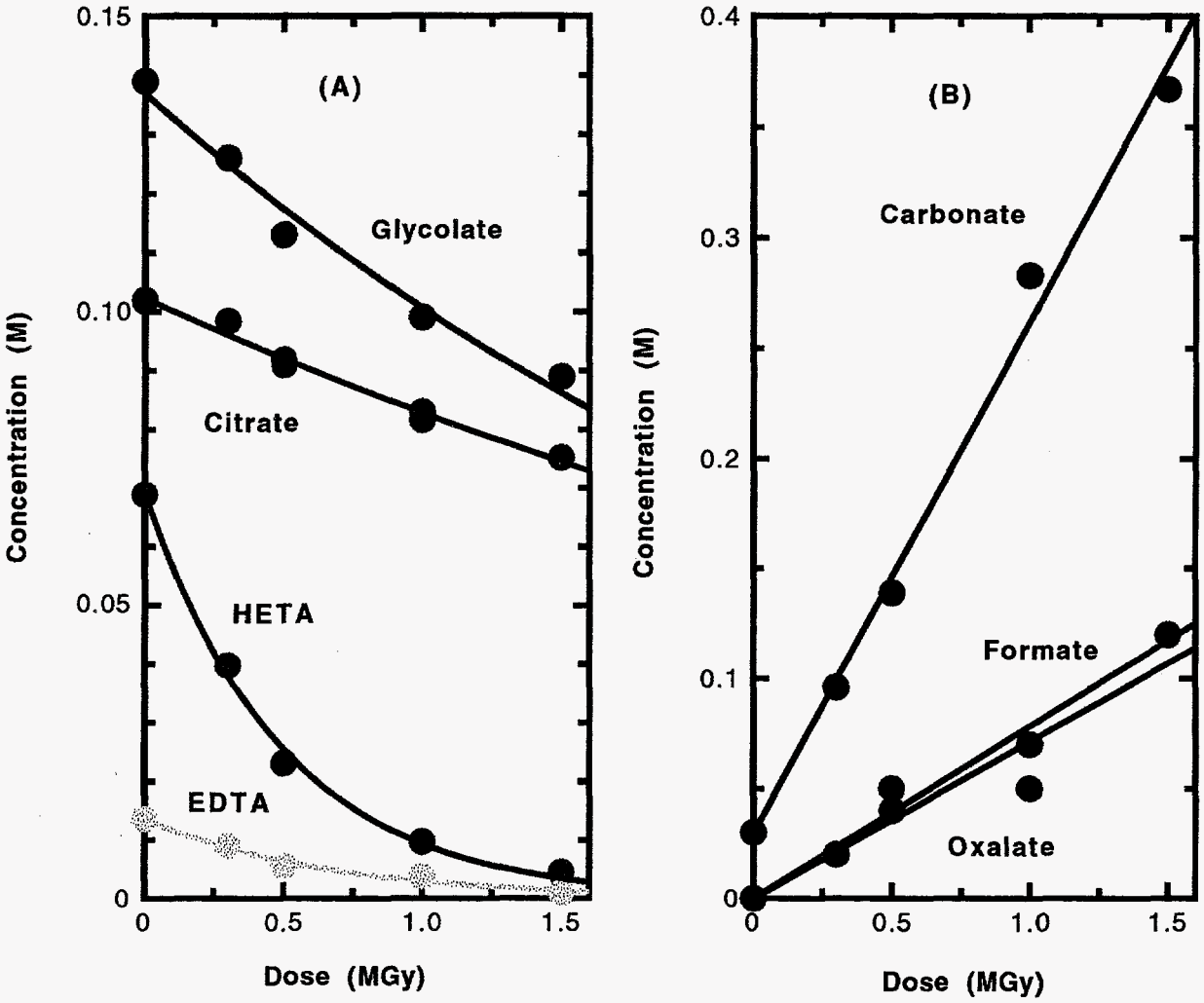

Figure 3.1. Disappearance (A) of Starting Organic Compounds and Appearance (B) of Products vs. Radiation Dose at 70 °C

Rate parameters and radiolytic yields (G) derived from speciation of the reactants and products are presented in Table 3.3. The first column lists the half-dose ($D_{1/2}$) of the starting compounds, i.e., the dose required to lower a compound to half its starting concentration. These values are obtained from fitting the disappearance data to the first order rate equation,

$$A=A_o e^{-kD} \quad (3.1)$$

where D is the dose and $D_{1/2}$ is ln(2)/k. The second column lists the rates of appearance of products and disappearance of nitrate. Nitrogen-containing organic compounds, HEDTA and EDTA are significantly more reactive than glycolate and citrate; concentration normalized relative rates of disappearance are HEDTA: 13; EDTA: 11; glycolate: 2.3; citrate: 1. However, glycolate may be more reactive than the rate constants suggest; because HEDTA, EDTA, and citrate may partly degrade to glycolate. The absolute and relative reactivities of EDTA and citrate are similar to the reactivities observed in aging studies of SY1-SIM-94C (see Section 2.0). Thus, the rate constants for reaction of these compounds may not be strongly affected by the presence or absence of other organic compounds.

Table 3.3. Kinetic Rate Constants and Radiolytic Yields Exhibited by Reactants and Products in SIM-PAS-95-1c

Compound	$D_{1/2}$[(a)] (MGy)	Initial Rate (M/MGy)	Radiolytic Yield, G[(b)]
HEDTA	0.38	-1.25	-1
EDTA	0.46	-0.021	-0.16
Glycolate	2.2	-0.043	-0.33
Citrate	3.3	-0.014	-0.11
Carbonate		0.25	1.9
Oxalate		0.073	0.55
Formate		0.080	0.6
Nitrate		-0.40	-3.0
Nitrite		0.28	2.1
Inorganic N		-0.061	-0.9

(a)Dose required to react half of the compound in the simulant mixture
(b)Molecules/100 eV; values for HEDTA, EDTA, glycolate, and citrate are derived using initial rates.

The fourth column of Table 3.3 lists Gs for the disappearance of starting compounds and appearance of products. The Gs for product formation are significant: ~1 for oxalate and formate and ~3 for carbonate and nitrite. Nitrate, with a G of ~-3, disappears faster than nitrite appears. The G for loss of inorganic nitrogen is -0.5. Results of aging studies of other simulants (Section 2 of this report; Meisel et al. 1993; Bryan and Pederson 1995, 1994; Lilga et al. 1996; Ashby et al. 1994; Barefield et al. 1996) and actual wastes (Person 1996; Bryan et al. 1996), suggest that this nitrogen is probably converted to N_2, N_2O, and NH_3. For comparison, G of 0.25 for combined production N_2 and N_2O was obtained from irradiation of SY1-SIM-94C at 70 °C.

3.1.2 Effects of Radiation Dose on TOC and Nitrate Reaction Energies

Figure 3.2 and Table 3.4 show how the radiolytic dose affects the concentrations of organic carbon in the simulant. The figure plots the concentrations of carbon in the starting compounds (glycolate, citrate, ETDA, HEDTA), oxalate, and formate carbon, and carbon in other organic compounds (e.g., NTA, ED3A, IDA, EDDA). The smooth lines through the data points are the concentrations predicted by the rate parameters listed in Table 3.3. Table 3.4 provides a more detailed distribution of carbon as a function of radiolytic dose. Although the other organic compounds have not been quantified, their total concentration is estimated here as the difference between the total carbon initially present and the sum of carbon in speciated compounds including carbonate.

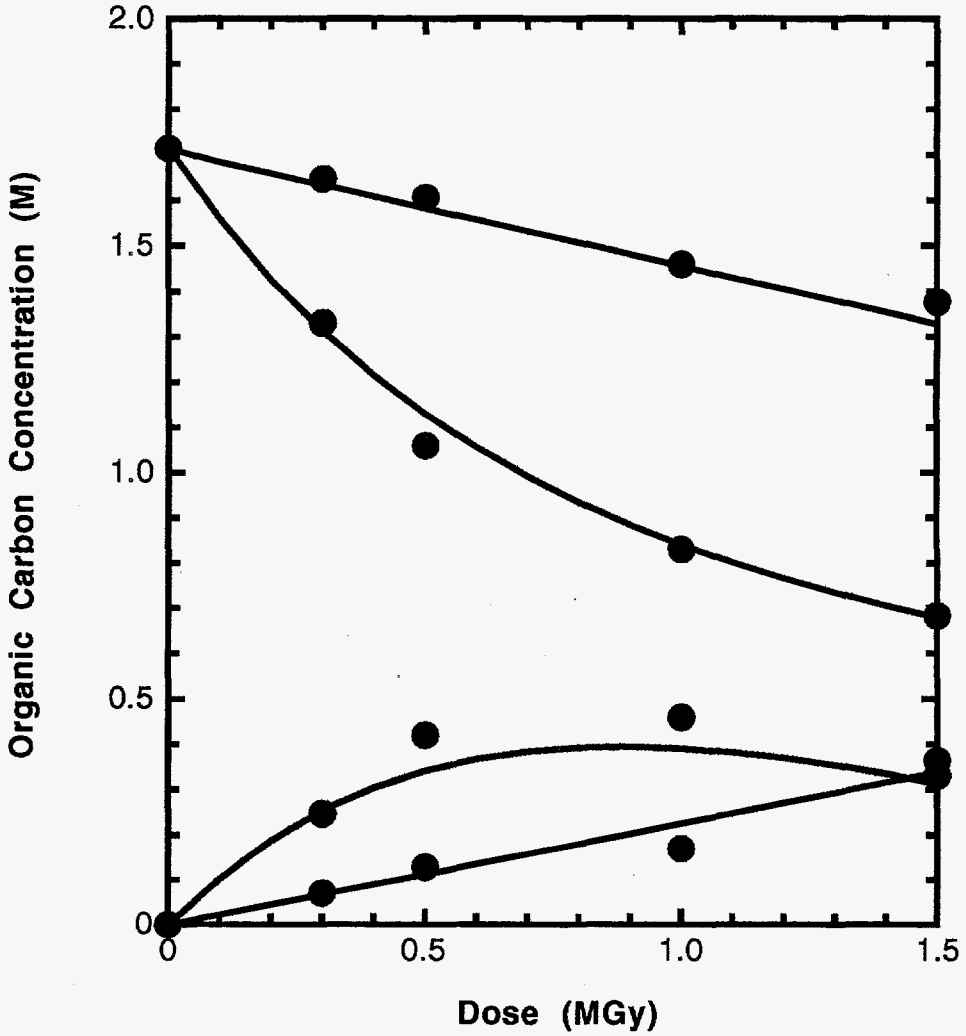

Figure 3.2: Plot of Carbon Content vs Dose: (●) Total Organic Carbon, (●) Carbon in Organic Starting Compounds, (●) Oxalate and Formate Carbon, (●) Carbon in Other Organic Compounds, e.g., ED3A, NTA, IDA, etc. Solid lines are calculated using kinetic parameters in Table 3.3.

Radiolytic doses on the order of 1 to 1.5 MGy convert significant fractions of the chelator carbon (glycolate, citrate, HEDTA, and EDTA) to oxalate, formate, and carbonate. The total organic carbon starts at 20.6 mg/L (4.8 % dry wt) and declines linearly with dose. By 1.5 MGy, organic carbon is 15.9 mg/L (3.5 % dry wt), which corresponds to a 33 mg/L decrease in TOC for a MGy of radiation. Furthermore, HEDTA and EDTA are nearly consumed by a dose of 1.5 MGy, and the carbon in chelator fragments is 0.4 wt%–and decreasing. The carbon in chelator fragments reaches a maximum of 0.7 wt% at 0.9 to 1 MGy.

Table 3.4. Organic Carbon Content and Nitrate Reaction Enthalpies[a] of SIM-PAS-95-1c as a Function of Radiation Dose

Dose MGy	Formate	Oxalate	Glycolate	Citrate	HEDTA	EDTA	Chelator Fragments	Total
Organic C, g/L								
0	0.00	0.00	3.34	7.33	8.27	1.63	0.00	20.6
0.3	0.26	0.59	3.02	7.08	4.77	1.08	2.95	19.7
0.5	0.57	0.96	2.71	6.55	2.78	0.66	5.03	19.3
1	0.83	1.20	2.37	5.97	1.17	0.45	5.51	17.5
1.5	1.49	2.88	2.12	5.42	0.54	0.12	3.29	15.9
wt% C								
0	0.00	0.00	0.73	1.60	1.81	0.36	0.00	4.8
0.3	0.06	0.13	0.66	1.55	1.04	0.24	0.65	4.6
0.5	0.13	0.21	0.59	1.43	0.61	0.15	1.10	4.5
1	0.18	0.26	0.52	1.31	0.26	0.10	1.21	4.1
1.5	0.33	0.63	0.46	1.18	0.12	0.03	0.72	3.7
-ΔHrxn, J/g mix								
0	0	0	186	402	637	115	0	1340
0.3	22	24	151	360	214	47	353	1232
0.5	10	14	168	389	367	77	207	1171
1	33	29	132	328	90	32	387	1031
1.5	58	71	118	297	41	9	231	825

ΔH_{rxn} calculated from ΔH_{rxn} (J/g C) values listed in Table 3.5. ΔH_{rxn} for chelator fragments assumed to be the average of Na_3NTA, Na_3ED3A, Na_2IDA, Na_2EDDA, and sodium glycinate.

The last entries in Table 3.4 are estimates of ΔH_{rxn} of the simulant (dry basis) as function of dose. The contribution of each component to ΔH_{rxn} is obtained by multiplying the concentration (mg/g dry mix) of the compound times the ΔH_{rxn} (kJ/g C) of the compound (Table 3.5). The ΔH_{rxn} for chelator fragments is assumed to be the average of values for Na_3ED3A, Na_2EDDA, Na_3NTA, Na_2IDA, and sodium glycinate. The initial enthalpy of the simulant is about 1340 J/g. After a 1.5 MGy dose, the enthalpy was ~800 J/g. Figure 3.3 is a plot of $-\Delta H_{rxn}$ vs. dose. The line through the data points is generated from the rate parameters in Table 3.3 and the reaction enthalpies of the carbon-containing species. The slope of the line (343 J/g dry mix/MGy) corresponds to the rate of change in the energy content of the simulant. The actual rate of change depends somewhat on the energy of the chelator fragments. Choosing a smaller average ΔH_{rxn} for the chelator fragments leads to a more curved line with a more rapid initial decrease in ΔH_{rxn}. Estimates of ΔH_{rxn} after high doses are not strongly dependent on ΔH_{rxn} of the chelator fragments. They make up less of the carbon in the simulant after exposure to high doses of radiation (Figure 3.2 and Table 3.4) and therefore, they contribute little to energy content. When analyses of

chelator fragments have been completed, our description of the trend with dose will be more accurate.

Table 3.5. Nitrate Reaction Enthalpies (ΔH_{rxn}) for Organic Chelators and Degradation Products of SIM-PAS-95-1c

	ΔH_f	ΔH_{rxn} [a]	
Compounds[a]	kJ/mol	kJ/mol	kJ/g C
Na_3HEDTA	-128.3	-242.3	-35.4
Na_4EDTA	-155.0	-219.7	-32.1
Na_3ED3A	-117.2[b]	-185.0	-33.8
Na_2EDDA	-79.3[c]	-150.4	-36.6
Sodium Glycinate	-43.7	-43.9	-32.1
Na_3NTA	-115.5[d]	-117.1	-28.5
Na_2IDA	-79.6[e]	-80.5	-29.4
Sodium Glycolate	-51.4	-28.3	-20.7
Trisodium Citrate	-129.0	-82.6	-20.1
Disodium Oxalate	-75.2	-9.4	-6.9
Sodium Formate	-38.0	-10.0	-14.7
Sodium Acetate	-40.5	-42.1	-30.7

[a]-ΔH_{rxn} and ΔH_f from Burger (1995) except as noted.
[b][ΔH_f(EDTA)+ ΔH_f(EDDA)]/2.
[c][ΔH_f(EDTA)+ΔH_f(ethylenediamine)]/2.
[e]ΔH_f(NTA)-716 kJ/mol, the correction converting the free acid to the trisodium salt (Burger 1995).
[e][ΔH_f(NTA)+ΔH_f(sodium glycinate)]/2.

3.2 Discussion

A radiation dose of 1 MGy at 70 °C decreases the energy content of the waste simulant by ~25% from a starting value of 1340 j/g dry mix. Much of the enthalpy that remains after 100 MRad dose, is due to undegraded glycolate, citrate, and chelator fragments. Since the longest experiments occurred over ~40 days at 70 °C, thermal pathways for aging did not contribute significantly to organic aging. To the extent that these compounds undergo thermal degradation in parallel with radiolytic aging, further reductions in enthalpy should be expected during long term aging. For example, glycolate degrades thermally with a half life of ~0.4 y at 60 °C (Barefield et al. 1995). If the glycolate remaining after a 1 MGy dose thermally degraded to a 1:1:1 mix of carbonate, formate, and oxalate, then the energy content would decrease by an additional 100 J/g to ~900J/g.

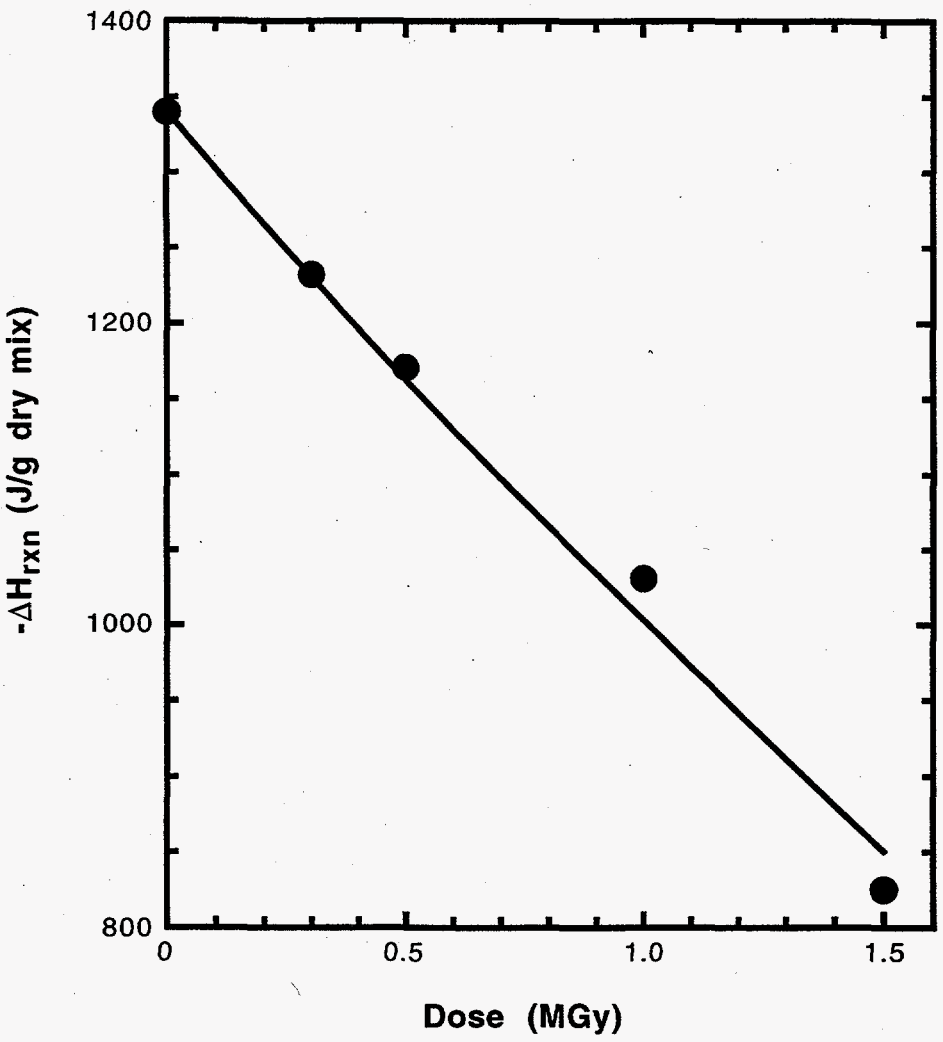

Figure 3.3. Nitrate Reaction Enthalpy of the Simulant vs. Dose. Solid line is calculated using kinetic parameters in Table 3.3 and reaction enthalpies for compounds (Table 3.5).

Thermal degradation of citrate is expected, too. Ashby et al. (1994) observed that citrate degraded to acetate and oxalate in a 2:1 ratio at 120 °C. After 1000 hours approximately half of a 0.021 M solution in 2 M NaOH had reacted. The same concentration in SY1-SIM-91B was 70% reacted. Unfortunately, the lifetime of citrate at temperatures comparable to tank wastes has not been determined. Since very little production of acetate (approximately 0.005 M) had occurred after 1.5 MGy (500 h), we estimate that the half-life of citrate is >5 y at 70 °C. Nonetheless, conversion of citrate to oxalate and acetate reduces the nitrate reaction enthalpy by 40 J/g for each mg/g (dry basis) of sodium citrate that degrades thermally.

Finally, although both TOC and $-\Delta H_{rxn}$ decrease with dose, the average energy content of a gram of carbon ($-\Delta H_{rxn}$ in kJ/g C)[1] is not constant. Rather, as shown in Table 3.6, the energy content per gram of carbon also decreases with increasing dose. The value starts out at 28.1 kJ/g C. After a dose of 1.5 MGy, the value is 22.5 kJ/g C. Correlating average $-\Delta H_{rxn}$ with dose and TOC leads to the following rate factors: 1) the average $-\Delta H_{rxn}$ decreases by 3.5 kJ/g C per 1 MGy dose, and 2) the $-\Delta H_{rxn}$ of the simulant decreases by 45 J per mg decrease in TOC during aging. This finding lends support to the idea that aging reduces the energy value of TOC in the tank wastes.

Table 3.6. Effect of Dose on Average ΔH_{rxn} of SIM-PAS-95-1c

Dose (MGy)	ΔH_{rxn} (kJ/g C)[a]
0	28.1
0.3	26.9
0.5	26.2
1	25.4
1.5	22.5

a) ΔH_{rxn} (J/g dry mix) divided by TOC (mg C/g dry mix)

3.3 Experimental Section

All of the chemicals used in this study were purchased from Aldrich Chemical Company, Eastman Kodak, or Baker Chemicals. Their purities were reagent grade or better, as defined by the American Chemical Society, and the chemicals were not further purified. Water used for preparing the simulant was deionized by a Milli-Q™ Deionization System (Millipore Corporation, San Francisco, CA).

The reactor used for this study was made from 316 stainless steel. The volume of the reactor was approximately 350 mL. Reaction temperatures were measured by a K-thermocouple that inserted through a port in the reactor cover to within 5 mm from the bottom. Another port was connected to the gas manifold via small diameter stainless-steel tubing.

The reactor was heated to operating temperature by heating tape wrapped around the outside of the vessel. Reaction temperatures were maintained at 70 °C by feedback control (Bryan and Pederson 1994). Reaction pressure and vessel temperature were monitored with a data logger.

[1]The average is calculated as the ΔH_{rxn} (J/g dry mix) divided by the TOC (mg C/g dry mix).

3.3.1 Simulant Preparation and Irradiation

The SIM-PAS-95-1c simulant is a based on recipes published in the test plan (Carlson and Babad 1996) for tube propagation experiments (Fauske 1996). We noted that addition of solid ferric nitrate to alkaline solutions containing nitrite ion produced copious amounts of NO_2 gas. On varying the order and timing of addition, we found that if sufficient time (~2 h) were allowed for ferric nitrate to dissolve and hydrolyze to ferric hydroxide before addition of nitrite, then no gas was evolved. Therefore, due caution should be taken in mixing the reagents in proportions or orders different from that recommended here or in the test plan (Carlson and Babad 1996).

To avoid errors associated with dispensing aliquots of a heterogeneous simulant, the simulant was prepared in the reaction vessel before each irradiation by mixing together three homogeneous stock solutions (Table 3.7). These solutions were stored at approximately 4 °C and were allowed to warm to room temperature before volumetric transfers were made. For each test run, 100 mL of solution 1, 20 mL of solution 2, and 10 mL of solution 3 were added sequentially to the reactor. No NO_2 gas was evolved on mixing the solutions. Control runs were similarly mixed and analyzed without exposure to radiation. The measured density of the simulant was 1.27 g/mL. The reactor was sealed and transported to the γ irradiation facility, where the irradiation experiments were performed according to the procedures described in Section 2.2.4 of this report. The gases generated during the irradiations were not collected and analyzed.

3.3.2 Condensed Phase Analyses

The reactor was cooled to room temperature, removed from the gas manifold at the γ-irradiation facility, sealed, and transported to PNNL's Advanced Analytical Methods Development Group for analysis. The reactor's contents were removed and diluted with water to a volume 500 mL. Aliquots of this irradiated mixture were subjected to a variety of analytical methods to determine the composition after irradiation. Ion chromatography (IC) was used to measure citrate, glycolate, acetate, formate, and oxalate, and ion-pair chromatography (IPC) was used to analyze EDTA and HEDTA. Descriptions of the IC and IPC methods are found in Section 2.2.6. A Dionex AS11 IC column was used for citrate, oxalate and formate analyses. Glycolate coeluted with acetate on this column. So, a second set of analyses used a Dionex AS6 column to quantify glycolate, acetate, succinate, and citrate. Analyses of nitrate and nitrite were also performed by IC. Total inorganic carbon was performed with a carbon analyzer.

Table 3.7. Composition of Solutions Used to Prepare SIM-PAS-95-1c

COMPONENT	Mol. Wt. (g/mol)	Mass (g)	Conc. (M)
Solution 1			
NaOH	40	142	3.55
$Al(NO_3)_3 \cdot 9H2O$	375.13	32	0.085
$Na2SiO_3 \cdot 9H2O$	284.2	0.9	0.003
$NaNO_3$	84.99	187	2.20
NaF	41.99	4.4	0.10
Na_2SO_4	142.04	1.2	0.01
$Na_3PO_4 \cdot 12H_2O$	380.13	3.1	0.01
$Na_3HEDTA \cdot 2H_2O$	344.18	36.2	0.11
$Na_4EDTA \cdot 3H_2O$	380.2	8.79	0.02
$Na_3Citrate$	294	35.8	0.12
$HOCH_2CO_2Na$	98.0	23	0.23
H_2O	18	735	40.83
Solution 2			
$Fe(NO_3)_3 \cdot 9H_2O$	404	29.1	0.72
H_2O	18	64.8	36.00
Solution 3			
$NaNO_2$	69	87.3	6.33
$Cr(NO_3)_3 \cdot 9H_2O$	400.15	0.5	0.01
$Ni(NO_3)_2 \cdot 6H_2O$	290.81	0.8	0.01
$Mn(NO_3)_2$	178.95	0.3	0.01
KNO_3	101.1	0.4	0.02
$Pd(NO_3)_2$	230.41	0.012	0.0003
$RuCl4 \cdot 5H_2O$	332.96	0.02	0.0003
$Rh(NO_3)_3 \cdot 2H_2O$	324.93	0.019	0.0003
$Ce(NO_3)_3 \cdot 6H_2O$	434.23	1.8	0.02
$Bi(NO_3)_3 \cdot 5H_2O$	485.07	1.5	0.02
$Pb(NO_3)_2$	331.23	2.6	0.04
H_2O	18	162.5	45.14

4.0 Measurements of TOC in Aged Simulants

The total organic carbon (TOC) content of samples pulled from individual tanks is used as an indicator of the energy content in the Hanford waste storage tanks (Web et al. 1995). A considerable database of TOC measurements exists, and some tank wastes have been sampled repeatedly. We ran TOC analyses on selected samples of aged simulants to learn whether TOC measurements may correlate with organic aging.

4.1 Results of the TOC Measurements on Aged Simulants

The samples for TOC analyses were from SY1-SIM-94C experiments (Section 2) and from a series of simulants (SIM-95) that were prepared and aged in FY95. The TOC analyses were performed by the hot persulfate method (Baldwin et al. 1994).

4.1.1 SY1-SIM-94C

Table 4.1 lists the conditions (temperature and MGy) and TOC results for select aged samples of SY1-SIM-94C. Although heat and radiation significantly changed the concentrations of the starting compounds (see Section 2), the measured TOC values were essentially unchanged by aging; all values are within the experimental precision of the method. Furthermore, the TOC found in an unaged sample was significantly below the value (55.9 g/mg) expected from the amounts of organic compounds used to prepare the simulant.

4.1.2 SIM-95 Simulants

A series of experiments was run with simulants that contained only EDTA and citrate.(1) The samples were speciated before and after irradiation with approximately 0.9 MGy at 70°C under 80/20 argon/oxygen. Table 4.2 lists the concentrations of organic and inorganic carbon (carbonate) in the starting and aged simulants, and the measured TOC values. The TOC values of aged samples were within the 10% experimental error of those of the starting simulants. Carbonate concentrations in the simulants before and after aging changed by less than 10% of the organic carbon initially present. Thus, the reduction of TOC by aging is within the method's limits of uncertainty.

---

(1)The inorganic components of the simulants were Na^+, NO_3^-, NO_2^-, PO_4^{3-}, and SO_4^{2-}. Water content varied from 60 to 70 %. EDTA and citrate were added in equimolar amounts or in a ratio of 0.6 g C of citrate per g C of EDTA.

Table 4.1. TOC Measurements of Starting and Aged Samples of SY1-SIM-94C

Run	Dose (MGy)	T (°C)	TOC (mg/g)
Starting simulant			20.0[a]
26	0.130	50	20.5
28	0.070	72	17.7
24	0.204	70	22.0
8	0.584	70	22.8
12	0.753	70	22.1
B3	0.000	90	22.0
23	0.207	90	21.6
6	0.576	92	20.9
13	0.771	90	21.1

[a]The organic carbon content in the starting simulant is 55.9 mg/g.

Table 4.2. TOC Measurements[a] of Starting and Aged Samples of SIM-95 Simulants

Run	Dose (MGy)	Initial TOC Found (Expected)	Final TOC Found (Expected)
C-1	0.939	36.9 (38.9)	37.3 (35.2)
C-2	0.869	30.4 (31.6)	30.7 (28.9)
C-3	0.927	27.3 (27.4)	25.7 (24.0)
C-5	0.912	22.3 (21.7)	22.6 (19.6)
C-6	0.908	24.1 (23.4)	22.4 (20.3)

[a]mg/g; expected initial TOC values are based on amounts of citrate and EDTA added to the simulants. Expected final TOC values are based on expected initial values less the increase in inorganic carbon.

4.2 Discussion

The accuracy of TOC measurements varies with the types of organic compounds present in the samples. Baldwin et al. (1994) measured the response of a variety of organics to the TOC method and found that recoveries are less than quantitative for many organic structures. For example, the method recovers ~84 % of the carbon from EDTA. Recovery of carbon from breakdown

products, glycolate, formate, and oxalate, exhibit recoveries of 102%, 93%, and 93%, respectively. Recoveries of the organic solvent components, dodecane, TBP, and hexone are 1%, 40%, and 22%, respectively (Baldwin et al. 1994). Thus, the low recovery of organic carbon from the SY1-SIM-94C is explained by the large fraction of carbon in organic solvent components (Table 2.1). The negligible change in TOC of the aged samples might reflect the loss of organic carbon offset by increased recovery of carbon in aged organic structures. For example, the carbon recoveries from TBP hydrolysis products exceed the 40% recovery from TBP, i.e., ~75% for DBP and ~58% for butanol. Similarly, even minor conversion of dodecane (NPH) to the ketones and carboxylate salts could raise the overall TOC.

For the SIM-95 simulants, the TOC method gives a good accounting of the carbon expected to be in the samples. Presumably, this is becausere recoveries of EDTA and citrate, and their aging products, exhibit good to excellent recoveries. Unfortunately, the amounts of inorganic carbon produced by the aging reactions of these simulants are within the experimental precision of the method.

In summary, TOC measurements are relatively insensitive indicators of organic aging, as a result of both the inherent uncertainty in the measurements and the widely varying responses of organic compounds. Because detectable changes in TOC require significant conversions of organic carbon to inorganic carbon, significant decreases in tank waste TOC values over time would seem to reflect significant aging to lower energy content, or they might be attributable to sampling artifacts.

5.0 Aging Studies of Dibutyl Phosphate

This study was undertaken to investigate the fate of dibutyl phosphate (DBP) and monobutyl phosphate (MBP) in the underground storage tanks at Hanford. The tanks have collectively received 720 metric tons of tributyl phosphate (TBP) (Webb et al. 1995, Sederburg and Reddick 1994) and significant quantities of di-2-ethylhexyl phosphate. TBP readily hydrolyzes to DBP and butanol when contacted with strongly alkaline aqueous solutions; however alkaline hydrolysis of dialkyl phosphates is extremely slow (Cox and Ramsey 1964).

Dialkyl phosphates have significant energy content and are hydrolytically stable in the alkaline tank wastes. Thus, it is of interest to know how susceptible they may be to radiolysis and whether they degrade to lower energy compounds. In the following subsections, we review the literature on hydrolysis of alkyl phosphates report on radiolytic aging studies we performed on alkaline nitrate and nitrite solutions of DBP.

5.1 Hydrolysis of Alkyl Phosphate Esters

The review of literature on alkaline hydrolysis of tri-, di- and monoalkyl phosphates yielded reaction rate data for each step in equation 5.1

$$(BuO)_3PO \xrightarrow[HO^-]{k_1} (BuO)_2PO_2^- + BuOH \xrightarrow[HO^-]{k_2} BuOPO_3^{2-} + BuOH \xrightarrow[HO^-]{k_3} PO_4^{3-} + BuOH \qquad (5.1)$$

The data are listed in Table 5.1 and discussed in the following sections.

5.1.1 TBP Hydrolysis

TBP exhibits zero order kinetic behavior in highly alkaline solutions because its solubility in water is low (Burger 1955). Burger reported a rate of 8.8×10^{-4} g/L/h for TBP hydrolysis in 1 M aqueous NaOH at 30 °C and rates 5-fold and 200-fold faster for reactions at 50 °C and 100 °C, respectively. Comparisons of these rates to lifetimes of TBP in tank waste simulant SY1-SIM94C (Camaioni 1995; Section 2) indicate that, even in the absence of radiation, TBP degrades much more rapidly than expected in mixtures approaching the chemical complexity of tank wastes. The cause may be catalysis by divalent metal ions and metal oxides, or the TBP may have been more soluble, possibly due to the formation of microemulsions by high-shear mixing (see Sections 2.2.1 and 2.2.4).

5.1.2 DBP Hydrolysis

The reports that the alkaline hydrolysis of DBP is negligible (Burger 1955) suggest that the rate must be exceedingly slow. While no rate constants have been reported for DBP, rate constants have been measured for structurally-related dimethyl phosphate (DMP) (Baran 1995, Cox and Ramsey 1964), diethyl phosphate (DEP) (Cox and Ramsey 1964), and poly(trimethylene)phosphate (Baran 1995). These constants are approximately 2 orders of magnitude lower than those for alkaline hydrolysis of trialkyl phosphate esters (Table 5.1). Our estimate of the DBP hydrolysis rate ($<2 \times 10^{-12}$ L/mol/s) in Table 5.1 is based on our detection by ^{31}P NMR of a trace (just above the limit of detection) of MBP in molar NaOH solutions of DBP stored for 10 months at room

temperature. This estimate obviously contains a high degree of uncertainty. Significantly faster DBP hydrolysis rates are to be expected at 70 to 100 °C. At room temperature $2x10^{-12}$ L/mol/sec yields a pseudo first-order rate constant of $6x10^{-12}$ sec^{-1} and a half life of over 3000 years in 1 M NaOH. The half life at 100°C could be tens-of-years.

Table 5.1 Second Order Rate Constants for the Base Hydrolysis of Alkyl Phosphates

Phosphate	Reaction Medium	Rate Constant (L/mol/s)	Temperature (°C)
Trimethyl	Aqueous Base	3.4×10^{-4}	35
Trimethyl	pH 12.7	1.1×10^{-4}	35
Trimethyl	pH 13.2	2.5×10^{-4}	45
Triethyl	Aqueous Base	3.7×10^{-4}	37.5
Triethyl	2M NaOH	5.5×10^{-4}	90
Tributyl	1M NaOH	1.53×10^{-6}(a)	30
Tributyl	1M NaOH	7.53×10^{-6}(a)	50
Tributyl	1M NaOH	4.94×10^{-4}	100
Dimethyl	Aqueous Base	5×10^{-6}	125
Dimethyl	pH 10.8	1.3×10^{-6}	70
Poly(trimethylene)	pH 11.7	5.9×10^{-6}	70
Dibutyl	1 M NaOH	$< 6 \times 10^{-12}$(b)	20
Methyl	Acidic/strongly alkaline	10^{-12}(c)	100
Ethyl	acidic/strongly alkaline	10^{-12}(c)	100

(a) Calculated from Kennedy and Grimley (1953) data using TBP solubility data from Higgins (1959).
(b) This work.
(c)First order rate constant for hydrolysis of monoanions ($CH_3CH_2OPO_3H^-$) is 8×10^{-6} s^{-1}.

5.1.3 MBP Hydrolysis

Studies of the hydrolysis of monoalkyl phosphates show that hydrolysis occurs mainly from the monoanion (Cox and Ramsey 1964) and is therefore at a maximal rate pH 4.5. Rate constants for methyl and ethyl phosphates in Table 5.1 are first order rate constants for the equation

$$\text{Rate} = k[RO(OH)(O^-)P{=}O] \qquad (5.2)$$

The dianion is in equilibrium with the monoanion by the reaction

$$RO(O^-)_2P{=}O + H_2O \rightleftarrows RO(OH)(O^-)P{=}O + HO^- \qquad (5.3)$$

so that the rate equation may be recast to show an inverse dependence on HO-.

$$\text{Rate} = k\frac{K_w}{K_a}\frac{[RO(O^-)_2P{=}O]}{[HO^-]} \qquad (5.4)$$

If K_a is approximately equal to the second dissociation constant of phosphoric acid, $K_2=2\times10^{-7}$ M (Lange 1985), then a first order rate constant of ~10^{-12} is expected in 1 M NaOH at 100 °C. Therefore, in strongly alkaline solutions, MBP is expected to be even more resistant to hydrolysis than DBP.

5.2 Radiolysis of Dibutyl Phosphate Solutions

We investigated radiolysis of DBP in homogeneous alkaline solutions with and without nitrate or nitrite. The solutions were irradiated in the γ facility with doses ranging up to 1.14 MGy and analyzed by two complimentary analytical techniques, ^{31}P NMR spectroscopy and ion chromatography (IC). The ^{31}P NMR spectroscopy was used to quantify the total concentrations of diorganophosphates, monoorganophosphates, and inorganic phosphate in each control and irradiated sample. The IC method was used to quantify DBP, MBP, and organic acids in two series of experiments.

A typical set (run 55674-81-12) of ^{31}P NMR spectra collected after different radiation doses is shown in Figure 5.1. This reaction mixture consisted of 0.30 M DBP, 1.20 M OH-, and 3.12 M $NaNO_3$. This solution, in a 5 mm o.d. NMR sample tube, was exposed to a flux of 3381 Gy/h (3.381×10^5 rad/h) with a total dose of 1.136 MGy. A sealed capillary tube containing a known concentration of triphenylphosphine (PPh_3) was added to the tube just before NMR analysis for reference and quantification purposes. The peak at 3.2 ppm (A) decreases relative to PPh_3 (-3.1 ppm), while peaks at 7.2 ppm (B) and 8.8 ppm (PO_4^{3-}) grow. A peak at 31.4 ppm is present initially and remains relatively unchanged after all applied doses. The identity of this peak is unknown. The ^{31}P NMR peak positions of phosphorus-containing compounds are affected mainly by the number of organic groups attached through the P-O-R linkage. Thus, peak A starts out as DBP, and at later times it represents DBP and other diorganophosphates, e.g., $BuOPO(O^-)OCH_2CH_2COCH_3$. Similarly, peak B at 7.2 ppm may be monobutyl phosphophosphate and other monoorganophosphates. Thus, Equation 5.5 describes the reactions observed by NMR:

$$\text{diorganophophate} \xrightarrow{k_4} \text{monoorganophosphate} \xrightarrow{k_5} PO_4^{3-} \qquad (5.5)$$

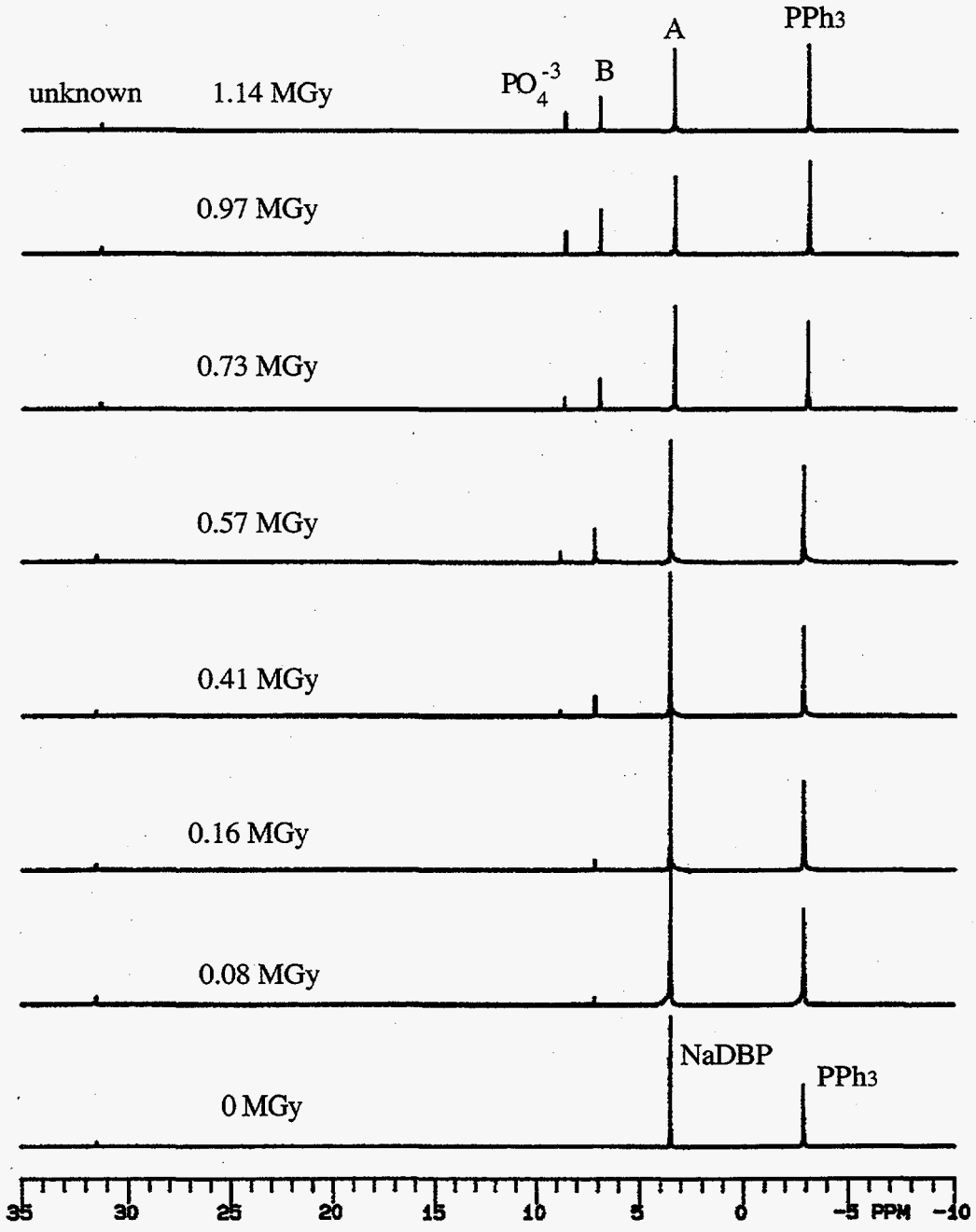

Figure 5.1. The ^{31}P NMR Spectra of γ-Irradiated Aqueous Solutions Containing 0.30 M NaDBP, 1.20 M NaOH, and 3.12 M $NaNO_3$. Peaks labeled A and B are diorganophosphates and monoorganophosphates. PPh_3 is an internal standard added for reference and quantification of other peaks.

We examined the effects of starting DBP ($[DBP]_0$) HO^-, NO_3^-, and NO_2^- concentrations on rates of conversion in a series of 13 experiments. Concentrations obtained by integrating NMR peaks A, B, PO_4^{3-}, and PPh_3 for these experiments are tabulated in Appendix C. Table 5.2 lists the experiment conditions and resulting conversions and radiolytic yields. Experiments 1 through 10 were run to learn the kinetic order of Equation 5.5 with respect to DBP and HO^-. The decrease in diorganophosphate was linear with increasing dose in all these experiments. Conversions of DBP to monoorganophosphates and inorganic phosphate ranged from 8% for 1 M DBP to 55% for 0.13 M DBP. With the exception of experiment 6, which did not contain excess NaOH, the conversion rate was relatively insensitive to the changes in initial concentrations of DBP and HO^-.

Table 5.2 Conversion, Rate, and Yield Data for Radiolysis of NaDBP Solutions Experiments 55674-81-1 through 55674-81-15

No.	$[NO_3^-]$	$[NO_2^-]$	$[OH^-]$	$[DBP]_0$	$[PO_4^{3-}]$ + [B](a)	R_4(b) x10^2	G(c)
1			1.10	1.00	0.067	7.2	0.61
2			1.02	0.48	0.096	8.7	0.75
3			0.94	0.26	0.085	6.7	0.59
4			0.92	0.13	0.072	5.8	0.51
6			(d)	0.30	0.025	2.2	0.20
7			0.29	0.31	0.099	7.7	0.69
8			0.60	0.30	0.10	7.9	0.71
9			1.19	0.31	0.079	8.1	0.70
10			2.10	0.30	0.12	9.1	0.77
12	3.12		1.20	0.30	0.11	10.2	0.77
13		1	1.19	0.31	0.12	9.5	0.80
14	1.98		1.21	0.29	0.12	11.1	0.93
15	1.98	1	1.20	0.30	0.73	6.9	0.57

(a)Concentration after 1.14 MGy dose; B: monoorganophosphates
(b)R_4 is the rate (mole/L/MGy) of diorganophosphate disappearance
(c)Units of molecules/100 eV
(d)Solution prepared by neutralizing 0.3 M dibutyl phosphoric acid with 0.3 M NaOH

With few exceptions, radiolytic yields (G) varied even less with initial DBP and HO^- concentrations. The calculation of G takes into account the different densities of the solutions thereby normalizing for the amount of absorbed energy. Thus, we surmise that the conversion is zero order in DBP and HO^-. The lower conversion rate and smaller G in experiment 6 may be due to differences in yields and types of oxidants in weakly versus strongly alkaline solutions, e.g. $HO^\bullet$ vs. $O^{-\bullet}$. The presence of NO_3^- and/or NO_2^- may have minor effects on the conversion rate.

Experiments 12 to 14 (Table 5.2) show that adding either NO_3^- or NO_2^- increased the conversion rate and G slightly. However, the addition of NO_3^- and NO_2^- appears to have inhibited conversion and G.

Table 5.3 shows the concentrations of DBP, MBP, and PO_4^{3-} that were determined for experiment 55674-81-15 by ion chromatography and the ^{31}P NMR results. The nearly identical concentrations determined by ^{31}P NMR and by IC for the non-irradiated samples and for PO_4^{3-} show that the analytical methods are in agreement. Secondly, the concentrations of MBP and especially DBP in the irradiated samples determined by IC are lower than the corresponding concentrations of diorganophosphates and monoorganophosphates determined by NMR. Thus, DBP converts to other diorganophosphate as well as MBP and that MBP converts to other monoorganophosphates as well as to phosphate. These other organophosphates probably derive from partial oxidation of the butyl groups in DBP and MBP. Finally, the material balance on phosphorus is excellent. Similar recoveries were obtained for the other experiments.

Table 5.3. Molar Concentrations and Phosphate Balance of Phosphorus Species in Experiment 55674-81-15 Determined by Ion Chromatography and ^{31}P NMR

Dose	Ion Chromatography			^{31}P NMR[a]			Other[b]		P
(MGy)	DBP	MBP	PO_4^{3-}	A	B	PO_4^{3-}	A-DBP	B-MBP	Balance[c]
0.00	0.31	0.00	0.0001	0.306	0.000	0.000	-0.006	0.000	0.981
0.08	0.33	0.01	0.0003	0.291	0.014	0.000	-0.034	0.005	0.978
0.16	0.23	0.02	0.0004	0.282	0.023	0.001	0.056	0.004	0.979
0.41	0.17	0.04	0.002	0.261	0.050	0.004	0.095	0.009	1.012
0.73	0.12	0.06	0.006	0.222	0.078	0.014	0.100	0.022	1.005
0.97	0.10	0.06	0.022	0.193	0.088	0.019	0.097	0.024	0.962
1.14	0.08	0.06	0.024	0.186	0.097	0.027	0.103	0.035	0.994

[a]A: diorganophosphates; B: monoorganophosphates.
[b]A-DBP: diorganophosphates other than DBP; B-MBP: monoorganophosphates other than MBP.
[c]Sum of A, B, and PO_4^{3-} divided by initial DBP concentration.

Figure 5.3 combines the IC and NMR data from experiment 55674-81-15 to show how the concentrations of DBP, MBP, other organophosphates, and phosphate change with radiation dose. Note that diorganophosphates other than DBP grow in faster than MBP. Also, monoorganophosphates other than MBP grow in faster than phosphate. Furthermore, DBP disappears by a non-zero order process; that is, its disappearance is not linear with dose. All this suggests a rather complex reaction scheme, such as that shown in Scheme 5.1.

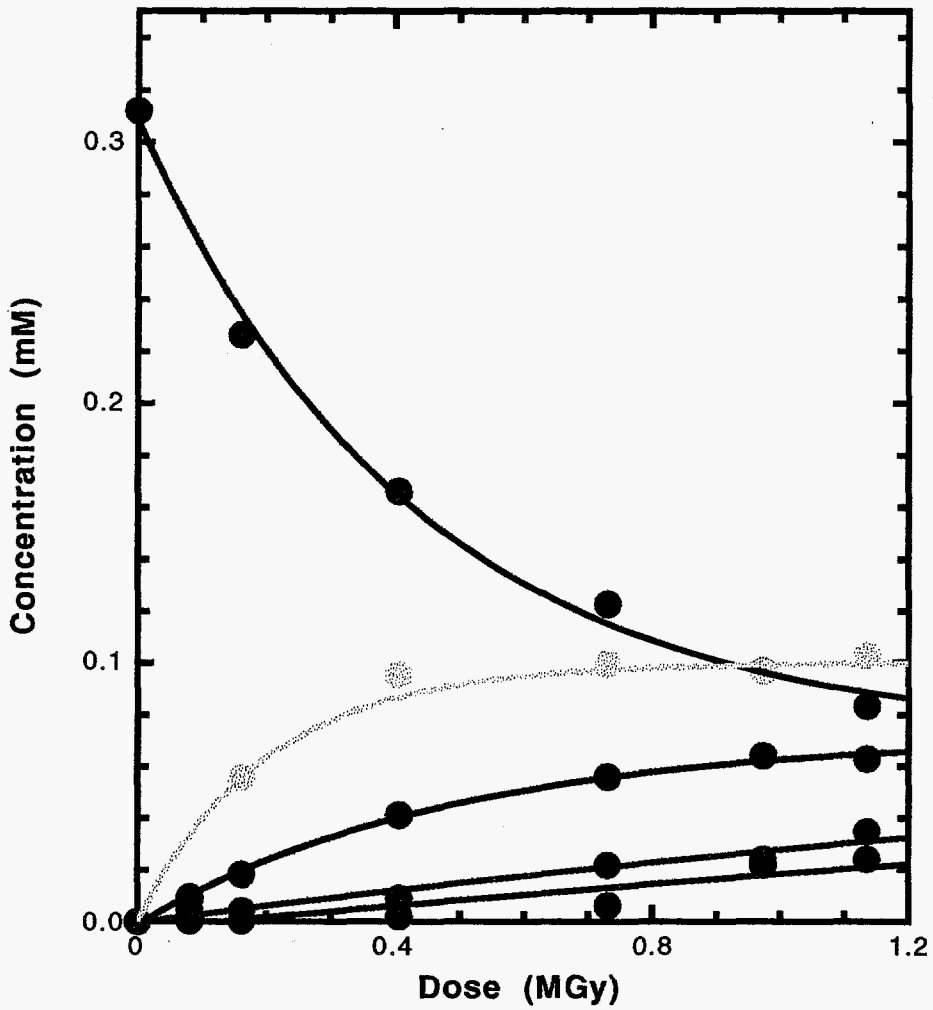

Figure 5.3. Concentrations of Phosphorus-Containing Species vs. Radiolytic Dose for Experiment 55674-81-15 (Table 5.3): (●) DBP; (●) MBP; (●) PO_4^{3-}; (●) other diorganophosphates; (●) other monoorganophosphates.

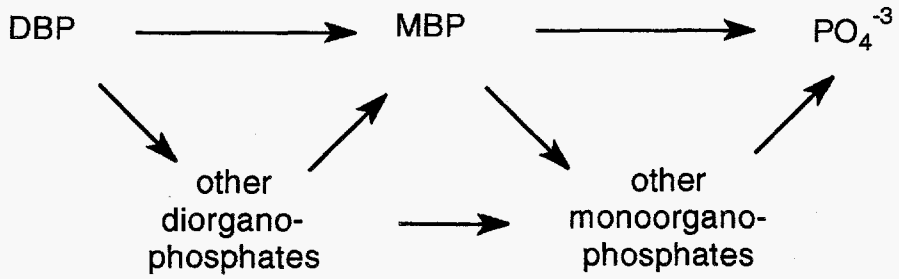

Scheme 5.1. Reaction Scheme for Radiolysis of DBP

Scheme 5.2 shows 2 possible diorganophosphates that might be produced by oxidizing a butyl group in DBP. Oxidation of an α-CH_2 group produces a diorganophosphate that hydrolyzes readily to MBP. But, oxidation of the γ-CH_2 group produces a hydrolytically stable diorganophosphate. Thus, depending on the position of attack on the butyl group, various horizontal and diagonal paths in Equation 5.6 may be taken during the radiolytic conversion of DBP to PO_4^{3-}.

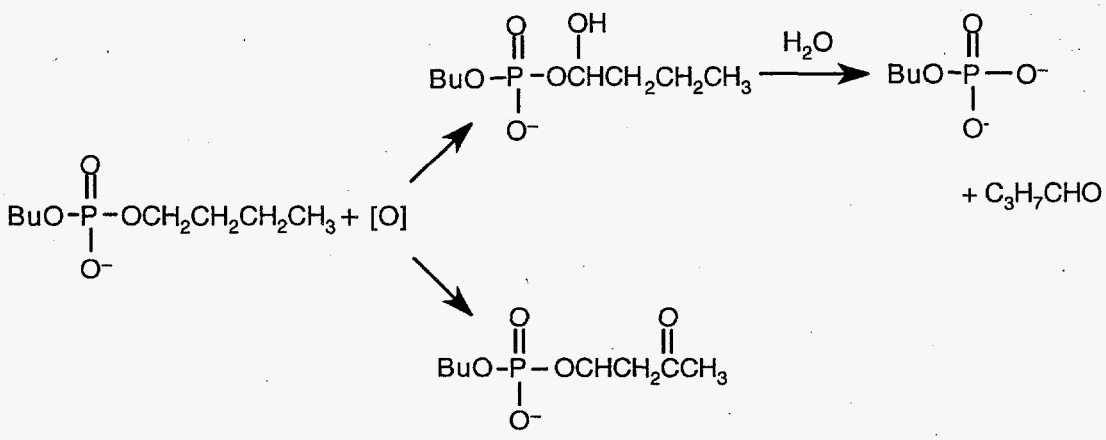

Scheme 5.1. Illustration of Pathways for Converting DBP to MBP and Other Diorganophosphates. Analogous pathways hold for converting MBP to PO_4^{3-} and other monoorganophosphates.

Table 5.4 shows the yields of organic carboxylate salts produced in experiments 55674-81-15 and 55674-81-14. The IC analyses could not resolve formate from butyrate, nor acetate from glycolate. Acetate is listed rather than glycolate because we had observed in aging studies of butyrate (see Section 6) that acetate predominated over glycolate by a factor of ~5. Concentrations of butyrate and formate are calculated in the table as though the other were not present. However, aging studies of butyrate (Section 6) and formate (Lilga et al. 1996) suggest that butyrate is more reactive than formate, so that formate is expected to be the predominant product, especially at the higher doses.

The distribution of organic carbon, total organic carbon, and organic carbon balance in experiment 55674-81-15 is shown in Table 5.5. We used the analytical results for formate rather than butyrate and for acetate rather than glycolate. Independent experiments had demonstrated that butyrate disappeared rapidly (half-life of 0.15 MGy) during radiolysis. The >70% organic carbon mass balance suggests that most of the organic species were detected. The missing carbon probably is carbonate, which was not measured in these experiments, but is known to form during radiolysis of formate (Lilga 1996), and organic simulants (Sections 2.0 and 3.0). We assumed that organophosphates other than DBP and MBP have C/P ratios of either 8 or 4, although, the ratios could be as low as 2 or 1. Therefore, since these compound are significant intermediates, the total organic carbon may be less and the conversion of organic carbon to carbonate may be more rapid than the results indicate.

Table 5.4. Concentrations (μM) of Organic Acid Salts Produced in Radiolysis of DBP Alkaline Nitrate/Nitrite Solutions

Dose (MGy)	Acetate[a]	Butyrate (Formate)[b]	Oxalate
Experiment 14			
0.00	0.0	1.9 (1.6)	0.0
0.08	0.0	7.6 (6.5)	0.6
0.16	0.0	11.0 (9.4)	1.0
0.41	8.0	24.7 (21.1)	2.5
0.57	11.7	31.7 (27.0)	3.2
0.73	14.9	39.0 (33.3)	4.0
0.97	13.3	46.1 (39.4)	5.8
1.14	25.8	52.8 (45.1)	7.2
Experiment 15			
0.00	0.0	0.0 (0.0)	0.0
0.08	3.0	5.0 (4.2)	0.0
0.16	3.7	6.6 (5.6)	0.0
0.41	9.2	15.1 (12.9)	0.8
0.73	14.5	22.0 (18.8)	1.8
0.97	27.2	29.4 (25.1)	2.3
1.14	24.3	29.4 (25.1)	0.0

[a]Glycolate are not resolved from acetate in the IC analysis. If the peak were glycolate instead of acetate, then quantities would be 0.75 smaller.
[b]Butyrate and formate not resolved by IC analysis. Quantities shown for each are calculated assuming none of the other is present.

Table 5.5. Distribution of Organic Carbon (mM) vs. Radiolytic Dose for Expt. 55674-81-15

Dose MGy	MBP	DBP	Acetate	Formate	Oxalate	A-DBP	B-MBP	Total Org. C	Org. C Balance
0.00	0.00	2.50	0.000	0.000	0.000	0.00	0.00	2.50	1.00
0.08	0.04	2.60	0.006	0.004	0.000	0.00	0.02	2.67	1.07
0.16	0.07	1.81	0.007	0.006	0.000	0.45	0.02	2.36	0.94
0.41	0.16	1.33	0.018	0.013	0.002	0.76	0.04	2.33	0.93
0.73	0.22	0.98	0.029	0.019	0.006	0.80	0.09	2.14	0.86
0.97	0.26	0.77	0.054	0.025	0.007	0.77	0.10	1.99	0.80
1.14	0.25	0.67	0.049	0.025	0.000	0.82	0.14	1.95	0.78

Finally, we analyzed the samples by NMR shortly after radiolysis and again several months later after the IC analyses were performed. The concentrations of monoorganophosphates and phosphate did not change significantly even though storage was at room temperature. Thus, the diorgano and monoorgano phosphates did not hydrolyse during storage.

5.3 Discussion

The published data and our control experiments suggest that alkaline hydrolysis of DBP and MBP probably is of minor importance in aging tank wastes. However, under radiolytic conditions, DBP and MBP decompose readily by oxidation of the butyl groups, and we detected oxidized organic species in irradiated DBP solutions (see Table 5.4). Combining the NMR and IC results for experiment 15 shows that conversion of diorganophosphates to monoorganophosphates is slower than the rate of disappearance of DBP. Evidently, only a fraction of the oxidative attacks leads to scission of C-O or P-O bonds.

The rate of disappearance of DBP does not fit simple first order kinetic behavior. In experiment 15 (Figure 5.3 and Table 5.4), we followed the disappearance of DBP for about 2 half-lives. The second half-life is longer than the first. By the second half-life, concentrations of MBP and other organophosphates had become comparable to that of DBP. Apparently, these species compete effectively with DBP for radiolytically-generated oxidants, thereby slowing the rate of disappearance of DBP more than would be expected for first order behavior.

The concentration of DBP in experiment 15 decreased to half the starting DBP concentration (0.3 M) after a dose of approximately 0.5 MGy at room temperature. This suggests that DBP is less reactive than either butanol or butyrate, which had half lives on the order of 0.06 MGy at room temperature. The half-life for DBP is comparable to that of EDTA at 70 °C in SY1-SIM-94C (see section 2.1.4) and in SIM-PAS-95-1 (see Table 3.3). Higher temperatures should accelerate the rates at which DBP ages. Thus, DBP and MBP appear to be more reactive than EDTA, and DBP and butanol (from TBP hydrolysis) rank among the more reactive organics added to tank wastes.

5.4 Experimental Section

The solutions and emulsions were produced using reagent grade TBP (Aldrich), DBP (99%,TCI America), $NaNO_3$ (Aldrich), $NaNO_2$ (Aldrich), and NaOH (Aldrich) and tap water. An approximate 50:50 mixture of DBP and MBP (Aldrich) was used to identify the MBP peak in the ^{31}P NMR spectra. The prepared NaDBP solutions showed no signs of decomposition during the > 6-month lifetime of these studies.

The ^{31}P NMR spectra were collected at 121.4 MHz on a Varian VXR-300 NMR spectrometer. A 75° pulse with a 5-second recycle time and proton decoupling during data acquisition were used to collect the spectra. Investigation of the effect of recycle time on the peak areas show that 5 seconds did not violate phosphorus T_1 and thus did allow sufficient time for spin relaxation between pulses. The peak positions were externally referenced to a chloroform solution of triphenylphosphine (-3.1 ppm) sealed in a capillary tube. The peak position of triphenylphosphine is -3.1 ppm when referenced to 1 M phosphoric acid in water. The peak positions of DBP, MBP, and PO_4^{3-} vary up to 0.3 ppm under the changing conditions in this experiment. The peak positions are dependent on concentration, pH, and ionic strength but the peak positions for the three species do not overlap under any conditions. The approximate peak positions of DBP, MBP,

and PO_4^{3-} were 3.2 ppm, 7.2 ppm, and 8.8 ppm respectively. In completely homogeneous solutions, the peak shape of the phosphate species is narrow and guassian. The peaks may be split, or the peak shape may broaden and become asymmetric when solutions are multiphasic.

We tested the reproducibility of the ^{31}P NMR technique in radiolytic experiments on the three samples subjected to the highest dose. Samples 55674-37-9a, 55674-37-9b, and 55674-37-9c, were loaded at the same time and subjected to identical doses. The amounts of A, B, and PO_4^{3-} were reproducible to ±1%.

The radiolyses were performed on 0.50 ml aliquots of the reaction solutions in a 5-mm o.d. borosilicate glass NMR tube which was sealed with a plastic NMR cap and wrapped with Parafilm®. Sets of 10 NMR tubes were loaded in the γ-irradiation facility for each DBP reaction mixture. An NMR tube from each set was removed from the γ-irradiation facility after an appropriate dose. Each of these were was analyzed by first placing a sealed capillary tube containing a known amount of PPh_3 in the NMR tube and then recording a ^{31}P NMR spectrum. The ratio of the phosphate peak areas to the PPh_3 peak area was used, after calibration with NaDBP, to determine the actual phosphate concentration. A sample calibration curve is shown in Figure 5.7.

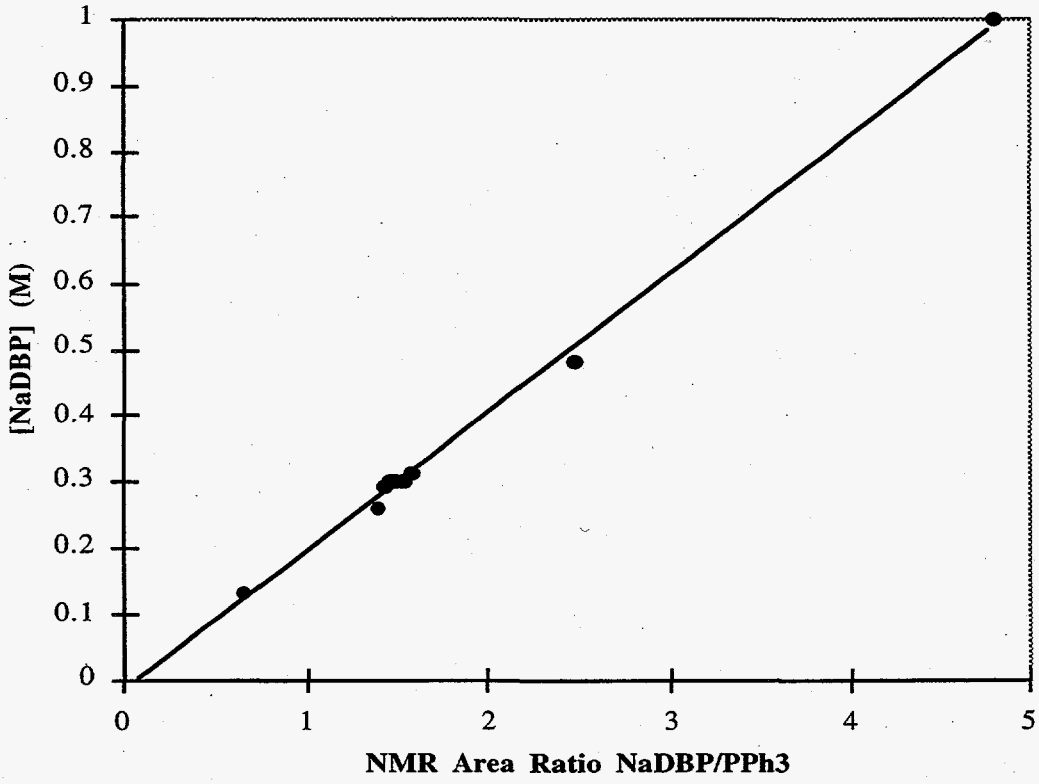

Figure 5.4. Calibration Plot of NaDBP Concentration vs. Area Ratio of DBP to Triphenylphosphine (PPh_3) for ^{31}P NMR Analyses.

6.0 Butanol and Sodium Butyrate Aging Studies

This study was undertaken to learn the radiolytic aging rates and products of butanol and sodium butyrate in tank wastes. The underground storage tanks at the Hanford site have collectively received 720 metric tons of tributyl phosphate (Webb et al. 1995; Sederburg and Reddick 1994). Because tributyl phosphate hydrolyzes in strongly alkaline solutions (Burger 1955, 1958), we expect that much of this tributyl phosphate has converted to butanol and dibutyl phosphate. The fate of butanol is uncertain. Some butanol (bp 118 °C) may have been stripped from the wastes by evaporation, the possibility that butanol degraded to butyrate raises concern because butyrate is more energetic than acetate.

Radiolysis of normal paraffinic hydrocarbons probably leads to production of aliphatic carboxylates of various carbon numbers. A clear indication that aliphatic carboxylates are being formed is given by the detection of a homologous series of nitriles and ketones in the headspace of Tank C-103 (Huckaby and Story 1994) and in other tanks which emit hydrocarbon vapors. Nitriles hydrolyze to carboxylate salts in strongly alkaline solutions. Our aging studies with SY1-SIM-94C (Camaioni et al. 1995) suggest that hexone oxidizes to sodium isobutyrate during γ-radiolysis. Therefore, aging probably produces solvent-derived carboxylate salts. Study of the fate of sodium butyrate is relevant to the fate of these carboxylate salts.

Solubility studies (Barney 1995) of related compounds suggest that butanol and butyrate will be soluble in supernate liquids. Therefore, we investigated the aging reactions in solutions that were representative of tank waste supernates. The two simulant solutions we prepared for γ-irradiation tests were homogeneous and colorless, differing only in organic content: one contained butanol, and the other contained sodium butyrate (Table 6.1).

Table 6.1. Composition of Simulants

	Butanol Simulant			Butyrate simulant		
Component	M	mg/mL	mg/g	M	mg/mL	mg/g
organic	0.08	5.9	4.5	0.047	4.1	3.1
Na^+	4.25	98	75	4.25	98	75
NO_3^-	4.44	275	210	4.44	275	210
Al^{+3}	0.06	1.7	1.3	0.06	1.7	1.3
total HO-	4.25	72	55	4.2	71	54.4
H_2O	47.6	857	654	47.8	860	656

6.1 Results

Irradiated simulant solutions were homogeneous. Simulants that received intermediate doses, (0.30 to 0.60 MGy) had the most intense yellow color. Which species cause(s) the color is unknown. None of the organic products thus far identified (Table 6.2) are colored. Similar

simulants irradiated this year which contained ethylenediaminetetraacetate (EDTA) and citrate, have been yellow to orange.

The GC-MS and IC analyses found several organic products in the irradiated simulants. Table 6.2 summarizes the analytical results, listing concentrations of compounds in millimolar (mM) units (Table B.1 lists these results in mg/g).

Table 6.2. Concentrations (mM) of Compounds Found in Irradiated Butanol and Butyrate Simulants

Dose MGy	GC Analyses			Acids by IC Analyses[a]					Carbon balance %[b]
	Butanol	Butyric Acid	Propion-ic Acid	Butyric/ (Formic)	Glycolic/ (Acetic)	Oxalic/ (Fumaric)	Malonic	Malic	
Butanol simulant									
0	79.5								100
0.036	56.6	0.0							71
0.125	26.5	0.8	<0.9			0.3 (0.4)			35
0.25	12.4	0.7	<0.9			0.7 (0.8)			18
0.357	1.0	0.8	<0.9	10 (6.6)		1.1 (1.2)			6
0.589		<0.7	<0.9			3.1 (3.5)	3.7	0.4	8
0.765		<0.7		12 (7.7)	15 (10)	6.5 (7.1)	7.3	0.8	21
0.959		<0.7		13 (8.5)	45 (31)	8.1 (8.9)	7.9	1.0	37
Butyrate simulant									
0		45		48					100
0.036		37		37					82
0.125		18		19		0.9 (1.0)			41
0.25		3.4		6.5		2.1 (2.4)	4.7		18
0.357		1.5		5.0	21 (15)	4.9 (5.4)	7.3		38
0.589		<0.7				9.5 (10.4)			12
0.765		<0.7				11.0 (12.1)	6.8	0.8	27
0.959		<0.7				11.2 (12.3)	6.9	0.9	28

[a]IC analyses did not resolve butyrate and formate, glycolate and acetate, or oxalate and fumarate; values listed for these compounds assume that the compound is either one or the other; numbers in parentheses are for the corresponding compounds in parentheses.
[b]From GC analyses for butyric acid and butanol and IC analyses for formic (from butanol only), glycolic, oxalic, malonic, and malic acids.

Only butanol, butyric acid, and propionic acid were detected and positively identified by the GC-MS analyses. The other listed compounds were identified by matching retention times of peaks in ion chromatograms. As this approach is essentially a process of elimination, many compounds were run on the IC to make the assignments. Table 6.3 lists the compounds that were

run and their retention times. Note that the retention times of some pairs of compounds (acetate and glycolate, formate and butyrate, oxalate and furmarate) are so similar that IC analyses alone cannot resolve them if both are present. In these cases, we listed both compounds and the calculated the amounts by assuming that the IC peak represented either one or the other). Of course, other compounds could also elute at similar retention times, and the IC identifications must be viewed as tentative until assignments are corroborated.

Table 6.3. Compounds Run in the Ion Chromatograph and Their Retention Times[a]

Compound	Structure	Time (min)	Compound	Structure	Time (min)
Acetic	CH_3CO_2H	2.44	Maleic	(Z) $HO_2CCH{=}CHCO_2H$	9.53
Glycolic	$HOCH_2CO_2H$	2.44	Succinic	$HO_2CCH_2CH_2CO_2H$	9.65
Propionic	$CH_3CH_2CO_2H$	2.72	Malonic	$HO_2CCH_2CO_2H$	9.88
Formic	HCO_2H	3.17	Malic	$HO_2CCH_2CH(OH)CO_2H$	10.31
Butyric	$CH_3CH_2CH_2CO_2H$	3.24	Oxalic	HO_2CCO_2H	10.86
Glyoxylic	$HCOCO_2H$	5.58	Fumaric	(E) $HO_2CCH{=}CHCO_2H$	10.88

[a]Dionex AS6 column

IC analysis conditions using a using different column (Dionex AS6) resolved the co-eluting compound pairs, acetate/glycolate, formate/butyrate, and oxalate/fumarate. Subsequent analysis of the butyrate sample dosed with 0.96 MGy revealed no fumarate and only small amounts of formate, acetate and glycolate. The amount of acetate was 5 times greater than the glycolate amount. Therefore, it appears that oxalate and malonate are the main compounds left in this sample, accounting for 25% of the carbon initially present.

6.2 Discussion

A complete description of reaction pathways is not possible because many compound assignments remain to be corroborated. Furthermore, information on initial products is limited. Few products were detected at low to intermediate doses (see Table 6.2), evidently because the analytical methods could not detect many of the intermediate products. Neutral intermediates would not have been detected by the IC method. In the GC-MS analyses, low molecular weight compounds (C-1 to C-3 hydrocarbons, alcohols, ketones and aldehydes) would have either evaporated from the solutions or been obscured by the solvent peak (ethyl acetate). At higher doses, yields of carboxylic acids such as formic, acetic, oxalic, glycolic, and malonic acids are significant, accounting for about 25% of the initial carbon in the butyrate sample. In the case of butanol, about 40% of the starting carbon is accounted for in the 0.96 MGy sample. It is reasonable that a considerable fraction of the unaccounted for carbon has been converted to CO_3^{-2}, for example by decarboxylation of the carboxylate anions (Eq. 6.1 and 6.2).

$$CH_3CH_2CH_2CO_2^- \rightarrow CH_3CH_2CO_2^- \rightarrow CH_3CO_2^- \rightarrow HCO_2^- \rightarrow CO_3^- \qquad (6.1)$$

$$CH_3CH_2CH_2CO_2^- \rightarrow {}^-O_2CCH_2CO_2^- \rightarrow {}^-O_2CCO_2^- \rightarrow CO_3^- \qquad (6.2)$$

GC analyses of the butanol runs shows that butyrate never attains significant concentrations, which suggests that the formate/butyrate peak in the IC analyses observed at high doses is mostly formate. On the other hand, the absence of formate in significant quantities in aged butyrate simulants suggests that oxidation to butyrate is not the most important pathway for butanol aging. The presence of propionate and formate suggests that oxidation involves scission of the β C-C bond, such as would occur from butoxy radical, Eq. 6.3.

$$CH_3CH_2CH_2CH_2OH \rightarrow CH_3CH_2CH_2CH_2O\bullet \rightarrow CH_3CH_2CH_2\bullet + CH_2{=}O \qquad (6.3)$$

Figure 6.1 is a plot of butanol and butyrate concentrations as a function of dose. Both degrade with similar rates and follow first-order kinetic behavior. The dose required to reduce the concentration by half its original value is only ~0.06 MGy, considerably less than the corresponding doses for EDTA and citrate in our SY1-SIM-94C simulant and for NaDBP. Thus, butanol and butyrate may be less stable than these compounds in radiolytic fields. This possibility may be established more clearly through competitive experiments where mixtures of organic compounds are irradiated.

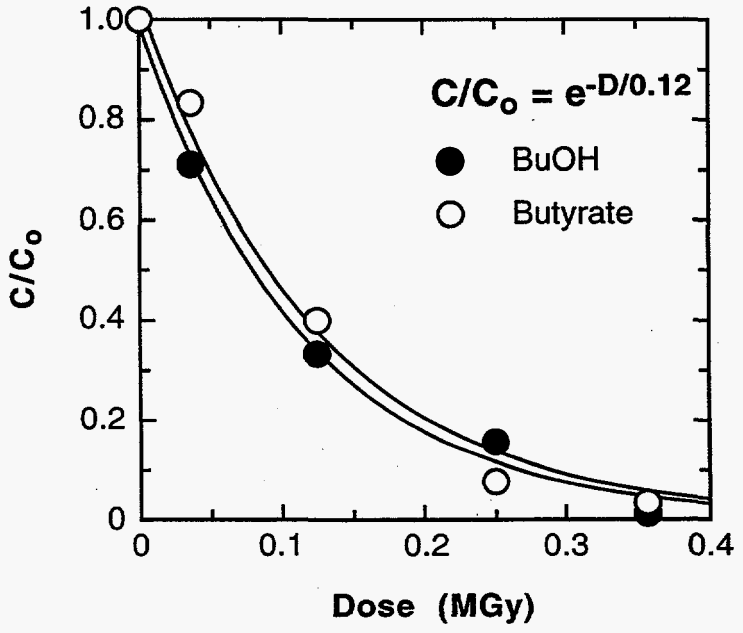

Figure 6.1. Disappearance of Butanol and Sodium Butyrate as a Function of γ Dose at 20 °C. Concentrations have been normalized and fit to a first-order rate equation (where C_0 is starting concentration, C is concentration after receiving D MGy of γ energy, and 0.12 is the kinetic life-time in units of MGy).

By analogy to this work, carboxylic acids derived from NPH may be expected to degrade readily in radiation fields to generate a variety of oxidized intermediate compounds. Ultimate degradation to oxalate, formate, and carbonate is plausible and partially demonstrated here by the butyrate results.

In summary, results of butanol and butyrate aging are consistent with aging reactions that tend to produce more highly oxidized organic compounds. Future work is needed to corroborate the compound assignments and learn how much carbon is converted to carbonate. Although butyrate does not appear to yield significant amounts of fumarate, some of the irradiated butanol samples should be reanalyzed to rule out fumarate production from butanol. Finally, the source of the yellow color produced by radiolysis should be investigated.

6.3 Experimental Section

The simulants were prepared by introducing and mixing components in the following order to make 100 mL of simulant: 50 mL water, 17 g sodium hydroxide, 24 g aluminum nitrate, 17 g sodium nitrate, organic component, remaining water. All chemicals were of reagent grade or better quality. Next, 0.5-mL aliquots of the simulants were dispensed into 5-mm-o.d. glass NMR tubes, and the tubes were capped with polyethylene caps. These tubes (7 containing butanol simulant and 7 containing butyrate simulant) were placed upright in a plastic bottle, and the bottle was irradiated in an upright position in the γ-irradiation facility. Tubes of each simulant were removed one at a time at scheduled intervals. The duration of the experiment was 63 days. The γ-flux was 2.6×10^5 rad/hr. Ambient temperature in the pit was ~20 °C throughout the experiment. Retrieved samples were stored at 4 °C until analysis.

Organic analyses were performed using gas chromatography-mass spectrometry (GC-MS) and ion chromatography (IC). For GC analyses, 0.200 mL samples of each solution were weighed in a tared vial to which the following were added with swirling: 0.050 mL valeric acid surrogate, 1 mL of 2 N phosphoric acid to neutralize hydroxide and carboxylate ions, and 0.5 mL saturated NaCl solution to promote organic phase separation. The contents of the vials were extracted 3 times in 2-mL aliquots of ethyl acetate. The extract was diluted to 10 mL and a portion was transferred to an autosampler vial. The analyses were performed on a 30 m × 0.25mm DBWAX™ (1 μm film thickness) capillary column (J&W Scientific). Samples for IC analyses were prepared by transferring 0.050 mL of sample to a 25-mL volumetric flask and diluting to volume with water. A portion of this solution was transferred to an autosampler vial. The analyses were preformed using a Dionex ion chromatograph equipped with an AS11 column.

7.0 Conclusions

The Waste Aging Studies task has made considerable progress in the past year. In our previous annual report, we could draw only qualitative conclusions of how organic compounds in the tank wastes may have changed since being added to the tanks. Now, our experiments are providing quantitative results on how the energy content of the waste may have changed during that time.

The aging studies show that radiation promotes redox reactions between organic compounds (reducing agents) and nitrates/nitrites (oxidizing agents) in the wastes. In aging studies with SY1-SIM-94C, we find that production of H_2, N_2, and N_2O by radiolysis is significant only when organic compounds are present in the waste simulant. Concurrent with production of these gases, organic compounds disappear and are replaced by oxidized products, organic carboxylates, and carbonyl compounds. The observations are consistent with progressive degradation of organic compounds to compounds with more C-O bonds and fewer C-H and C-C bonds, resulting in an overall lower energy content of the organic inventory. These facts are quantitatively established in our studies with the SIM-PAS-95 simulant. Carbonate, formate, oxalate, and chelator fragments have been quantified to yield estimates of the maximum theoretical energy content as a function of dose. The energy content declined steadily with increasing radiolytic dose. Analogous actual wastes receiving similar doses should have even lower energy content due to contributions by purely thermal aging reactions (Delagard 1987; Ashby et al. 1993; Barefield et al. 1995, 1996).

Our studies with simulants show that TOC is a poor indicator of aging and energy content. TOC measurements have much inherent uncertainty and organic compounds exhibit widely varying responses to the test method. Yet, TOC measurements have been obtained from a significant number of tank wastes. Accordingly, this data currently provides the main basis for assessing the risk that a particular tank waste might undergo propagating reactions (Webb et al. 1995). The assessment essentially converts TOC to enthalpy by assuming a proportionality factor, i.e.

$$\Delta H_{rxn}\,(\text{kJ/g waste}) = \text{TOC}\,(\text{mg/g waste}) \times \Delta H\,(\text{kJ/g C}) \qquad (7.1)$$

Presently, the conversion factor is taken to be the reaction enthalpy of sodium acetate. Results of our aging tests suggest that the actual conversion factor decreases with aging.

With respect to recommendations for FY97 work, we note that the disappearance of starting compounds and the appearance of products often follow simple kinetic rate laws. Thus, it may be possible to use a phenomenological kinetic model to predict aging effects under a wider variety of conditions than could be experimentally tested. The apparent rate parameters probably depend on temperature and radiation flux. Our results with SY1-SIM-94C suggest that radiolytic aging of EDTA and citrate is modestly dependent on temperature: rates increase by 10% to 25% per 10 °C increase in temperature. More experiments are needed to elucidate the dependence on radiation flux. More data is needed on thermal non-radiolytic decomposition rates for compounds not studied by the Flammable Gas Safety Program (Asby et al. 1994; Barefield et al. 1995, 1996). We also need more specific information on the degradation pathways of each major starting compound and some intermediates. For example, when EDTA degrades to ED3A, what are the resulting yields of carbonate, formate, and oxalate? How much glycolate is produced? When glycolate degrades, what are the resulting yields of carbonate, formate, and oxalate? Do oxalate and formate degrade to carbonate in the presence of complexants and other organic waste compounds? What are the relative reactivities? How does the heterogeneity of the waste affect absolute and relative

rates of aging? We recommend FY97 work be targeted to answer such questions as necessary to predict the organic species and energetic contents of tank wastes.

Many tank wastes will be speciated as part of the Flammable Gas and Organic Tank Safety programs. If organic content and species in these wastes are consistent with predictions, then it will be proven that organic tank wastes, in general, are aging to low energy species that do not or will not propagate under storage conditions.

8.0 References

Agnew SF. 1996a. *Hanford Defined Wastes: Chemical and Radionuclide Compositions.* LA-UR-94-2657 Rev. 2, Los Alamos National Laboratory, Los Alamos , New Mexico.

Agnew SF. 1996b. *Hanford Tank Chemical and Radionuclide Inventories.* LA-UR-96-858, Los Alamos National Laboratory, Los Alamos, New Mexico.

Agnew SF. 1996c. *History of Organic Carbon in Hanford HLW Tanks: HDW Model Rev. 3.* LA-UR-96-989, Los Alamos National Laboratory, Los Alamos , New Mexico.

Allen, GK. 1976. *Estimated Inventory of Chemicals Added to Underground Waste Tanks, 1944 Though 1975,* ARH-CD-610B, Atlantic Richfield Hanford Company, Richland, Washington.

Ashby EC, A Annis, EK Barefield, D Boatright, F Doctorovich, CL Liotta, HM Neumann, A Konda, C-F Yao, K Zhang, and NG Duffie. 1994. *Synthetic Waste Chemical Mechanism Studies.* WHC-EP-0823, Westinghouse Hanford Company, Richland, Washington.

Ashby EC, F Doctorovich, CL Liotta, HM Neumann, EK Barefield, A Konda, K Zhang, and J Hurley. 1993. *Concerningthe Formation of Hydrogen in Nuclear Waste. Quantitative Generation of Hydrogen via a Cannizzaro Intermediate.* J Am Chem Soc **115**:1171.

Baldwin DL, RW Stromat, and WI Winters. 1994. "Camparative Study of Total Organic Carbon (TOC) Methods for High -Level Mixed Wastes," *Proceedings of the International Topical Meeting on Nuclear and Hazardous Wastes -Spectrum 94, August 14-18,* American Nuclear Society: La Grange, Illinois, pp. 27-34; PNL-SA-23718, Pacific Northwest Laboratory, Richland, Washington.

Baran J and S Penczek. 1995. *Hydrolysis of Polyesters of Phosphoric Acid. 1. Kinetics and pH Profile* Macromol. **28**: 5167-5176.

Barefield EK, D Boatright, A Deshpande, F Doctorovich, CL Liotta, HM Neumann and S Seymore. 1995. *Mechanisms of Gas Generation from Simulated SY Tank Farm Wastes: FY1994 Progress Report,* PNL-10822, Georgia Institute of Technology, Atlanta, Georgia, and Pacific Northwest Laboratory, Richland, Washington.

Barefield EK, D Boatright, A Deshpande, F Doctorovich, CL Liotta, HM Neumann, and S. Seymore. 1996. *Mechanisms of Gas Generation from Simulated SY Tank Farm Wastes: FY1995 Progress Report,* PNNL-11247, Georgia Institute of Technology, Atlanta, Georgia, and Pacific Northwest Laboratory, Richland, Washington.

Barney GS. 1995. *The Solubilities of Significant Organic Compounds in HLW Tank Supernate Solutions,* WHC-SA-2565-FP, Westinghouse Hanford Company, Richland, Washington.

Bryan SA and LR Pederson. 1994. *Composition, Preparation, and Gas Generation from Simulated Wastes of Tank 241-101-SY,* PNL-10075, Pacific Northwest Laboratory, Richland, Washington.

Bryan SA and LR Pederson. 1995. *Thermal and Combined Thermal and Radiolytic Reactions Involving Nitrous Oxide, Hydrogen, and Nitrogen in the Gas Phase; Comparison of Gas Generation Rates in Supernate and Solid Fractions of Tank 241-SY-101 Simulated Waste*, PNL-10490, Pacific Northwest Laboratory, Richland, Washington.

Bryan SA and LR Pederson. 1996a. *Thermal and Combined Thermal and Radiolytic Reactions Involving Nitrous Oxide, Hydrogen, Nitrogen and Ammonia in Contact with Tank 241-SY-101*, Pacific Northwest National Laboratory, Richland, Washington.

Bryan SA, CM King, LR Pederson, SV Forbes and RL Sell. 1996b. *Gas Generation from Tank 241-SY-103*, PNNL-10978, Pacific Northwest National Laboratory.

Burger LL. 1955. *The Chemistry of Tributyl Phosphate - A Review*, HW-40910, General Electric Company, Richland, Washington.

Burger, LL. 1958. "The Decomposition Reactions of Tributyl Phosphate and Its Diluents and Their Effect on Uranium Recovery Processes." In *Progess in Nuclear Energy-Series III, Process Chemistry*, Vol. 2, Pergamon Press: New York, pp. 307-319.

Burger LL. 1995. *Calculation of Reaction Energies and Adiabatic Temperatures for Waste Tank Reactions*, PNL-8557-Rev 1, Pacific Northwest National Laboratories.

Camaioni DM, WD Samuels, SA Clauss, BD Lenihan, KL Wahl, JA Campbell, WJ Shaw. 1995. *Oganic Tanks Safety Program FY95 Waste Aging Studies*, PNL-10794, Pacific Northwest National Laboratory, Richland, Washington.

Camaioni DM, WD Samuels, BD Lenihan, SA Clauss, KL Wahl, JA Campbell. 1994. *Organic Tanks Safety Program Waste Aging Studies*, PNL-10161, Pacific Northwest Laboratory, Richland, Washington.

Campbell JA, S Clauss, K Grant, V Hoopes, B Lerner, R Lucke, G Mong, J Rau, and R Steele. 1994. *Flammable Gas Safety Program; Analytical Methods Development: FY 1993 Progress Report*, PNL-9062, Pacific Northwest Laboratory, Richland, Washington.

Carlson CD and H Babad. 1996. *Test Plan for Fauske and Associates to Perform Tube Propagation Experiments with Simulated Hanford Tank Wastes*, PNNL-10970 rev 1, Pacific Northwest National Laboratory, Richland, Washington.

Cleveland JM. 1967. *Plutonium recovery and waste disposal*, In Plutonium Handbook, OJ Wick, Ed.,Vol. II, Gordon and Breach, Science Publishers: New York.

Cox JR Jr, and OB Ramsey. 1964. *Mechanisms of nucleophilic substitution in phosphate esters* Chem Rev 64: 317-352.

Creed MJ and HK Fauske. 1990. *An Easy, Inexpensive Approach to the DIERS Procedure,* Chem. Eng. Prog. 45-49

Delegard CH. 1980. *Laboratory Studies of Complexed Waste Slurry Volumes Volume Growth in Tank 241-SY-101*, RHO-LD-124, Rockwell Hanford Operations, Richland, Washington.

Delegard CH. 1987. *Identities of HEDTA and Glycolate Degradation Products in Simulated Hanford High-Level Waste*, RHO-RE-ST-55P, Rockwell Hanford Operations, Richland, Washington.

Fauske HK. 1995. *Summary of Laboratory Scoping Tests Related to Organic Solvents Combustion by Nitrate Oxidation and Organic Solvent Ignitability*, Fauske & Associates, Burr Ridge, Illinois.

Fauske HK and M Epstein. 1995. *The Contact-Temperature (CTI) Criteria for Propagating Chemical Reactions Including the Effect of Moisture and Application to Hanford Waste*, WHC-SD-WM-ER-496 Rev 0, Westinghouse Hanford Company, Richland, Washington.

Fauske HK. 1996. *An Update of Requirements for Organic-Nitrate Propagating Reactions Including RSST and Tube Propagation Test Results with Simulants*, FAI/96-48, Fauske & Associates, Burr Ridge, Illinois.

Gerber M A, LL Burger, DA Nelson, JL Rayan and RL Zollars. 1992. *Assesment of Concentration Mechanisms for Organic Wastes in Underground Storage Tanks at Hanford.*, PNL-8339, Pacific Northwest Laboratory, Richland, Washington.

Goheen MW. 1988. *Quantitative Gas Mass Spectrometry*. PNL-ALO-284, Pacific Northwest Laboratory, Richland, Washington.

Herting DL, DB Bechtold, BA Crawford, TL Welsh, and L Jensen. 1992a. *Laboratory Characterization of Samples Taken in May 1991 from Hanford Waste Tank 241-SY-101* WHC-SD-WM-DTR-024 Rev 0, Westinghouse Hanford Company, Richland, Washington.

Herting, DL, DB Bechtold, BE Hey, BD Keele, L Jensen, and TL Welsh. 1992b. *Laboratory Characterization of Samples Taken in December 1991 (Window E) from Hanford Waste Tank 241-SY-101* WHC-SD-WM-DTR-026 Rev 0, Westinghouse Hanford Company, Richland, Washington.

Hohl TM. 1993. *Synthetic Waste Formulations for Representing Hanford Tankd Waste*, WHC-SD-WM-TI-549 Rev 0, Westinghouse Hanford Company, Richland, Washington.

Huckaby JL and MS Story. 1994. *Vapor Characterization of Tank 241-C-103*, WHC-EP-0780, Westinghouse Hanford Company, Richland, Washington.

Kennedy J, and SS Grimley. 1953. *Radiometric Studies with Phosphorus-32 Labelled Tri-n-Butyl Phosphate*, A.E.R.E. CE/R 1284, Atomic Energy Research Establishment, Harwell, United Kingdom.

Kingsley RS. 1965. *Solvent Extraction Recovery of Americium with Dibutyl Butyl Phosphonate,* RL-SEP-518, Hanford Atomic Productions Operation, Richland, Washington.

Lange, NA. 1985. *Lange's Handbook of Chemistry,* JA Dean, Ed., 13th ed., McGraw-Hill: New York.

Lilga MA, RT Hallen, EV Alderson, MO Hogan, TL Hubler, GL Jones, DJ Kowalski, MR Lumetta, WF Reimath, RA Romine, GF Schiefelbein and MR Telander. 1996. *Ferrocyanide Safety Project Ferrocyanide Aging Studies Final Report,* PNNL-11211, Pacific Nortwest Laboratory, Richland, Washington.

Meisel D, H Diamond, EP Horwitz, MS Matheson, MC Sauer Jr, JC Sullivan, F Barnabas, E Cerny, and YD Cheng. 1991a. *Radiolytic Generation of Gases from Synthetic Waste*, ANL-91/41, Argonne National Laboratory, Argonne, Illinois.

Meisel D, H Diamond, EP Horwitz, MS Matheson, MC Sauer Jr, and JC Sullivan. 1991b. *Radiation Chemistry of Synthetic Waste*, ANL-91/40, Argonne National Laboratory, Argonne, Illinois.

Meisel D, CD Jonah, S Kapoor, MS Matheson, and MC Sauer Jr. 1993. *Radiolytic and Radiolytically Induced Generation of Gases from Synthetic Wastes*, ANL-93/43, Argonne National Laboratory, Argonne, Illinois.

Meisel D, CD Jonah, MS Matheson, MC Sauer Jr, F Barnabas, E Cerny, Y Cheng and T Wojta. 1992. *Radiation Chemistry of High-Level Wastes ANL/CHM Task Force on Gas Generation in Waste Tanks*, ANL-92/40, Argonne National Laboratory, Argonne, Illinois.

Norton JD, and LR Pederson. 1994. *Ammonia in Simulated Hanford Double-Shell Tank Wastes: Solubility and Effects on Surface Tension*, PNL-10173, Pacific Northwest Laboratory, Richland, Washington.

Person, JC 1993. *Waste Generation Studies, January 1993*, WHC-SD-WM-DTR-028, Westinghouse Hanford Company.

Person, JC 1996. *Effects of Oxygen Cover Gas and NaOH Dilution on Gas Generation in Tank 241-SY-101 Waste*, WHC-SD-WM-DTR-043 Rev. 0, Westinghouse Hanford Company.

Pool KH, and RM Bean. 1994. *Waste Tank Organic Safety Project - Analysis of Liquid Samples from Hanford Waste Tank 241-C-103*, PNL-9403, Pacific Northwest Laboratory, Richland, Washington.

Reynolds DA. 1993. *Tank 101-SY Window E Core Sample: Interpertation of Results*, WHC-EP-0628, Westinghouse Hanford Company, Richland, Washington.

Scheele RD, JL Sobolik, RL Sell, and LL Burger. 1995. *Organic Tank Safety Project: Preliminary Results of Energetics and Thermal Behavior Studies of Model Organic Nitrate and/or Nitrite Mixtures and a Simulated Organic Waste,* PNL-10206, Pacific Northwest Laboratory, Richland, Washington.

Schmidt AJ, EO Jones, RJ Orth, JL Cox, ME Elmore, CD Meng, GG Newenschwander, and TR Hart. 1993. *Preliminary Conceptional Design for the Destruction of Organic/Ferrocynaides Constituents in the Hanford Tank Waste with Low Temperature Hydrothermal Processing*, PNL-SA-23181, Pacific Northwest Laboratory, Richland, Washington.

Schumpe A. 1993. *The estimation of gas solubilities in salt solutions*. Chem Eng Sci 48: 153-158.

Sederburg JP, and JA Reddick 1994. *TBP and Diluent Mass Balances in the PUREX Plant at Hanford 1955-1991*, WHC-SD-WM-ER-396-rev. 0, Westinghouse Hanford Company, Richland, Washington

Stromatt RW. 1989. *GC/MS Analysis of Extractable Semivolatile Organic Compounds*, PNL-ALO-345, Pacific Northwest Laboratory, Richland, Washington.

Webb AB, JL Stewart, DA Turner, MG Plys, G Malinovic, JM Grigsby, DM Camaioni, PG Heasler, WD Samuels and JJ Toth. 1995. *Preliminary Safety Criteria for Orgainc Watch List Tanks at the Hanford Site*, WHC-SD-WM-SARR-033 Rev. 0, Westinghouse Hanford Company, Richland, Washington.

APPENDIX A

Table A.1. Headspace Gas Pressure Data for SY1-Sim-94C Aging Experiments

Expt no.	T °C	Dose MGy	Pressure psi	Pressure Atm	Amount µmol	Change %
0	20	0	0.0	1.00	946	0
1	88.8	0.6	19.0	2.29	1757	86
3	48.0	1.1	11.0	1.75	1510	60
2	89.6	0.0	4.5	1.31	999	6
4	71.8	1.0	15.0	2.02	1625	72
5	89.3	1.0	30.0	3.04	2327	146
6	92.4	0.6	18.8	2.28	1729	83
7	51	1	6.6	1.45	1240	31
8	69	1	10.0	1.68	1361	44
9	90.7	1.21	31.0	3.11	2370	150
B1	50	0	1.5	1.10	947	0
B2	70	0	1.9	1.13	913	-4
B3	91	0	3.0	1.20	918	-3
9	48.7	0.416	8.0	1.54	1331	41
10	91.1	0.765	17.0	2.16	1642	74
11	50.5	0.779	8.0	1.54	1323	40
12	70	0.753	10.0	1.68	1358	44
13	90.4	0.771	21.0	2.43	1853	96
14	68	0.763	8.0	1.54	1255	33
15	50.4	0.745	8.0	1.54	1324	40
X1	50	0	0.0	1.00	858	-9
X2[a]	18.9	0.607	2.0	1.14	1079	14
23	90	0.207	6.5	1.44	1101	16
24	69.9	0.204	3.0	1.20	974	3
25	48.8	0.201	2.3	1.15	993	5
B4[b]	50	0.731	4.5	1.31	1121	18
B5[b]	70.2	0.814	2.9	1.20	967	2
B6[b]	88.4	0.805	3.6	1.25	956	1
16	50.7	0.925	9.9	1.68	1436	52
17	70	0.926	13.8	1.94	1567	66
18	87.6	0.912	22.7	2.55	1957	107
19	91.4	0.52	19.0	2.29	1744	84
29[a]	88	0.6	21.0	2.43	1863	97

Table A.1. Continued

Expt no.	T °C	Dose MGy	Pressure psi	Pressure Atm	Amount µmol	Change %
21	90.4	0.913	23.0	2.56	1957	107
26	49.9	0.132	1.5	1.10	946	0
27	49.8	0.068	1.25	1.09	932	-2
22	50.3	0.388	3	1.20	1033	9
28	71.6	0.065	3	1.20	969	2
31(c)	91	0.524	19	2.29	1746	85
32(c)	92.5	0.836	23	2.56	1945	106
30	71.7	0.445	7.5	1.51	1215	28
34(c)	89.1	0.707	19.5	2.33	1781	88
35	92.2	0.13	8	1.54	1172	24
36	92.7	0.065	6	1.41	1068	13
37	69.6	0.132	2	1.14	919	-3
38	50.5	0.128	1.7	1.12	956	1
39(a)	68.5	0.409	1	1.07	867	-8.7
40(a)	19.5	0.415	1	1.07	1010	7.0

(a)Flux is ~10% of standard flux.
(b)Only 0.01 M citrate present initially.
(c)No oxygen gas present initially in headspace.

Table A.2. Headspace-gas Analytical Data for SY1-SIM-94C Aging Experiments

Expt no.	T °C	Dose MGy	Flux KGy/h	Gases (µmol)							
				H_2	CH_4	N_2	O_2	N_2O	NO_x	C_2H_6	RH
1	88.8	0.60	3.10	288	7	135	75	356	2	2	19
2	89.6	0.00	3.10	3	4	9	86	0	0	0	9
3	48.0	1.05	3.07	185	9	143	73	299	7	1	12
4	71.8	0.95	3.04	225	11	182	77	330	8	0	18
5	89.3	1.00	3.04	672	19	215	77	500	0	3	32
6	92.4	0.58	3.00	432	11	85	74	206	1	0	23
7	51.0	0.58	3.00	109	7	64	110	119	6	1	8
8	69.2	0.58	3.00	172	8	101	72	193	1	0	13
9	90.7	1.21	2.97	569	11	251	78	506	0	3	22
10	91.1	0.77	2.94	700	7	134	85	281	0	0	29
11	50.5	0.78	2.91	133	4	105	72	160	0	9	7
12	70.0	0.75	2.91	195	6	137	71	242	0	1	11
13	90.4	0.77	2.87	572	11	133	78	308	0	1	23
14	68.0	0.76	2.87	187	6	128	65	198	1	0	10
15	50.4	0.75	2.87	140	4	104	94	184	0	1	6
16	50.7	0.93	2.78	161	5	122	86	243	0	1	9
17	70.0	0.93	2.76	150	14	167	61	295	0	4	9
18	87.6	0.91	2.75	373	18	186	78	491	0	0	18
19	91.4	0.52	2.75	491	7	79	77	137	0	0	16
21	90.4	0.91	2.72	605	20	116	70	205	0	0	20
22	50.3	0.39	2.69	48	1	26	130	36	0	0	3
23	90.0	0.21	2.87	171	2	45	88	78	0	1	10
24	69.9	0.20	2.87	41	0	35	131	18	0	0	4
25	48.8	0.20	2.84	3	0	9	173	3	1	1	2
26	49.9	0.13	2.69	1	0	8	175	0	0	0	1
27	49.8	0.07	2.69	0	0	1	177	0	0	0	1
28	71.6	0.07	2.69	6	2	10	172	1	0	0	1
29[a]	88.4	0.61	0.25	1017	32	216	25	151	0	0	24
31[b]	91.0	0.52	2.69	455	7	83	0.2	163	2	2	15
32[b]	83.6	0.93	2.66	297	5	67	0.5	172	1	0.1	13
34[b]	89.1	0.71	2.66	447	6	80	0.3	156	2	0	15
35	92.2	0.13	2.66	91	2	33	76	29	1	0	7

Table A.2. Continued

Expt no.	T °C	Dose MGy	Flux KGy/h	Gases (μmol)							
				H_2	CH_4	N_2	O_2	N_2O	NO_x	C_2H_6	RH
36	92.7	0.07	2.63	61	2	25	116	14	2	0	9
37	69.6	0.13	2.63	21	3	27	154	6	4	0	17
38	50.5	0.13	2.63	5	1	15	174	3	2	0	9
39[a]	68.5	0.41	0.24	224	6	286	46	131	3	0.1	17
40[a]	19.5	0.42	0.24	32	1	127	145	46	0.4	0.5	2
B1	49.7	0.00	0.00	0.01	1	18	155	0.06	0.2	0.2	9
B2	70.0	0.00	0.00	0.01	1	18	155	0.06	0.2	0.2	9
B3	90.6	0.00	0.00	5	1	16	32	0.06	0.01	0.01	7
B4[c]	50.0	0.73	2.81	12	1	24	181	89	0.01	0.01	0
B5[c]	70.2	0.81	2.81	16	1	39	129	67	0.01	0.01	0
B6[c]	88.4	0.81	2.81	16	3	21	86	35	0.01	0.01	0
X1	50.0	0.00	0.00	0.33	1.25	37	2.4	0.08	0.08	0.3	16
X2[a]	18.9	0.61	0.24	55	1.4	61	124	55	0.05	0.6	0.1

[a]Flux is ~10% of standard flux.
[b]No oxygen gas present initially in headspace.
[c]Only 0.01 M citrate present initially.

Table A.3. Concentrations (mg/g) of Starting Organic Compounds Found in SY1-SIM-94C after Aging

Run No.	Date Received	Date Analyzed	T°C	Dose MGy	Analytes, mg/g Na4EDTA	Trisodium Citrate	Hexone	Dodec-ane	NaDBP	TBP	Sodium Stearate
1	4/1/94	6/19/95	89	0.603	5.75	12.7	0.00	4.53	5.1	0.00	14.6
3	5/31/94	7/29/94	48	1.050	7.5	NA	0.92	7.70	6.9	0.02	9.5
4	6/14/94	6/19/95	72	0.950	5.2	12.0	0.00	7.48	3.4	0.00	13.2
5	6/29/94	6/19/95	89	1.002	4.10	10.4	0.00	10.53	3.6	0.00	11.2
6	7/8/94	11/30/94	92	0.576	5.83	11.4	1.05	5.89	3.8	0.00	8.8
7	7/22/94	11/30/94	51	0.580	9.78	12.9	1.86	6.78	0.9	0.08	10.1
8	11/18/94	11/30/94	69	0.584	8.29	12.7	1.47	5.78	3.3	0.00	9.5
9	9/20/94	11/30/94	91	1.210	3.11	10.6	0.825	6.30	3.3	0.00	8.7
10	9/20/94	11/30/94	91	0.765	5.29	11.8	0.799	5.51	2.3	0.00	8.2
11	10/7/94	11/30/94	51	0.779	8.20	11.4	1.79	6.41	2.7	0.12	9.5
12	10/26/94	11/30/94	70	0.753	6.65	13.6	1.07	6.20	1.6	0.00	9.6
13	11/1/94	11/30/94	90	0.771	5.65	12.3	1.27	6.13	2.7	0.00	8.3
14	11/18/94	6/19/95	68	0.763	6.48	12.7	0.00	8.91	3.2	0.00	11.8
15	12/6/94	6/19/95	50	0.745	8.41	17.0	0.01	10.85	2.2	0.00	13.2
16	2/22/95	6/19/95	50	0.930	18.3	14.6	4.03	11.3	1.5	6.89	14.6
18	4/11/95	6/19/95	88	0.912	4.24	9.3	0.00	8.5	3.4	0.00	12.1
19	4/11/95	6/19/95	91	0.520	8.55	15.8	0.00	6.81	0.4	0.00	11.1
21	6/1/95	6/27/95	90	0.910	5.94	12.6	0.00	7.48	1.1	0.00	9.6
22	6/1/95	6/27/95	50	0.390	14.2	13.1	0.66	10.2	0.3	0.00	12.2
23	12/19/94	6/19/95	90	0.207	12.6	14.6	0.72	8.68	2.5	0.00	13.2
24	12/19/94	6/19/95	70	0.204	13.8	14.5	2.04	10.55	1.7	0.00	14.0
25	12/19/94	6/19/95	49	0.201	13.9	14.4	2.93	10.26	0.5	0.18	12.1
26	6/1/95	6/27/95	50	0.130	16.9	13.8	1.52	9.71	1.2	1.75	12.1
27	6/1/95	6/27/95	50	0.070	18.0	14.0	1.93	9.84	1.4	2.37	12.9
28	6/1/95	6/27/95	72	0.070	16.6	13.8	1.04	9.85	1.3	0.00	12.8
29[a]	4/11/95	6/19/95	88	0.610	7.48	5.1	0.00	11.69	0.6	0.00	10.4
30	7/6/95	8/8/95	72	0.445	13.9	13.7	1.96	5.07	0.5	0.00	7.0
31[b]	NA	8/8/95	91	0.520	7.20	13.0	1.68	7.58	1.2	0.00	8.4
32[b]	NA	8/8/95	84	0.930	5.81	12.1	1.78	8.54	1.2	0.00	7.4
34[b]	7/6/95	8/8/95	89	0.710	6.65	11.2	2.09	7.80	1.1	0.00	7.4
35	7/6/95	8/8/95	92	0.130	10.7	13.1	1.68	7.93	0.9	0.00	7.4
36	7/13/95	8/8/95	93	0.070	15.6	13.9	1.77	6.17	0.5	0.00	7.5
37	7/24/95	12/7/95	70	0.130	15.6	13.9	4.14	8.30	0.6	0.00	12.6
38	7/24/95	12/7/95	51	0.130	16.7	14.5	4.28	7.73	0.9	0.56	12.1
39[a]	10/6/95	12/7/95	42	0.685	12.4	12.1	2.52	8.70	0.3	0.00	12.7
40[a]	NA	5/23/96	41	0.195	14.9	13.6	0.56	7.42	3.3	0.00	16.7
B1	8/3/94	11/30/94	50	0.000	18.5	13.0	4.08	7.10	1.8	0.05	12.2
B2	NA	11/30/94	70	0.000	15.3	0.0	3.56	7.01	4.2	0.00	12.9
B3	9/20/94	11/30/94	90	0.000	17.7	13.5	3.56	8.07	1.4	0.01	14.6
X1	10/26/94	11/30/94	50	0.000	18.6	13.8	4.10	7.46	1.8	0.00	12.8
X2[a]	12/16/94	6/19/95	19	0.607	12.8	13.1	0.83	11.94	3.2	0.53	14.4
94C	2/22/95	6/19/95	4	0.000	19.1	15.6	3.71	10.22	1.1	6.37	12.6
94C	7/6/95	8/8/95	4	0.000	19.1	15.5	5.29	9.66	0.5	4.85	8.8
94C	NA	5/23/96	4	0.000	18.25	14.6	3.62	8.79	0.8	2.48	18.9
94C	3/10/94	NA	4	0.000	16.8	NA	3.81	9.34	39.0	18.6	NA
94C	4/1/94	6/19/95	4	0.000	17.8	NA	2.09	3.54	0.7	8.89	15.2

NA: data not available. [a]Flux is ~10% of standard Flux. [b]No oxygen gas present initially in headspace.

APPENDIX B

Table B.1. Concentrations (mg/g) of Compounds Found in Irradiated Butanol and Butyrate Simulants

Dose	GC Analyses			Acids by IC Analyses[a]				
	Butanol	Butyric Acid	Propion-ic Acid	Butyric/ (Formic)	Glycolic/ (Acetic)	Oxalic/ (Fumaric)	Malonic	Malic
Butanol simulant								
0	4.5							
3.6	3.2	0.057						
12.5	1.5	0.054	<0.050			0.02 (0.03)		
25.0	0.70	0.049	<0.050			0.05 (0.07)		
35.7	0.055	0.052	<0.050	0.68 (0.23)		0.18 (0.11)		
58.9	0.0	<0.040	<0.050			0.22 (0.31)	0.30	0.04
76.5	0.0	<0.040		0.81 (0.27)	0.85 (0.47)	0.44 (0.63)	0.58	0.08
95.9	0.0	<0.040		0.89 (0.30)	2.62 (1.44)	0.56 (0.79)	0.63	0.10
Butyrate simulant								
0		3.0		3.23				
3.6		2.5		2.49				
12.5		1.2		1.26		0.06 (0.09)		
25.0		0.23		0.44		0.15 (0.21)	0.37	
35.7		0.10		0.33	1.25 (0.69)	0.33 (0.47)	0.45	
58.9		<0.040				0.65 (0.92)		
76.5		<0.040				0.76 (1.08)	0.54	0.08
95.9		<0.040				0.77 (1.09)	0.55	0.09

[a]IC analyses did not resolve butyrate and fomate, glycolate and acetate, or oxalate and fumarate; values listed for these compounds assume that the compound is either one or the other; numbers in parentheses are for the corresponding compounds in parentheses.

APPENDIX C

Table C.1. Molar Concentrations of Phosphorus-Containing Species Found by ^{31}P NMR Analyses of DBP Radiolyses Experiments (See Table 5.2): (A) Diorganophosphates, (B) Monorganophosphates, (C) PO_4^{-3}

Experiment Number	Dose (MGy)	A	B	C	Unknown	Total
81-1-0	0	1.003	0.000	0.000	0.014	1.017
81-1-1	0.0811	1.089	0.009	0.000	0.017	1.116
81-1-2	0.1623	1.024	0.012	0.000	0.015	1.051
81-1-4	0.568	1.241	0.058	0.000	0.018	1.318
81-1-5	0.7303	0.939	0.065	0.005	0.000	1.009
81-1-6	0.9737	0.923	0.082	0.009	0.016	1.031
81-1-7	1.136	0.935	0.089	0.005	0.015	1.045
81-2-0	0	0.516	0.000	0.000	0.006	0.522
81-2-1	0.0811	0.548	0.006	0.000	0.006	0.560
81-2-2	0.1623	0.541	0.006	0.000	0.006	0.553
81-2-3	0.4057	0.479	0.041	0.000	0.006	0.525
81-2-4	0.568	0.477	0.037	0.000	0.006	0.520
81-2-5	0.7303	0.434	0.049	0.002	0.000	0.486
81-2-6	0.9737	0.426	0.066	0.011	0.009	0.511
81-2-7	1.136	0.420	0.070	0.005	0.008	0.503
81-3-0	0	0.287	0.000	0.000	0.012	0.299
81-3-1	0.0811	0.281	0.006	0.000	0.013	0.300
81-3-2	0.1623	0.272	0.017	0.000	0.016	0.304
81-3-3	0.4057	0.257	0.027	0.000	0.013	0.297
81-3-4	0.568	0.492	0.071	0.001	0.031	0.596
81-3-5	0.7303	0.378	0.049	0.000	0.000	0.427
81-3-6	0.9737	0.234	0.057	0.005	0.015	0.311
81-3-7	1.136	0.203	0.056	0.005	0.016	0.280
81-4-0	0	0.138	0.000	0.000	0.013	0.151
81-4-1	0.0811	0.133	0.003	0.000	0.015	0.151
81-4-2	0.1623	0.131	0.014	0.000	0.013	0.158
81-4-3	0.4057	0.115	0.024	0.000	0.017	0.157
81-4-4	0.568	0.100	0.029	0.004	0.000	0.133
81-4-5	0.7303	0.097	0.038	0.006	0.014	0.157
81-4-6	0.9737	0.092	0.046	0.010	0.017	0.164
81-4-7	1.136	0.066	0.047	0.008	0.015	0.137
81-6-0	0	0.312	0.000	0.000	0.017	0.329
81-6-1	0.0811	0.313	0.003	0.000	0.016	0.332
81-6-2	0.1623	0.296	0.006	0.000	0.014	0.316
81-6-3	0.4057	0.300	0.000	0.000	0.014	0.314
81-6-4	0.57	0.303	0.000	0.000	0.000	0.303
81-6-5	0.7303	0.300	0.000	0.000	0.015	0.316
81-6-6	0.9737	0.290	0.000	0.000	0.013	0.303
81-6-7	1.136	0.287	0.000	0.000	0.015	0.302

Table C.1. Continued.

Expt. No.	Dose	A	B	C	Unknown	Total
81-7-0	0	0.329	0.000	0.000	0.013	0.342
81-7-1	0.0811	0.334	0.001	0.000	0.013	0.348
81-7-2	0.1623	0.312	0.010	0.000	0.016	0.338
81-7-3	0.4057	0.313	0.034	0.000	0.015	0.361
81-7-4	0.568	0.276	0.028	0.000	0.000	0.304
81-7-5	0.7303	0.275	0.039	0.000	0.015	0.330
81-7-6	0.9737	0.264	0.051	0.002	0.016	0.333
81-7-7	1.136	0.229	0.062	0.007	0.015	0.313
81-8-0	0	0.319	0.000	0.000	0.015	0.334
81-8-1	0.0811	0.322	0.004	0.000	0.014	0.340
81-8-2	0.1623	0.309	0.017	0.000	0.014	0.340
81-8-3	0.4057	0.300	0.026	0.000	0.014	0.341
81-8-4	0.568	0.267	0.034	0.000	0.000	0.301
81-8-5	0.7303	0.268	0.048	0.000	0.014	0.331
81-8-6	0.9737	0.245	0.055	0.006	0.012	0.319
81-8-7	1.136	0.218	0.062	0.004	0.014	0.298
81-9-1	0.0811	0.319	0.002	0.000	0.014	0.334
81-9-2	0.1623	0.314	0.010	0.000	0.014	0.338
81-9-3	0.4057	0.304	0.032	0.000	0.016	0.352
81-9-4	0.568	0.270	0.040	0.000	0.000	0.310
81-9-5	0.7303	0.272	0.050	0.003	0.015	0.339
81-9-6	0.9737	0.256	0.061	0.007	0.014	0.339
81-9-7	1.136	0.240	0.069	0.015	0.016	0.339
81-10-0	0	0.319	0.000	0.000	0.015	0.334
81-10-1	0.0811	0.314	0.007	0.000	0.013	0.334
81-10-2	0.1623	0.303	0.019	0.000	0.016	0.338
81-10-3	0.4057	0.290	0.030	0.001	0.015	0.336
81-10-4	0.568	0.257	0.039	0.003	0.000	0.299
81-10-5	0.7303	0.273	0.042	0.005	0.015	0.334
81-10-6	0.9737	0.230	0.058	0.009	0.013	0.310
81-10-7	1.136	0.204	0.063	0.008	0.015	0.291
81-12-0	0	0.303	0.000	0.000	0.014	0.317
81-12-1	0.0811	0.302	0.008	0.000	0.015	0.325
81-12-2	0.1623	0.270	0.019	0.001	0.013	0.303
81-12-3	0.4057	0.268	0.045	0.008	0.014	0.336
81-12-4	0.568	0.234	0.046	0.013	0.000	0.293
81-12-5	0.7303	0.225	0.060	0.017	0.014	0.316
81-12-6	0.9737	0.204	0.077	0.031	0.014	0.326
81-12-7	1.136	0.191	0.075	0.031	0.013	0.310

Table C.1. Continued.

Expt. No.	Dose	A	B	C	Unknown	Total
81-13-0	0	0.322	0.000	0.000	0.013	0.335
81-13-1	0.0811	0.334	0.007	0.001	0.017	0.359
81-13-2	0.1623	0.304	0.014	0.000	0.013	0.331
81-13-3	0.4057	0.298	0.043	0.002	0.022	0.366
81-13-4	0.568	0.274	0.054	0.004	0.000	0.331
81-13-5	0.7303	0.252	0.073	0.006	0.017	0.348
81-13-6	0.9737	0.220	0.091	0.008	0.013	0.332
81-13-7	1.136	0.213	0.101	0.010	0.013	0.337
81-14-0	0	0.306	0.000	0.000	0.013	0.319
81-14-1	0.0811	0.291	0.014	0.000	0.015	0.320
81-14-2	0.1623	0.282	0.023	0.001	0.015	0.320
81-14-3	0.4057	0.261	0.050	0.004	0.014	0.329
81-14-5	0.7303	0.222	0.078	0.014	0.015	0.328
81-14-6	0.9737	0.193	0.088	0.019	0.015	0.316
81-14-7	1.136	0.186	0.097	0.027	0.015	0.325
81-15-0	0	0.307	0.000	0.000	0.013	0.320
81-15-1	0.0811	0.298	0.006	0.000	0.014	0.319
81-15-2	0.1623	0.300	0.015	0.000	0.017	0.332
81-15-3	0.4057	0.275	0.033	0.004	0.016	0.329
81-15-4	0.568	0.268	0.044	0.004	0.000	0.316
81-15-5	0.7303	0.255	0.051	0.006	0.015	0.326
81-15-6	0.9737	0.234	0.063	0.012	0.015	0.325
81-15-7	1.136	0.233	0.073	0.017	0.014	0.338

Distribution

No. of Copies

Offsite

2 DOE/Office of Scientific and Technical Information

Steve F. Agnew
Los Alamos National Laboratory
P. O. Box 1663
CST-4MS-J586
Los Alamos, NM 87545

J. Antizzo
U.S. Department of Energy
EM-36/Trevion II
Germantown, MD 20874

E. C. Ashby
School of Chemistry/Biochemistry
Georgia Institute of Technology
Atlanta, GA 30332-0400

E. Kent Barefield
School of Chemistry/Biochemistry
Georgia Institute of Technology
Atlanta, GA 30332-0400

Ned Bibler
Westinghouse Savannah River
P. O. Box 616
Aiken, SC 29802

Jack Edwards
Los Alamos National Laboratory
P. O. Box 1663
Los Alamos, NM 87545

L. Kovach
NUCON
P. O. Box 29151
Columbus, OH 43229-0151

B. R. Kowalski
Chemistry Department, BG-10
University of Washington
Seattle, WA 98195

No. of Copies

Offsite

Charles L. Liotta
School of Chemistry/Biochemistry
Georgia Institute of Technology
Atlanta, GA 30332-0400

D. Meisel
Chemistry Division
Argonne National Laboratory
9700 South Cass Avenue
Argonne, IL 60439

H. M. Neumann
School of Chemistry/Biochemistry
Georgia Institute of Technology
Atlanta, GA 30332-0400

C. O'Dell
U. S. Department of Energy
EM 36/Trevion II
Germantown, MD 20874

Leon Stock
6022 S.W. Texas Ct.
Portland, OR 97219

H. Sutter
SAIC
20300 Century Boulevard
Germantown, MD 20874

Billy C. Hudson
PO Box 271
Lindsborg, KA 67456

David O. Campbell
102 Windham Road
Oak Ridge, TN 37830

Thomas S. Kress
102-B Newridge Road
Oak Ridge, TN 37830-8118

No. of Copies

Offsite

Thomas E. Larson
2711 Walnut St.
Los Alamos, NM 87544

Dana A. Powers
Sandia National Laboratories
PO Box 5800
Albuquerque, NM 87185-0744

Scott E. Slezak
Sandia National Laboratories
PO Box 5800
Albuquerque, NM 87185

Onsite

7 *DOE Richard Operations Office*

S. O. Branch	S7-54
R. F. Christensen,	S7-54
M. F. Jarvis,	S7-54
G. W. Rosenwald,	S7-54
Public Reading Room	
RL Docket File (2)	B3-11

FAI

M. G. Plys	A3-37

2 *MACTEC*

M. H. Campbell	S7-73
S. T. Murff	S7-73

17 *Westinghouse Hanford Company*

H. Babad	S7-14
G. S. Barney	T5-12
W. B. Barton	R2-11
R. E. Bauer	S7-14
D. B. Bechtold	T6-09
R. J. Cash	S7-14
W. L. Cowley	A3-37
D. L. Herting	T6-09
J. R. Jewett	T6-09

No. of Copies

Onsite

Westinghouse Hanford Company

G. D. Johnson	S7-14
N. W. Kirch	R2-11
J. E. Meacham	S7-14
J. C. Person	T6-09
F. R. Reich	L5-55
D. A. Reynolds	R2-11
E. R. Siciliano	H0-31
A. B. Webb	A3-37

56 *Pacific Northwest National Laboratory*

D. L. Baldwin	P7-22
G. H. Beeman	P7-75
J. W. Brothers (5)	K9-20
S. A. Bryan	P7-25
D. M. Camaioni (10)	K2-44
J. A. Campbell	P8-08
C. D. Carlson	P7-25
S. A. Clauss	P8-08
S. D. Colson	K9-62
D. M. Friedrich	K2-14
P. A. Gauglitz	P7-41
M. A. Gerber	P8-38
S. C. Goheen	P8-08
R. T. Hallen	P8-38
D. W. Koppenaal	P7-07
M. A. Lilga	P8-38
P. K. Melethil	P7-22
G. M. Mong	P8-08
L. R. Pederson	K2-44
W. D. Samuels	K2-44
R. D. Scheele	P7-25
A. K. Sharma	P8-08
C. W. Stewart	K7-15
M. R. Thompson	K2-50
J. M. Tingey	P7-25
J. J. Toth	K7-94
K. L. Wahl	P8-08
Organic Tank Project File	K9-89
Publishing Coordination	
Technical Report Files (5)	